Stars and **Galaxies**

Tom Theuns
Office OCW 207
Institute for Computational Cosmology
Ogden Centre for Fundamental Physics
Durham University
tom.theuns@durham.ac.uk

- ⋆ **Chapter 1: Introduction**
- ⋆ **Chapter 2: The discovery of the Milky Way and of other galaxies**
- ⋆ **Chapter 3: The modern view of the Milky Way**
- ⋆ **Chapter 4: The Interstellar Medium**
- ⋆ **Chapter 5: Dynamics of galactic disks**
- ⋆ **Chapter 6: The dark halo**
- ⋆ **Chapter 7: Elliptical galaxies**
- ⋆ **Chapter 8: Groups and Clusters of galaxies**
- ⋆ **Chapter 9: Galaxy statistics**
- ⋆ **Chapter 10: Active Galactic Nuclei**
- ⋆ **Chapter 11: Gravitational lensing**

Aim

The *Hubble Deep Field* shows how even a tiny patch of sky contains thousands of galaxies of different sizes and shapes, lighting-up the Universe with a dazzling display of colours. When did they form? Which physical processes shaped them? How do they evolve? Which types are there, and whence the huge variety? How does the Milky Way galaxy fit in?

12 lectures are too few to answer any of these fundamental questions in any detail. In addition, galaxy formation and evolution require a cosmological setting, see the later lecture courses on cosmology (L3) and galaxy formation (L4). The more modest aim of these lectures is to give an overview of the properties of galaxies (galaxy types, properties of spiral galaxies in general and the Milky Way galaxy in particular, properties of elliptical galaxies), look at some of the more spectacular phenomena (quasars, gravitational lensing), and investigate the extent to which all this can be described with simple physics. These lectures will *use* the physics you've learnt in other lectures (in particular classical mechanics, electricity and magnetism, quantum mechanics, and of course the earlier parts Observational Techniques and Stars) to galaxies, rather than teach new physics.

The beauty of galaxies is for most people enough to warrant their study, but of course astronomy and cosmology enable one to study physics in situations which cannot be realised in a laboratory. Examples of fundamental physics made possible by astronomy and cosmology are tests of general relativity (Mercury's orbit, dynamics of pulsars), investigations whether the fine-structure constant evolves (from quasar absorption spectra), the discovery of dark matter (from the motions of galaxies), and more recently the discovery of dark energy (from the expansion of the Universe). Several of these fundamental discoveries rely on a basic understanding of galaxies, the building blocks of the Universe.

Learning outcomes:

- ability to classify galaxies and state defining properties of spiral, elliptical and irregular galaxies
- explain observational basis for discovery of the Milky Way
- explain observational basis of the modern view of the Milky Way
- apply classical mechanics to dynamics of galactic disks, including arguments for the presence of dark matter
- apply classical mechanics and other basic physics to the properties of the interstellar medium in spirals (properties of gas and dust, 21-cm radiation, concept and application of Jeans mass)
- apply mechanics and hydrostatics to describe elliptical galaxies and clusters of galaxies
- understanding of galaxy scaling relations and statistical properties of galaxies
- observational manifestations of active galactic nuclei, and the connection to central supermassive black holes
- basics of gravitational lensing, and its applications

Additional information
There are many excellent sites with images of galaxies, and explanations of some of the issues discussed below. The latest version of *Google Earth* has the option to look at the night sky, with images of galaxies taken from the *Sloan Digital Sky Survey* and the *Hubble Space Telescope*.

Most of the images shown during the lectures come from one of

- http://www.seds.org/
- http://www.aao.gov.au/images.html/
- http://hubblesite.org/newscenter/archive/
- http://teacherlink.ed.usu.edu/tlnasa/pictures/picture.html

- http://astro.estec.esa.nl
- http://space.gsfc.nasa.gov/astro/cobe/cobe_home.html
- http://astro.estec.esa.nl/Hipparcos/
- http://astro.estec.esa.nl/GAIA/

Much of what is discussed in the notes can be found often with additional explanations and diagrams in several text books. The lectures here will refer very often to Carroll & Ostlie: paragraphs refer to the corresponding section in that reference book (*e.g.* CO 6.2 refers to Section 6.2 of that text book, CO p. 310 to page 310.)

Additional explanations can be found in

1 Carroll & Ostlie, *Modern Astrophysics*, Addison-Wesley, second edition, 2007

2 Zeilik & Gregory, *Astronomy & Astrophysics*, Saunders College Publishing, 1998

3 Binney & Merrifield, *Galactic Astronomy*, Princeton, 1998

4 Binney & Tremaine, *Galactic Dynamics*, Princeton, 1987

(These are referred to as CO. ZG, BM, and BT in these notes) The first two are general and basic texts on astronomy, which, together with the web pages, should be your first source for more information. [3] is a much more advanced text on galaxies, and [4] is a superb and detailed discussion of the dynamics of galaxies.

http://burro.astr.cwru.edu/Academics/Astr222/index.html

is a truly excellent web site where you'll find additional material on what is discussed in these lectures, and several images in these notes originate from there.

Summary

Chapters 1-6: spiral galaxies

Galaxies come in a range of colours and sizes. In **spiral** galaxies such as the Milky Way, most stars are in a thin disk. The disk of the Milky Way has a radius of about 15 kpc, and contains $\sim 6 \times 10^{10} M_\odot$ of stars. The disk stars rotate around the centre of the galaxy on nearly circular orbits, with rotation speed $v_c \sim 220$ km s^{-1} almost independent of radius r (unlike the motion of planets in the solar system where $v_c \propto 1/r^{1/2}$). Such *flat rotation curves* require a very extended mass distribution, much more extended than the *observed* light distribution, indicating the presence of large amounts of invisible *dark matter*. Curiously, the spiral arms do not rotate with the same speed as the stars, hence stars may move in and out of spiral arms.

Stars are born in the large molecular gas clouds that are concentrated in spiral arms. Massive short-lived stars light-up their natal gas with their ionising radiation, and such 'HII' regions of ionised hydrogen follow the arms as beads on a string. The blue light from these massive and hot stars affects the colour of the whole galaxy, one reason why spirals are blue. Remember that the luminosity L of a star is a strong function of its mass M, with approximately $L \propto M^3$ on the main sequence, hence a single $100 M_\odot$ star outshines nearly 10^6 solar-mass stars: the colour of a galaxy may be affected by how many massive (hence young) stars it harbours.

The stars in the central region of the Milky Way (and most spirals) are in a nearly spherical *bulge*, a stellar system separate from the spiral disk, with mass $\approx 10^{10} M_\odot$. Dust in the interstellar medium of the disk prevents us from seeing the Milky Way's bulge on the night sky. Disk and bulge are embedded in a much more extended yet very low-density nearly spherical *halo*, consisting mostly of dark matter. The stellar halo contains a sprinkling of 'halo' stars, but also globular clusters, very dense groups of $10^5 - 10^6$

stars of which the Milky Way has ~ 150. The total mass of the Milky Way is $\sim 10^{12} M_\odot$, but stars and gas make-up only $\sim 7 \times 10^{10} M_\odot$ with the rest in dark matter.

Chapter 7: elliptical galaxies

Elliptical galaxies are roundish objects which appear yellow. The redder colour as compared to spiral galaxies is due to two reasons: firstly the stars in elliptical galaxies tend to have higher metallicity than spiral galaxies of comparable mass, and the metals in the stellar atmospheres redden the stars. Secondly, elliptical galaxies have no current star formation, and hence they do not contain the massive and short-lived stars that produce the blue light in spirals.

The stars move at high velocities, and it is these random motions, not rotation, that provides the support against gravity. This is similar to how the velocities of atoms in a gas generate a pressure, $p \sim \rho v^2 \sim \rho T$. However, unlike the atoms in a gas, the stellar velocities are in general *not* isotropic, meaning that also the pressure is not isotropic. The result is that, whereas stars are round, elliptical galaxies are in general flattened, *i.e.* elliptical in shape.

The observed stellar motions, but also the hot X-ray emitting gas detected in them, both suggest the presence of dark matter in elliptical galaxies.

Chapters 8-9: galaxy statistics

Roughly half of all stars in the Universe are in spirals, and half are in ellipticals. Spiral galaxies tend to live in region of low galaxy density. The Milky Way is part of a 'local group' of galaxies, containing in addition to Andromeda a swarm of smaller galaxies. Ellipticals in contrast tend to cluster in groups of tens to hundreds of galaxies, called clusters of galaxies. Such clusters contain large amounts of hot, X-ray emitting gas. Together with the large observed speeds of the galaxies, this hot gas provides evidence that a large fraction of the cluster's mass is invisible dark matter.

Chapter 10: Active Galactic Nuclei

A small fraction of galaxies contains an active nucleus, which may generate as much or even more energy than all the galaxy's stars combined. The observational manifestations of such active galactic nuclei, or AGN, are quite diverse, with energy being emitted from visible light in quasars, to immensely power full radio lobes, to X-rays and even gamma-rays. Some fraction of energy may even be released in the form of a powerful jet.

The energy source is thought to be accretion onto a supermassive black hole, with masses from 10^6 to as high as $10^9 M_\odot$. It is thought that most, if not all, massive galaxies contain such a supermassive black hole in their centres. The evidence is particularly convincing for the presence of a $\sim 10^6 M_\odot$ black hole in the centre of the Milky Way.

Clearly, if most galaxies contain the engine but have little or no observational AGN manifestations, it must imply that the majority of black holes is dormant.

Chapter 11: Gravitational lensing

A gravitational field bends light. In general this is only a small effect and our view of the distant universe is not significantly deformed by the gravitational lensing caused by the intervening potentials generated by stars, galaxies or clusters of galaxies. The phenomenon has been used to test Einstein's theory of relativity, to constrain the nature of dark matter in the Milky Way, to determine the masses of galaxies and clusters, and even to enable astronomers to use clusters of galaxies as truly giant telescopes enabling the detailed study of distant galaxies.

Chapter 1

Introduction

CO §25.1 & 25.2

1.1 Historical perspective (*CO §24.1*)

Galaxies are extended on the night sky as can be seen even without using a telescope[1]. *Andromeda* is similar in size to the Milky Way and extends over several degrees, whereas the *Large Magellanic Cloud* or LMC, visible from the Southern hemisphere on a clear night, extends over six degrees (diameter of full moon is 1/2 a degree). The Sagittarius dwarf galaxy, a small galaxy gravitationally bound to the Milky Way, extends over a large fraction of the sky.

The Milky Way galaxy is a spiral galaxy, in which most of its $\sim 200 \times 10^9$ stars lie in a thin ($\sim$ 1/2kpc) disk of radius $\sim$ 15 kpc, with the Sun at a distance $\sim$ 8kpc from the centre. The Milky Way's disk can be seen as a faint trail of light on the night sky, while the other visible stars are not obviously part of a disk simply because they are nearby.

Other extra-solar objects which appear extended on the night sky include planetary nebulae, supernova remnants, and star clusters. Before intergalactic distances were first measured in the 1920s it was not realised that galaxies were a separate class, and both Messier's catalogue (1780, in which Andromeda is M 31) and Dryers (1988) *New General Catalogue* (in which it

[1]The disks of stars on the sky can only be resolved with special techniques, and even then only for very nearby stars.

is NGC 224) make no distinction between galaxies and these other 'nebulae'. Emmanuel Kant was one of the first to suggest that galaxies were other Milky Ways. The study of galaxies therefore only started in the 20th century, and we now know that the observable Universe contains $\sim 10^{11}$ galaxies more massive than the Milky Way. Surveys of galaxies now regularly catalogue properties of $10^4 - 10^6$ galaxies.

1.2 Galaxy classification (*CO §25.1*)

The light from normal galaxies is produced predominantly by stars. Luminosities of stars vary widely: recall from the earlier lectures that along the main sequence luminosity L depends on mass M as $L \propto M^\alpha$, with $\alpha \approx 3$, hence a single $100 M_\odot$ star outshines nearly 10^6 solar-mass stars. For given M, L depends strongly on the phase of stellar evolution, with giant and asymptotic giant branch stars *much* more luminous than the earlier main sequence phase. Therefore the observed luminosity of a galaxy will be dominated by its giant stars.

1.2.1 Observables

- *Luminosity* L Total luminosity of all stars combined.
- *Spectrum* The spectrum of a galaxy is the combined spectrum of all of its stars, weighted by luminosity.
- *Colour* A measure of the fraction of light emitted in long versus short wavelengths. *True colour* images of galaxies[2] are made by combining photographs of the galaxy taken through standard broad-band filters (see observational techniques), and mapping these to RGB colours. Since massive stars are young, hot and blue, galaxies which contain massive stars will tend to be bluer than those without them.
- *Extent* The angle the galaxy extends on the sky.
- *Flux* Just as for stars, the flux F of a galaxy with luminosity L at distance d is $F = L/4\pi d^2$, and is usually expressed using a system of

[2]Sometimes narrow-band filters are used to stress the presence of particular emission lines, for example the Hα emission line produced in star-forming regions.

magnitudes. Whereas L is an intrinsic property of the galaxy, the flux also depends on the distance to the observer.

- *Surface brightness and intensity* Approximate a galaxy as a slab of stars, with surface density σ (in stars per unit area), each of identical luminosity L. The total luminosity $d\mathcal{L}$ of an area dS of this galaxy is $d\mathcal{L} = \sigma L\, dS$. The *intensity* I is the luminosity per unit area, therefore $I = d\mathcal{L}/dS = \sigma L$ for a slab. It is an intrinsic quantity, *i.e.* it does not depend on the distance to the observer. The flux dF an observer at distance d receives from this surface area is

$$\begin{aligned} dF &= \frac{d\mathcal{L}}{4\pi d^2} \\ &= \frac{\sigma L dS}{4\pi d^2} \\ &= \frac{I}{4\pi}\, d\Omega\,. \end{aligned} \tag{1.1}$$

  Here, $d\Omega = dS/d^2$ is the solid angle the surface area dS extends on the sky. The quantity $dF/d\Omega = I/4\pi$, the flux received per unit solid angle, is called the *surface brightness*,

$$\text{Surface brightness} = \frac{dF}{d\Omega} = \frac{I}{4\pi}\,. \tag{1.2}$$

  Note that it is independent of distance[3]. Since σ decreases with radius r from the centre, surface brightness is higher in the centre than in the outskirts. Surface brightness is usually expressed in magnitudes per square arc seconds but this is not correct. What is meant is that one has converted the flux dF, measured in a solid angle of 1 square arc seconds, into magnitudes.

1.2.2 Galaxy types

Images of galaxies immediately show there are two types, called *elliptical* (E, also called early type, or spheroidal) and *spiral* S, also called disk type, or late type. Large galaxies that do not fit into either category have usually

[3]This is only true for nearby galaxies with redshift $z \ll 1$. When z is not $\ll 1$, surface brightness dims with redshift $\propto 1/(1+z)^4$.

undergone a recent violent collision, and most small galaxies are of type *irregular*.

Defining characteristics for E and S galaxies are

	Elliptical	Spiral
Shape	spheroidal	most stars in a disk
Colour	red	blue
Stars	old stars	old and young stars
ISM	little gas or dust	gas and dust
Stellar Dynamics	large random motions (hot)	circular orbits (cold)
Environment	dense (clusters)	low density (groups and field)

Ellipticals Isophotes (lines of constant surface brightness) of Es are smooth and elliptical and are further classified as En, where $n = 10(1 - b/a)$, where a and b are the major and minor axis of the isophotes, respectively. A round elliptical ($a = b$) is E0, whereas the most flattened ellipticals, E7, have $b = 0.3a$. There is little evidence for rotation in elliptical galaxies (except may be small ellipticals), so their flattening is not due to angular momentum. The intrinsic (as opposed to projected) shapes of Es are thought to be triaxial, with iso-density contours $a > b > c$.

Spirals The very thin flattened disk of spirals galaxies is due to rotation, and the stars in the disk are on nearly circular orbits around the galaxy's centre. Gas collects in Giant Molecular Clouds in the spiral arms of disks, where some fraction collapses into new stars. The massive, newly formed stars ionise their natal gas, and such HII regions of ionised hydrogen follow the arms as beads on a string. Once the cloud is dispersed, the blue light of these stars contributes to making the whole spiral appear blue, in contrast to the yellow/red light emitted by the older stars in Es. Spirals also contain dust which causes dark bands across the disk as the dust obscures background stars. The presence of dust prevents us from seeing the Milky Way's central bulge in visible light. The *bulge* is the central spheroidal stellar system, with many properties in common with elliptical galaxies. Spirals are further divides as Sa to Sc, where along the sequence the ratio of bulge-to-disk luminosity decreases, and the spiral arms become more loosely wound.

Some spirals also contain a *bar*, an almost rectangular stellar system in the disk, sticking-out of the bulge. These are designated as SB. So for example, an SBc galaxy is a barred (B) spiral (S), with loosely wound spiral arms

and a small bulge (c), where an Sa has no bar, and a big bulge. The Milky Way is between types SBb and SBc, Andromeda is type Sb.

Hubble's classification

Hubble used the above classification ordering galaxies in a tuning fork diagram called the Hubble Sequence (Fig. 1.1). The commonly used nomenclature of early types (for Es) and late types (for Ss) comes from the mistaken belief that Es evolve in Ss.

The range in physical scales of Es is huge, from masses as little[4] as $10^7 M_\odot$ to as much as $10^{13} M_\odot$, with linear sizes ranging from a few tenths of a kpc to hundreds of kpc. In contrast, spirals tend to be more homogeneous, with masses 10^9–$10^{12} M_\odot$, and disk diameters from 5 to 100kpc or so.

cDs and S0s are unusual types of Es and Ss, respectively. cDs are very large ellipticals, found in the centres of clusters, with a faint but very large outer halo of stars[5]. S0s (or SB0 when barred) or lenticulars are the divide in Hubble's sequence between E and S, they have disks without gas or dust, and no recent star formation.

Most small galaxies like *e.g.* one of our nearest neighbours, the Small Magellanic Cloud or SMC, have no well defined disk, nor a spheroidal distribution of stars, and hence are neither of type E nor S, they are classified as type *Irregular*. The two main types of galaxies are then elliptical and spiral, with most small galaxies being irregulars.

1.3 Summary

After having studied this lecture, you should be able to

- Describe the Hubble Sequence
- Describe the main galaxy types, Es and Ss, and list five defining characteristics
- Define surface brightness, and show it to be independent of distance

[4]It has been suggested that globular clusters are small ellipticals and should represent the low-mass end.

[5]cD refers to properties of the spectrum, but think of it as standing for **c**entral **D**ominant.

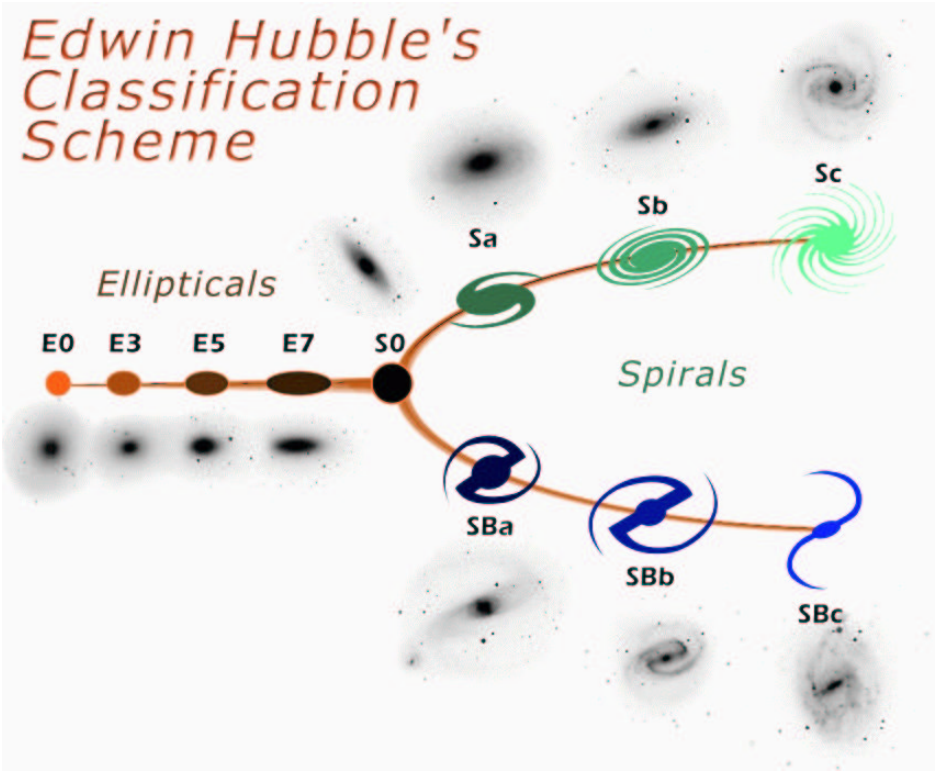

Figure 1.1: The Hubble sequence.

- Derive the relation between the surface density of stars in a galaxy, and its surface brightness

Chapter 2

The discovery of the Milky Way and of other galaxies

CO §25.1

Before distances to galaxies were measured, their nature and that of the Milky Way itself, was unclear. One possibility was that nebulae where stages of stellar evolution, such as *e.g.* proto-planetary systems. Observations gave contradictory results, with star counts suggesting the Sun was near the centre of the Milky Way, while globular clusters suggested it was not. The reason for the confusion is interesting and discussed below.

2.1 The main observables

Star clusters

- *Globular clusters* (GCs) are small ($\sim$1pc) dense concentrations of $10^5 - 10^6$ stars of low-mass, old stars. Most galaxies contain 10s to 1000s of GCs, spherically distributed around their centres; the MW galaxy has about 150 GCs.

- *Open clusters* contain typically 10^4 stars, are much less dense than GCs, and are restricted to the galactic plane. They are gravitationally bound systems left-over after star formation has ceased in a Giant Molecular Cloud, and the remaining gas has been dispersed. They are of crucial

importance for testing theories of stellar evolution: since their stars are thought to be coeval, any differences in properties should be a consequence of differences in initial mass.

Star counts (CO p.878)

Star counts can probe the number density of stars in a stellar system, as a function of position. William Herschel and his sister counted the numbers of stars as function of their magnitude in many (700!!) directions in the sky. Kapteyn and his collaborators used photographic plates for counting stars.

Suppose for simplicity that all stars have the same luminosity, L. The flux of a star, $F = L/4\pi r^2$, then only depends on distance r, and $dF/F = -2dr/r$. If the number density of stars at distance r in direction $\hat{\Omega}$ is $n(r, \hat{\Omega})$, the number of stars with flux between F and $F + dF$ in that direction, is

$$\begin{aligned} dN(F, \hat{\Omega}) &= n(r, \hat{\Omega}) r^2 dr \, d\Omega \\ &= -\frac{1}{2} n(F, \hat{\Omega}) \, (\frac{L}{4\pi})^{3/2} \, F^{-5/2} \, dF \, d\Omega \, . \end{aligned} \tag{2.1}$$

Therefore counting $dN(F)$ allows one to infer the density $n(r)$.

Parallax

Nearby stars appear to move with respect to more distant stars as Earth moves around the Sun. The extent of the excursion θ depends on the Earth-Sun distance and the distance to the star. Measuring θ gives a *parallax* distance to the star. A star at 1pc distance has by definition a yearly parallax of 2 arcsec. The name derives from **par**allax of one **sec**ond of arc.

Standard candles

Standard candles are objects with a known absolute property, for example a known size, or known luminosity. If the intrinsic size D is know, the distance can be determined by measuring angular extent. If the luminosity is known, distance can be determined by measuring flux.

Cepheid variables are an important example. Henrietta Leavitt studied variable stars in the Magellanic Cloud in 1912. She found a relation between the period P of the periodic variation Δm, and the magnitude m of

these Cepheids. Since all these stars are at (nearly) the same distance, this must mean it is actually a relation between the *absolute* magnitude M and P. Calibrating this relation makes Cepheids standard candles. In addition, Cepheids have a very characteristic saw-tooth shaped $m(t)$, making it easy to recognise them. Leavitt's discovery was therefore of great importance.

Parallax and Cepheid variables are the first two steps in the *distance ladder*, which use one method (e.g. parallax) to calibrate another distance measure (e.g. Cepheids), that then can be used to calibrate another distance indicator, and so on to ever greater distances. *Hubble Space Telescope* recently measured Cepheids in the Virgo cluster (at a distance of $\sim$ 17Mpc), thereby providing the first accurate distance to that cluster of galaxies, and getting an accurate measurement of Hubble's constant in the process.

2.2 Discovery of the structure of the Milky Way (CO p 875)

Star counts

Jacobus Kapteyn confirmed in the beginning of the 20th century using photographic plates the star count results first obtained by Herschel. The MW is a flattened elliptical system, with stellar density n decreasing away from the centre. n drops to half its central value at 150pc perpendicular to the MW plane, and 800pc in the galactic plane. The Sun is at 650pc from the centre. Although the star counts are correct, the interpretation to the shape of the MW and the position of the Sun are wrong.

The conversion from F to r, for given L, assumes $F \propto 1/r^2$, which neglects possible absorption of the light on route. But how can one test whether absorption is important? A plausible source of absorption is light scattering off atoms or molecules along the line of sight (Rayleigh scattering). The strength of scattering is colour dependent (stronger for shorter wavelengths): scattering of Sun light off molecules in the atmosphere makes the sky appear blue. Therefore if this were important, distant (hence fainter) stars should appear redder than more nearby stars. Kapteyn did measure the predicted reddening, but the amount was too small to be important.

However the reddening is not due to scattering off atoms, but due to scattering off *dust* (Tyndall scattering). The colour dependence of dust scattering is much less, so the small amount of reddening actually implies that

absorption is quite important.

Globular clusters

Harlow Shapley estimated the distances to the brightest globular clusters using their RR Lyrae variables, and found they were not centred around the Sun, but around a point 15kpc away in the direction of Sagittarius. This implied a much bigger MW than Kapteyn's, and relegated the Sun to the MW outskirts. But who was right?

Other nebulae

Another famous Dutch astronomer, *van Maanen*, observed galaxies over several years, and decided he could see them move with respect to the stars. This must mean they are relatively nearby, certainly within the MW.

But another astronomer Slipher measured large (1000s km s^{-1}) velocities for some Nebulae, and finds evidence for rotation. He also claims the light is produced by stars, not by gas. This suggests the nebulae are galaxies, and outside of the MW, in conflict with van Maanen'sand Kapteyn's MW picture.

Hubble's discovery

Hubble used the 100-inch Hooker Telescope on Mount Wilson in 1919 to identify Cepheid variables in other nebulae, including Andromeda. He inferred[1] a distance of $\sim$ 0.3 Mpc, much larger than even Shapleys size for the MW, and final prove that the nebulae were other galaxies outside of the Milky Way. Hubble went on to discover that the more distant galaxies move away from us at ever increasing speed. It is difficult to overstate the importance of this discovery. In one great swoop, the size of the Universe increased dramatically. The Sun got relegated to the outskirts of the MW, and the MW itself was found to be just one out of billions of other galaxies. And the Universe was found to be expanding, making Einstein's attempts to build a static cosmological model out of his theory of relatively irrelevant.

[1]The modern value is $\sim$ 0.7Mpc.

Epilogue

Trumpler found in the 1930s what had been wrong with Kapteyn's interpretation, by studying MW Open Clusters. He assumed the size of Open Clusters to be a standard candle, and hence assumed you could infer their distance from their angular size. Using this distance indicator, he found that the stars in the more distant clusters (as inferred from cluster size) were invariable much fainter than stars in more nearby clusters. He concluded that the light from distant stars was attenuated much more than expected from scattering off atoms. It had to be absorption by dust, and Kapteyn's neglect of this lead to his error in interpretation.

Time-line

1610 Galileo resolves the MW into stars

1750 Immanual Kant suggests that some of the other Nebulae are other galaxies, similar to the MW.

end of 1700s Messier and Herschel catalogue hundreds of Nebulae. Herschel counts stars, and deduces that the Sun lies near the centre of an elliptical distribution with axes ratio 5:5:1

1900-1920 Kapteyn counts stars, decides wrongly that extinction is unimportant, and deduces the MW to be 5kpc $\times$ 5kpc $\times$ 1kpc big, with the Sun at 650pc from the centre.

1912 Leavitt discovers the $P(L)$ relation for Cepheids.

1914 Slipher measures large (1000s km s^{-1}) velocities for some Nebulae, and finds evidence for rotation. The spectra he takes suggests presence of stars, not of gas. A clear indication these are not proto-planetary structures in the MW, but other galaxies.

1915 Shapley finds the centre of the MW's globular cluster system to be far away from Kapteyn's MW centre.

1920 van Maanen claims (erroneously) that some spiral nebulae have a large proper motion, suggesting they are within the MW.

1920 Shapley and Curtis debate publicly over the size of the MW, but the matter is not settled.

1923 Hubble resolves M31 (Andromeda) into stars, using the newly commissioned 100-inch telescope. Given the large inferred distance means that M31 must be outside the MW. He also discovers Cepheids, and the distance to M31 is estimated at 300kpc. So Andromeda is indeed another galaxy.

1926 Lindblad computes that Kapteyn's MW is so small, it cannot gravitationally bind its Globular Clusters. But Shapley's much bigger MW could.

1927 Jan Oort shows that several aspects of the local motion of stars can nicely be explained if the Sun (and the other nearby stars), is on a nearly circular motion around a position 12kpc away in the direction of Sagittarius. Nearly the same position as found by Shapley, and implying a much larger MW than Kapteyn's.

1927 larger MW picture, where many of the nebulae are extra-galactic MWs, gains general acceptance.

1929 Hubble discovers his expansion law. His derived value is a factor of 10 too large!

1930 Trumpler uses open clusters to show the importance of extinction, and explains why Kapteyn's measurement were faulty

1930-35 Hubble's new data confirm the modern picture of galaxies, and demonstrates van Maanen's measurements must have been wrong.

2.3 Absorption and reddening (CO p.878)

Consider a light ray of intensity I traversing a space containing very large dust grains (bricks). The bricks will absorb a fraction of the incoming light, and the intensity of the ray will decrease as

$$\frac{dI}{dr} = -A\,I\,, \tag{2.2}$$

which expresses the fact that each distance dr will absorb a constant *fraction* $dI/I = -A\,dr$ of the light. The constant A depends on the number density of bricks, and their size.

The solution to this equation is

$$I(r) = I_0\,\exp(-Ar)\,. \tag{2.3}$$

In terms of magnitudes, $\Delta m = -2.5\log(I/I_0) = \hat{A}\,r$, where the relation between $\hat{A}$ and A is left to you. $\hat{A}$ therefore has units of magnitude per unit length. Absorption therefore changes the usual relation $(m-M) = 5\log(r) - 5$ between apparent and absolute magnitude to $(m-M) = 5\log(r) - 5 + \hat{A}\,r$.

If the size of the particles is of order of the wavelength λ of the light, then the value of A will be wavelength dependent. This leads to reddening of the star, since smaller wavelengths (blue light) will be absorbed more strongly than longer wavelengths (red light).

If we apply this reasoning to light in the B versus V band, for example, we obtain

$$\begin{aligned}
(m-M)_{\rm B} &= 5\log(r) - 5 + A_{\rm B}\,r \\
(m-M)_{\rm V} &= 5\log(r) - 5 + A_{\rm V}\,r \\
E_{\rm B-V} &\equiv (m_{\rm B} - m_{\rm V}) - (M_{\rm B} - M_{\rm V}) = (A_{\rm B} - A_{\rm V})\,r\,.
\end{aligned} \tag{2.4}$$

The quantity $E_{\rm B-V}$ is called the *colour excess*, note that it is the difference between the observed and intrinsic colour of the star,

$$E_{\rm B-V} = ({\rm B-V})_{\rm observed} - ({\rm B-V})_{\rm intrinsic}\,. \tag{2.5}$$

Trumpler's measurements, and also laboratory measurements, show that for interstellar dust grains

$$E_{\rm B-V} \approx \frac{1}{3} A_{\rm V}\,r\,. \tag{2.6}$$

This is a crucial result. Reddening and hence $E_{\rm B-V}$, is easy to measure, and so if we do this for stars of known distance, we find[2] $A_{\rm V} \approx 1{\rm mag\,kpc^{-1}}$. If we now measure $E_{\rm B-V}$ for another star of *known* colour (from stellar evolutionary models say) we can estimate r.

[2]The amount of dust is not the same everywhere: there are regions where the absorption is much stronger, not surprisingly called dark clouds, and some directions along which the absorption is much less, a well known direction is called Baade's window.

2.4 Summary

After having studied this lecture, you should be able to

- Describe what are Open and Globular clusters
- Explain and apply the relation between star counts and the density of stars
- Explain what a standard candle is.
- Explain why Cepheids are good standard candles.
- Explain and apply parallax measurements
- Explain how parallax and Cepheids can be used to walk-up the distance ladder.
- Explain how Hubble's observations revolutionised our view of the MW and the realm of the Nebulae.
- Derive and apply the effect of scattering by dust on the apparent magnitude and colour of distant stars.

Chapter 3

The modern view of the Milky Way

CO §24.2

Our current picture of the Milky Way is based on a observations using a range of different techniques, often developed for military purposes (*e.g.* radar).

3.1 New technologies

3.1.1 Radio-astronomy

Radio-waves are EM-radiation with long wavelength λ and therefore are not susceptible to absorption by interstellar dust. Therefore they can probe the dense, dusty regions where stars are formed. Earth's atmosphere is nearly transparent for 1 cm $< \lambda <$ 10 m. Radio telescopes usually consist of a (large) single dish (for example at Jodrell bank; the Physics department has a small dish on its roof) or an *interferometer* with many inter-connected dishes, for example the *Giant Meter Radio-telescope* in India. Radio-observatories separated by 100-1000s of kilometers sometimes combine their signal to obtain very high angular resolution[1] Radio-waves are usually produced by one of:

[1]Recall that the angular diffraction limit depends on telescope diameter D and observed wavelength λ as $\theta \propto \lambda/D$. A radio-interferometer with $D = 10^3$ km and $\lambda = 1$ mm has $\theta \approx 10^{-9}$, whereas an optical telescope with $D \sim 10$ m and $\lambda \sim 5{\times}10^{-5}$ m has $\theta \approx 5{\times}10^{-8}$.

1. Roto-vibrational transitions in molecules
2. Thermal radiation from (cold) dust
3. Synchrotron radiation from electrons moving in a magnetic field
4. Hyperfine transitions, *e.g.* the 21-cm line in hydrogen (see Ch 4)

Roto-vibrational transitions correspond to the rotational or vibrational transitions in molecules. For example energy can be stored in the vibration of the C and O atoms in a CO molecule, whereby the distance between C and O varies. A quantum transition whereby the amount of vibration in the molecule decreases is associated with the emission of a photon. A diatomic molecule such as CO can also store energy in rotation along one of the two axes perpendicular to the C-O molecular bond. A decrease in the amount of rotation again results in the emission of a photon. The associated energies ΔE are in general much less than of *electronic transitions* hence the associated wavelengths $\lambda = hc/\Delta E$ are longer (IR or radio-waves, as opposed to optical or UV-radiation).

Thermal radiation Dust heated by nearby stars cools by radiating radio/infrared waves. If the temperature are low, the blackbody may peak in micro/mm wavelengths[2]

Synchrotron radiation Electrons moving in a magnetic field may emit radiation at radio-wavelengths depending on their speed (just as in a terrestrial synchrotron). Astronomical examples include supernovae remnants.

3.1.2 Infrared astronomy

IR photons are not significantly absorbed by dust. In fact, much of the visible and UV-light absorbed by dust grains, is re-emitted in the IR and sub mm, and so IR observations can look deep inside star forming regions. The DIRBE instrument on the COBE (Cosmic Background Explorer) satellite provided us with one of the best views of the the Milky Way, because it could see through the dust clouds that obscure large parts of the MW in the

[2]Recall Wien's displacement law, relating the peak emission wavelength λ and temperature T as $\lambda = b/T$, with $b = 3 \times 10^{-3}$ m K .

optical. Unfortunately earth's atmosphere absorbs most IR radiation, except in some narrow bands. IR observations therefore require balloon, rocket or satellites, or are limited to narrow regions of EM radiation in between the atmosphere's absorption bands.

3.1.3 Star counts

The Hipparcos satellite used diffraction limited observations above the atmosphere to obtain superbly accurate positions of stars on the night sky. By repeating measurements over several years, the satellite measured parallaxes of many 1000s of stars, and in addition proper motions for some stars (*i.e.* the velocity of some stars in the plane of the sky). Parallax distances are the crucial first step to the distance-ladder: parallax distances to Cepheids are required to calibrate the period-luminsity relation.

GAIA[3], the successor to HIPPARCOS, was launched in November 2013 and is currently being tested. It will measure positions of stars up to 15-th magnitude with a resolution of 10^{-5}arcsec. Gaia's expected scientific harvest is 'of almost inconceivable extent and implication' (according to their modest web page). In total, about 10^9 MW stars will be measured (as compared to 10^4 measured by Hipparcos). Gaia will be so accurate that it can even measure proper motions of some of the nearest globular clusters and galaxies. It will revolutionize the study of the MW.

3.2 The components of the Milky Way

The techniques above have shaped our view of the MW: it consist of three well-defined separate stellar systems: *disk*, *bulge* and *halo*. A summary of the properties of these is in Tables 3.1 and 3.2.

3.2.1 Disk

The disk is a round, thin distribution of stars. The Sun is part of the MWs disk.

- luminosity $L \sim 2 \times 10^{10} L_\odot$ in the B-band, ≈ 70 per cent of the MWs total B-band luminosity.

[3]http://astro.estec.esa.nl/GAIA/

- radius[4] $R \sim 15$kpc.
- Define the thickness t of the disk as the ratio $t \equiv \rho/\sigma$ of the volume density of stars, ρ, at the galactic plane, and the surface density σ. The thickness t depends on the type of star, and is ~ 200pc for young stars, ~ 700pc for stars like the Sun.

The disk also contains gas and dust (see lecture 4 on the interstellar medium). On top of the smooth disk are spiral arms, traced by young stars, molecular clouds, and ionised gas. The disk stars are in (nearly) circular motion around the centre, with speeds ~ 220km s^{-1}. The oldest disk White Dwarfs are $\sim 10 - 12 \times 10^9$ years old, but these could have formed *before* the disk.

The density distribution of stars in disk in cylindrical coordinates (R, ϕ, z) can be written as

$$n(R, \phi, z) \propto \exp\left(\frac{-R}{R_h}\right) \exp\left(\frac{-|z|}{z_h}\right), \tag{3.1}$$

i.e. independent of ϕ since it is cylindrically symmetric, and falling exponentially both in radius R and height z above the disk, with *scale-length* $R_h \approx 3.5$ kpc and *scale-height* $z_h \approx 0.3$ kpc.

Note that there isn't really an edge to the disk, either in radius or height. It can be traced to a distance of around 30kpc. With a height of 0.3kpc, this is a ratio 100:1, which is thinner than a compact disk!

The thick disk About 4 per cent of the MW's stars belong to a thicker disk, aligned with the (thin) disk, but with a larger scale height of $z_h \approx 1$kpc. Stars in this thick disk differ from the thin disk stars discussed above both in composition (having a lower metal content) and kinematically.

3.2.2 Bulge

The bulge is a spheroidal distribution of stars in the centre of the MW (and of most spirals).

- central spheroidal stellar system with radius of ~ 1kpc

[4]The distance from Sun to the galactic centre has recently been determined with remarkable accuracy to be $R_0 = 7.94 \pm 0.42$ kpc, from the observed motions of stars around the galactic centre (see lecture 11 for more details).

- luminosity ≈ 30 per cent of total MW luminosity
- luminosity profile is a de Vaucouleurs or '$r^{1/4}$' profile, defined as

$$I(r) = I_e \exp[-7.67(r/r_e)^{1/4} - 1]\,, \tag{3.2}$$

  with *effective radius* $r_e \approx 0.7$kpc.

The bulge stars are generally older and more metal poor than disk stars, suggesting the bulge formed before the disk, and before stellar evolution had managed to pollute the gas from which stars form with metals. In contrast to the disk, there is little or no star formation in the bulge.

The MW's bulge is elongated with axis ratio 5:3, with strong evidence for a bar. Whereas the disk stars are rotating in ordered fashion around the MW centre, the bulge has little net rotation, but the stars have large random velocities. All these properties: no star formation, large random stellar motions, spheroidal geometry, are reminiscent of the properties of an elliptical galaxy: it is as if there is a small elliptical galaxy at the centre of each spiral.

The bulge is bright but obscured in the visible due to dust: we need IR observations to make it visible.

3.2.3 Halo

A very small fraction (≤ 1 per cent) of the MWs stars are contained in a large, spheroidal, extremely tenuous stellar system called the halo, mostly (99%) made-up out of single 'field' stars with a sprinkling of Globular Clusters. The halo does not appear to rotate, and the halo stars have very low metallicities, typically 1/10 to 1/100 times the solar metallicity. When a halo star occasionally plunges through the disk, it is spotted because of its very high velocity, which is partly due to its intrinsic high random velocity, partly due to the fact the the Sun (and other disk stars) races with 220 km s^{-1} around the MW centre, but the halo star does not partake in this rotation. The halo contains ≈ 150 Globular Clusters (GCs), although there is some evidence that younger GCs may be associated with the disk.

The density of halo stars, and of GCs, falls spherically as

$$n(r) = n_0(\frac{r}{r_0})^{-3.5}\,, \tag{3.3}$$

and extremely distant field stars have been detected out to more than $\approx$ 50 kpc.

3.2.4 The dark matter halo

See lecture 5 for evidence that as much as 90 per cent of the mass in the MW is invisible, and consists of some unknown type of matter.

3.3 Metallicity of stars, and stellar populations (CO p.885)

Nuclear-synthesis during the first three minutes after the Big Bang produced mostly Hydrogen and Helium, and trace-amounts of other elements such as Li and B[5]. By mass, a fraction $X \approx 0.76$ was Hydrogen, with most of the remaining mass fraction $Y \approx 1-X \sim 0.24$ in Helium. All other elements were synthesised in stars and flung into space either due to winds (in AGB stars), during a Planetary Nebula phase, or during supernova explosions[6]. These elements are usually (but erroneously) referred to as 'metals' in astronomy, and their mass fraction denoted as $Z \equiv 1 - X - Y$.

A star formed out of gas already enriched in metals by (a) previous generation(s) of stars, will have a higher metal fraction Z than stars formed from more pristine gas. Since most of the stellar burning converts Hydrogen into Helium, such a star will have also tend to have $X < 0.76$ and hence $Y > 0.24$. For example the Sun has $X \sim 0.7$, $Y \sim 0.28$ leaving a total fraction of $Z = 1-X-Y \approx 0.02$ in 'metals'. The composition of a star therefore contains a wealth of information on the properties of earlier generations of stars. It is quite an awesome realisation that the metals in the Sun (and also in you and me) were produced by 1000s of stars and SNe that have long since perished.

Metallicity is often expressed relative to that of the Sun on a logarithmic scale, denoted (for example for Fe) as

$$[\mathrm{Fe/H}] \equiv \log_{10}\left[\frac{M_{\mathrm{Fe}}/M_{\mathrm{H}}}{(M_{\mathrm{Fe}}/M_{\mathrm{H}})_{\odot}}\right], \tag{3.4}$$

that is (the logarithm of) the ratio of Fe-to-H mass, divided by that ratio for the Sun. A star with [Fe/H]=0 has the same Fe abundance as the Sun,

[5] See L3 and L4 lectures.

[6] Elements heavier than ^{56}Fe are endothermic, meaning energy is required to synthesise them, as opposed to elements that release energy during synthesis, and are almost exclusively produced during SNe explosions.

Table 3.1: Disk parameters

	Neutral Gas	Thin Disk	Thick Disk
$M/10^{10}M_\odot$	0.5	6	0.2 to 0.4
$L_B/10^{10}L_\odot$		1.8	0.02
$M/L_{\rm B}$ $(M_\odot/L_\odot)$		3	
Diameter (kpc)	50	50	50
Distribution	$\exp(-z/0.16{\rm kpc})$	$\exp(-z/0.325{\rm kpc})$	$\exp(-z/1.4{\rm kpc})$
[Fe/H]	> 0.1	-0.5 – 0.3	-1.6 – -0.4
Age (Gyr)	0 – 17	< 12	14 – 17

a star with [Fe/H]=-1 is ten times more Fe poor, a star with [Fe/H]=1 ten times more Fe rich.

Disk stars have $-0.5 \leq$ [Fe/H] $\leq +0.3$, with a clear trend of increasing [Fe/H] toward the centre of the disk, hence the MWs material has been processed more vigourously in its interior than towards its outskirts. The disk population of relatively metal rich stars, still undergoing star formation is called *population I* stars. The true nature of the thick disk stars is not completely clear, but thick disk stars tend to be more metal poor, [Fe/H]≈ -0.6

Bulge stars have a wide range of $-3 \leq$ [Fe/H] ≤ 0.3, with no significant ongoing star formation. This population of relatively metal rich stars without star formation is called *population II*[7].

Halo stars have much lower abundances $-3 <$ [Fe/H]< -1. A population with such extremely low abundance, composed of old stars, is called *extreme population II*.

3.3.1 Galactic Coordinates (CO §24.3)

The position of an object on the sky as seen from the Sun can be characterised by two angles (see Fig. 3.1) : (1) *galactic latitude*: the angle b above the Milky Way plane and (2) *galactic longitude*: the angle l between the direction Sun-Galactic centre, and the projection Sun-star onto the Milky Way disk.

[7]The stellar population of elliptical galaxies is similar

Table 3.2: Spheroid parameters

	Central Bulge	Stellar Halo	Dark Matter Halo
$M/10^{10}M_{\odot}$	1	0.1	55
$L_B/10^{10}L_{\odot}$	0.3	0.1	0
M/L_{B} $(M_{\odot}/L_{\odot})$	3	~ 1	-
Diameter (kpc)	2	100	> 200
Distribution	bar	$r^{-3.5}$	$(a^2 + r^2)^{-1}$
[Fe/H]	-3 – 0.3	-4.5 – -0.5	
Age (Gyr)	10 – 17	14 – 17	17

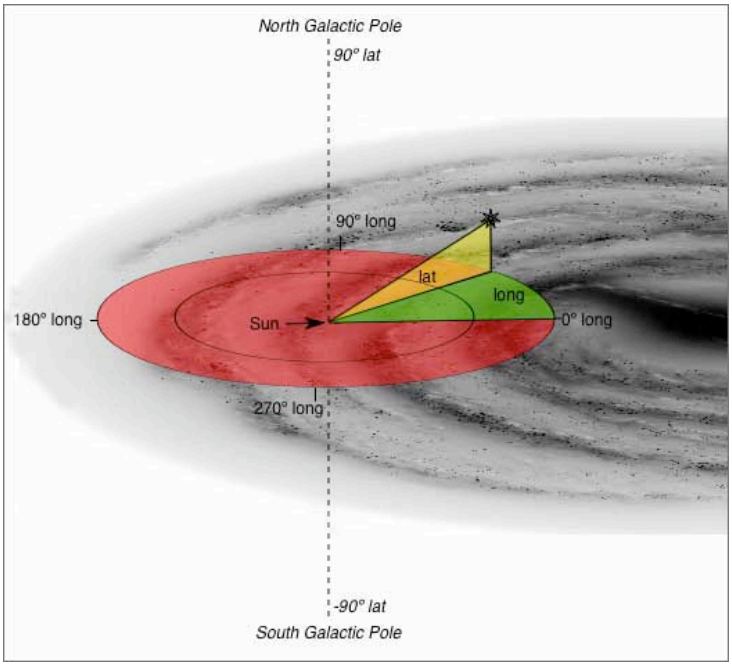

Figure 3.1: Diagram illustrating galactic longitude l and galactic latitude b. From *thinkastronomy.com*.

3.4 Summary

After having studied this lecture, you should be able to

- Explain which processes generate observable radio and IR radiation, and why this radiation was important to clarify the MW structure.
- Explain how the Hipparcos satellite was a major step in setting the scale of the MW, by performing accurate parallax and proper motions measurements, and fixing a reference frame with respect to distant objects.
- Describe the three main stellar components of the MW, and give two characteristic properties of each
- Explain what is meant by the metallicity of a star, and how it is expressed
- Explain how the Galactic Coordinate system (l, b) is defined

Chapter 4

The Interstellar Medium

CO §12

The interstellar medium (ISM) is the *stuff* between the stars. It is a rich but complex physical system, with gas collecting in large molecular clouds (*Giant Molecular Clouds*), which form stars that then destroy the clouds, polluting the gas with metals. Stellar winds and super nova explosions stir the gas, and may even expell some gas from the MW into the surrounding intergalactic medium. Dust, magnetic fields and cosmic rays[1] play an important but poorly understood rôle. The L4 course on the ISM treats some of the issues in more detail. This chapter concentrates on the composition of the ISM, how the different components can be observed, how stars and gas interact, and the important concept of Jeans mass, relevant for how stars form in clouds.

4.1 Interstellar dust (CO §12.1)

Interstellar dust is composed of metals (*e.g.* Si), affects the chemistry of the ISM, and also the propagation of light. Dust particles interact with light both through *scattering* and *absorption*. Sunlight passing through the

[1] Cosmic rays are energetic particles (photons, protons, nuclei of heavier elements), with energies up to orders of magnitude higher than what can presently be achieved in labs such as SLAC or Cern. With Profs Rochester and Wolfendale, Durham has a rich history in cosmic ray physics, and continues to do so with its involvement in the HESS telescope in Namibia.

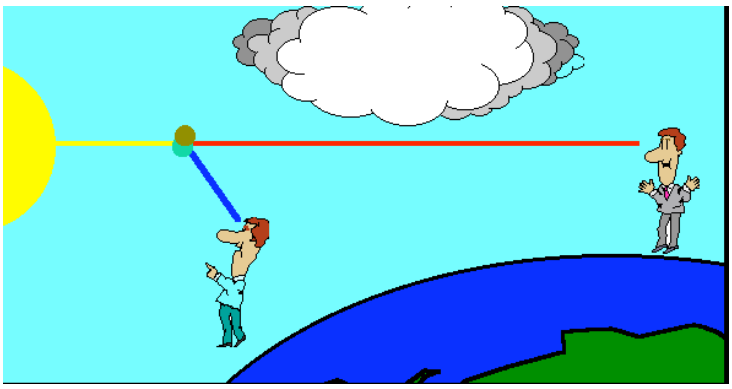

Figure 4.1: Scattering of Sunlight in the Earth's atmosphere, from The Physics and Relativity FAQ.

Earth's atmosphere scatters off molecules (mostly N and O molecules), with blue light scattered more strongly than red light. Away from the Sun, we see the scattered Sun light on the sky, which is hence much bluer than the Sun itself: this is why the sky is blue. Conversely, looking at the Sun itself, we see a larger fraction of red light: the Sun reddens at sunset or sunrise. Sunlight can also scatter on dust (for example following a volcanic eruption or a desert storm): this makes the sun appear even redder at sunset/rise. Figure 4.1 illustrates this phenomena:

The scattered light is also *polarised*. Sun glasses are sometimes polarised to block sunlight scattered from the Ocean, or from road surfaces. Light may also be absorbed by clouds our dust, darkening the day. The same process of scattering and absorption occur in the ISM: distant stars appear redder, the light detected from reflection nebulae is blue and polarized, all due to the effects of dust grains.

Scattering: changes the direction of the incoming photon, but not its energy. EM radiation with wavelength much longer than the size of a grain scatters must less efficiently, hence red light, and in particular IR and radio-waves, is hardly affected by dust.

Absorption: a photon interacting with a dust grain may break a molecular bond, or simply heat the dust grain. This destroys the photon, which is lost to the observer. The grain may cool by emitting EM radiation, with black-

body spectrum corresponding to its temperature: the typical energies of this cooling radiation is much less than those of the incoming photon. The net effect is that the dust grain has converted short wavelength (blue) photons to long wavelength (red or IR) ones. Dust in the surroundings of star forming regions for example reprocesses the blue light emitted by the hot stars into IR radiation. This obscures the star forming region in the visible, but makes it glow in the IR.

Although in general the amount of scattering/absorption increases with decreasing wavelength λ, some λs correspond to resonance transitions in the molecules or dust grains, allowing determination of their composition[2].

4.2 Interstellar gas (CO §12.1)

Gas in the ISM can be in molecular, neutral, or ionised form. What determines which phase the gas is in? How are the different phases observed? The processes discussed below are illustrated in Fig. 4.2.

Notation Astronomers use the (confusing) notation XIII to denote the *doubly* ionised state of element X, for example CIII≡C^{2+}, HI is neutral Hydrogen, HII ionised Hydrogen, and OVI is five-times ionised O.

4.2.1 Collisional processes

Kinetic theory of gases The typical velocity v of particles with mass m in a gas with temperature T is $v^2 \sim kT/m$. A collision between such particles will have typical kinetic energy $E \sim mv^2 \sim kT$, and will be elastic (energy conserving) when E is much less than any excitation energies of the particle. Rotational and vibrational excitation energies are small, and so even at relatively low temperatures $T \sim 100$ K, the kinetic and roto-vibrational energy levels are in equipartition ('thermal equilibrium'). Because of such 'internal degrees of freedom' a diatomic gas (*e.g.* H_2) does not behave the same as a

[2] A typical example is the detection of the Si-O resonance in dust grains, showing they contain both Si and O.

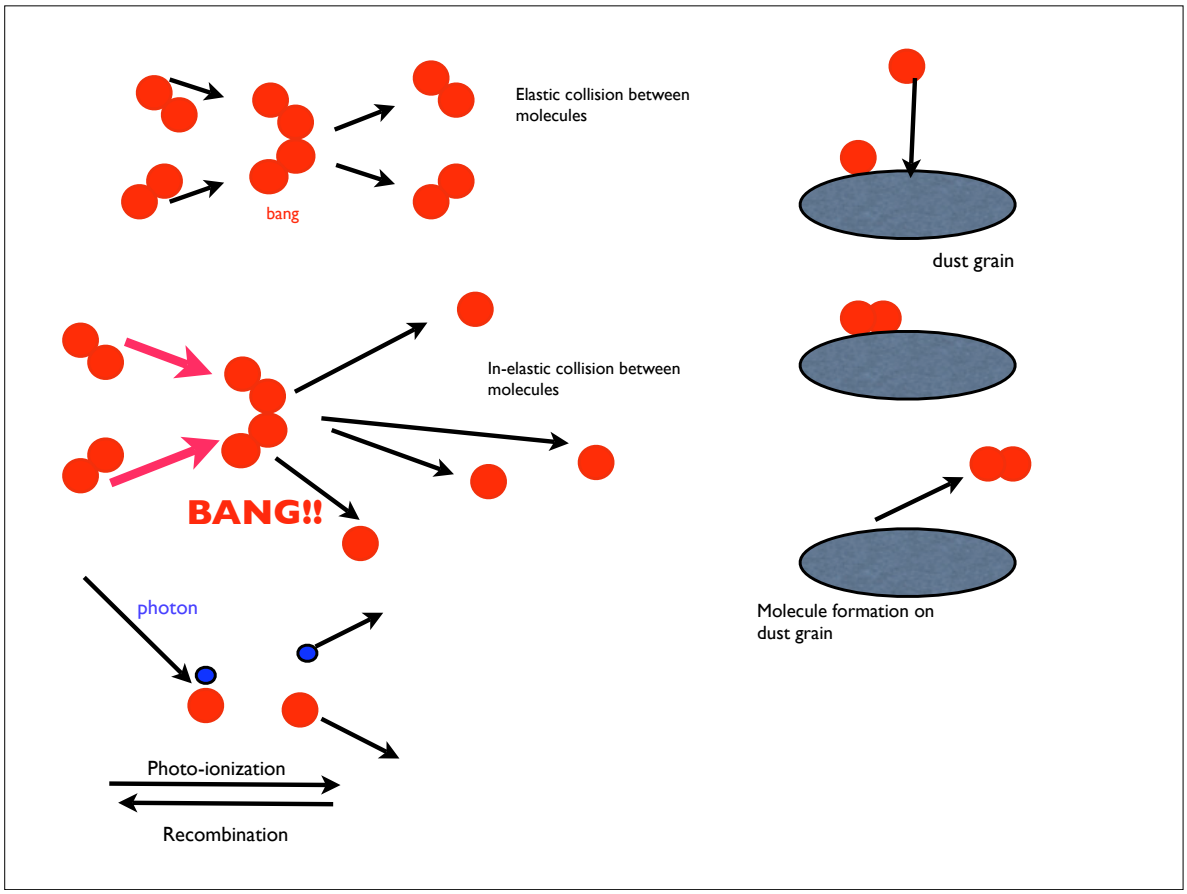

Figure 4.2: Important physical processes in the ISM.

mono-atomic gas (*e.g.* HI)[3].

At higher T, the kinetic energy may be high enough for collisions to break the molecular bond in the particles: collisions are no longer elastic, but destroy molecular bonds. The molecular binding energy in H_2 is ~ 11eV[4], so gas at temperatures of $T \geq 10^3$K will cease to be molecular. At even higher T, E is enough to ionise the atoms. For example the binding energy of the Hydrogen atom is 13.6eV, hence for $T \sim 10^4$K, Hydrogen will tend to be ionised. This suggests that **increasing T leads to initially molecular gas to become first neutral, then ionised.**

How about the reverse processes? Ionised gas can become neutral through recombinations. This process produces a photon which could escape from the gas, taking energy with it. This energy loss means the gas is cooling: it is called *radiative cooling*. Neutral gas can become molecular through gas-phase reactions, but in the ISM mostly because of reactions on dust grains.

The ISM has regions where the gas is cold, warm , and hot . Because we expect the *pressure* in these regions to be similar (since otherwise gas would flow from high to low pressure regions, equilibrating the pressure), the cold regions tend to be dense and molecular (called molecular clouds), the warm regions tend to be neutral, whereas the hot regions are at low density and contain ionised gas.

4.2.2 Photo-ionisation and HII regions (CO p.431)

When a photon impinging on an atom has enough energy, it may ionise the atom in a process called *photo-ionisation*. The ionisation energy for HI is 13.6eV, and the corresponding wavelength of the photon is in the UV. The ionised Hydrogen nucleus may catch a free electron and recombine: it is the inverse process. On its way to the $n = 1$ ground-state, the electron will pass through one or more allowed electronic energy levels, emitting photons with characteristic energies 13.6eV $(1/n_1^2 - 1/n_2^2)$ for a transition $n_2 \rightarrow n_1$. The series of emission lines which end in the ground state ($n_1 = 1$) are called the

[3]Recall that a diatomic gas has adiabatic exponent $\gamma = 7/5$ in contrast to the ideal (mono-atomic gas) case $\gamma = 5/3$.

[4]An energy of 1eV corresponds to a temperature T=1eV/$k_B \approx 10^4$K.

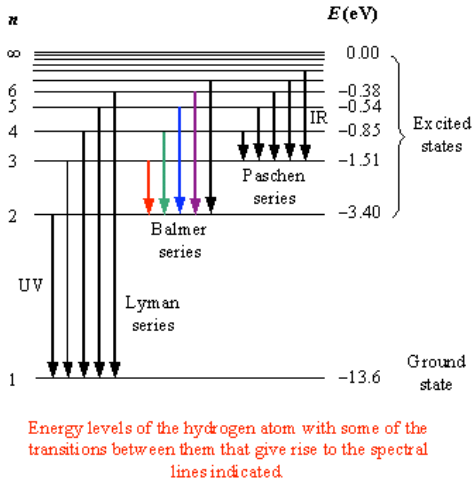

Figure 4.3: Electronic transitions in the Hydrogen atom, and nomenclature of the corresponding emission lines. Figure taken from the internet encyclopedia.

Lyman-series, with Lyman-α corresponding to $n_2 = 2$, Lyman-β to $n_2 = 3$, *etc.* Transitions with $n_1 = 2$ are called the Balmer series, with Balmer-α or Hα corresponding to $n_2 = 3$, Hβ to $n_2 = 4$, *etc.* Fig 4.3 illustrates these transitions.

Only massive stars are hot enough to produce Hydrogen ionising photons in abundance. Since massive stars have such short lifetimes, they are almost exclusively found in the star forming region where they were born. As the hot stars ionise the gas, most of Hydrogen gas is ionised and the region is therefore called an **HII region**. Recombinations make HII regions emit the very characteristic pattern of recombination lines discussed above. It is the Hα emission lines which is used to trace HII regions in spiral galaxies[5]. Such HII regions follow spiral arms as beads on a string: this is because the spiral structure sweeps gas into dense clouds, which can then form stars, which subsequently ionise the gas making it radiate in recombination lines and be observable. All this stellar feedback destroys the cloud, the massive stars die, and so there are no HII regions nor massive stars, in between spiral arms. The Rosetta Nebula and Orion are well known HII regions in the Milky Way.

[5]Other lines are too far into the UV to be easily observable from the ground

4.2.3 Strömgren spheres

Suppose a hot star starts at time $t = 0$ to emit ionising photons at a rate $\dot{N}$ into a gas cloud, which initially contains neutral Hydrogen gas with uniform density n. The radius R of the sphere within which the gas is ionised will increase in time. We can find $R(t)$ by requiring that the number of photons emitted by the source in time t, $\dot{N}\,t$, equals the number N of (initially) neutral Hydrogen atoms within $R(t)$, $N = (4\pi/3)\,n\,R^3(t)$, hence

$$\dot{N}\,t = \frac{4\pi}{3}\,n\,R^3(t)\,. \tag{4.1}$$

This simply expresses the fact that the source needs to emit one ionising photon per neutral atom. Take the time derivative to obtain the speed of the *ionisation front*,

$$\frac{dR(t)}{dt} = \frac{\dot{N}}{4\pi n R^2(t)}\,. \tag{4.2}$$

Initially when R is small the speed of the front is high, then decreases $\propto 1/R^2$. Equation (4.2) predicts the speed becomes arbitrarily large for small R, but this cannot be right: it must be limited by the speed of light, so our treatment cannot be applied at very early times

As the ionisation front runs into the cloud, some of the Hydrogen ions behind the front will start to recombine. Each neutral atom within the HII region will absorb an ionising photon, which then can no longer ionise a neutral atom outside of the HII region: recombinations will slow the ionisation front. Eventually, there may be so many recombinations occuring within the HII region that the speed of the front decrease to zero: the front has reached its **Strömgren radius** R_s. The rate $(dn_{\rm HII}/dt)_{\rm rec}$ at which Hydrogen ions recombine, is given by

$$\frac{{\rm d}n_{\rm HII}}{{\rm d}t}|_{\rm rec} = -\alpha n_e n_{\rm HII}\,. \tag{4.3}$$

Figure 4.2 illustrates the recombination of a Hydrogen ion with an electron. Since both a proton and an electron should be present for a recombination, the recombination rate is proportional to the product of the densities

$n_e n_{\rm HII}$ of electrons and protons, respectively. The proportionality constant is denoted α[6]

When Hydrogen gas is highly ionised, $n_e = n_{\rm HII} \approx n$, and the Strömgren radius R_s is found by equating the rate of recombinations in a sphere of radius R, $\dot{N}_r \equiv |dn_{\rm HII}/dt_{|rmrec} \times (4\pi/3)\, R^3$, with the rate at which the source produces ionising photons, $\dot{N}$:

$$\begin{aligned} \dot{N} &= |\frac{dn_{\rm HII}}{dt}|_{\rm rec} \frac{4\pi}{3} R_s^3 \\ R_s &= (\frac{\dot{N}}{(4\pi/3)\,\alpha\, n^2})^{1/3}\,. \end{aligned} \tag{4.4}$$

Using typical values $n_{\rm H} = 5 \times 10^3 {\rm cm}^{-3}$ for the density of a cloud, $\dot{N} = 10^{49} {\rm s}^{-1}$ for the ionisation rate of a massive star, and using $\alpha \approx 3.1 \times 10^{-13}$ cm^3 s^{-1} (valid for temperatures $\sim 10^4$ K in HII regions) gives a Strömgren radius $R_S \approx 0.21$pc.

4.2.4 21-cm radiation (CO p. 405)

The Lyman and Balmer series discussed earlier corresponded to transitions of the electron between different *orbital* energy levels, but there are other possible transitions for an electron in an atom, which result from its **spin**. Spin is a purely quantum mechanical degree of freedom, with some similarities to angular momentum[7]. A spinning electric charge generates a dipole moment, and spin is also associated with a magnetic dipole. However, the electron's magnetic dipole $\mathbf{S}$ is *quantised*: along any axis, the dipole is either up or down: $\mathbf{S} = \pm 1/2$. The electron has a series of energy levels resulting from the interaction of this dipole moment with its orbital angular momentum, $\mathbf{L}$, and with the proton spin, $\mathbf{S_p}$. This is similar to the interaction between two bar magnets: when they are aligned, they will repel each other, since like-poles repel. When they are anti-alingned, they will attract each other.

fine-structure lines result from coupling between $\mathbf{S}$ and $\mathbf{L}$: for given $\mathbf{L}$, the electron's energy is slightly higher when $\mathbf{S}$ and $\mathbf{L}$ are parallel, than when

[6]Determine the units of α as an exercise.

[7]See later lectures on quantum mechanics

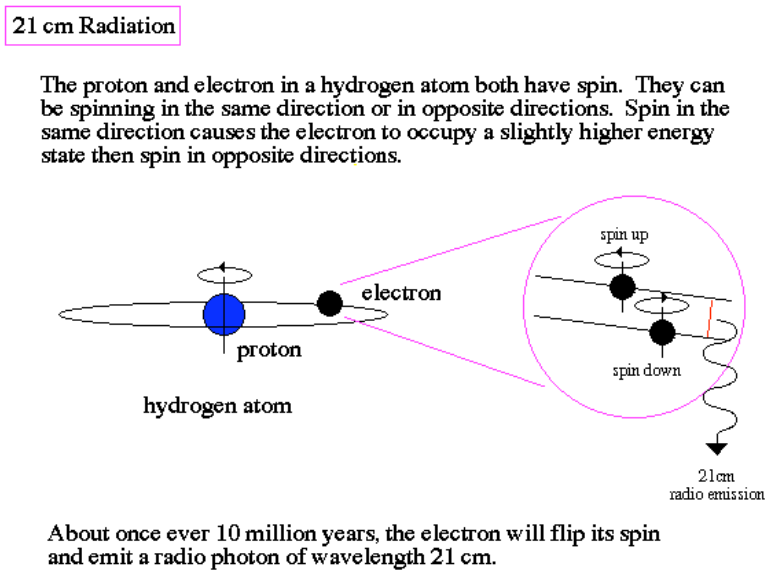

Figure 4.4: Emission of 21-cm radiation in Hydrogen due to a hyperfine transition, taken from Schombert.

they are anti-parallel.

hyperfine structure lines result from coupling between the electron spin $\mathbf{S}$ and the *proton* spin $\mathbf{S_p}$: the energy of the electron is higher for $\mathbf{S}$ and $\mathbf{S_p}$ parallel than when they are anti-parallel, see Fig.4.4.

The wavelength of the hyperfine transition in the Hydrogen atom is $\lambda \approx 21.1$ cm and it is therefore called the **Hydrogen 21-cm line**. The transition probability is very low, which is why it is very hard to observe it in the laboratory, because collisions between the particles will de-excite the aligned spin well before there has been a spontaneous transition. But in the ISM, densities are far lower than can be generated in the lab, and **this line is of great observational importance** because it can be used to detect neutral gas. The long wavelength also means it is not affected by dust[8].

[8]The radio-dish on top of the physics department can detect 21-cm radiation from neutral gas in the MW

An external magnetic field shifts the energy levels of the electron in a Hydrogen atom, the 'Zeeman effect', and the 21-cm radiation can be used to estimate the strength of the magnetic field in the ISM.

4.2.5 Other radio-wavelengths

The 21-cm line cannot be used to study gas in dense clouds, because the gas will tend to be molecular instead of atomic. But radio-telescopes can be used to detect roto-vibrational transitions of these molecules, enabling the study of molecular clouds.

The MW contains molecular clouds with a wide range in masses, up to *Giant Molecular Clouds*, (GMCs) with masses up to $10^7 M_\odot$. These enormous complexes of gas and dust are almost exclusively found in spiral arms, and are the sites of star formation in the MW: most, if not all, stars are thought to form in GMCs.

4.2.6 The Jeans mass (CO p. 412)

The masses of GMCs, $\sim 10^6 M_\odot$, are very much higher than those of the stars that form in them: why?

The **Jeans** mass M_J in a gas with uniform density, ρ, and temperature, T, is the characteristic mass for which the thermal energy, K, and gravitational energy, U, in a sphere are in virial equilibrium, $2K = U$. When $M > M_J$, gravity dominates, and the sphere will tend to collapse; when $M < M_J$, pressure dominates, and the sphere is stable to collapse.

The thermal energy K in a sphere with mass M is

$$\begin{aligned} K &= Mu \\ u &= \frac{3\mathrm{k_B}T}{2\,\mu\mathrm{m_H}}\,, \end{aligned} \tag{4.5}$$

where $\mathrm{k_B}$ Boltzmann's constant, and $\mu\mathrm{m_H}$ the mean molecular weight per particle. The gravitational potential energy U of the sphere is

$$
\begin{aligned}
U &= \frac{3}{5}\frac{GM^2}{R} \\
M &= \frac{4\pi}{3}\rho R^3 \,.
\end{aligned}
\tag{4.6}
$$

In virial equilibrium, $2K = U$, and the mass of the sphere is the Jeans mass[9]:

$$
M_J = \left(\frac{5\mathrm{k_B}T}{\mu \mathrm{m_H} G}\right)^{3/2} \left(\frac{3}{4\pi\rho}\right)^{1/2} \,. \tag{4.7}
$$

Fragmentation Consider the fate of a cloud with mass $M = M_J$ that starts to collapse. In general, both T and ρ will change, and hence M_J will change as well. If the gas behaves *adiabatically*, $\rho \propto T^{3/2}$, and hence $M_J \propto \rho^{1/2}$. Hence M_J *increases* at the cloud starts to collapse, pressure will increase faster than gravity, and the cloud will bounce back. However if the gas is *isothermally*, T =constant, then $M_J \propto 1/\rho^{1/2}$, and the Jeans mass will *decrease*. Now smaller spheres will have $M = M_J$ and hence the cloud may fragment.

[9]You may find expressions which differ by factors of order unity in other texts

4.3 Summary

After having studied this lecture, you should be able to

- Describe how we know the properties of interstellar dust from scattering and absorption of star light.
- Explain why we find different ionisation states of interstellar gas, depending on density, temperature, and ionising background.
- Compute the speed of an ionisation front.
- Derive the Strömgren radius for an HII region, and explain the concept.
- Explain the origin of the hydrogen 21-cm line, and explain its importance in understanding the structure of the MW.
- Explain the concept of Jeans mass, and its relation to fragmentation of clouds.

Chapter 5

Dynamics of galactic disks

CO §24.3

The stars in the Milky Way disk are on (almost) circular orbits, with gravity balancing centripetal acceleration. Given that most of the light of the disk comes from its central parts, we would expect the circular velocity in the outer parts of the disk to fall with distance as appropriate for Keplerian motion. We should also be able to compute how velocities of stars in the solar neighbourhood depend on direction. Observations do not follow these expectations at all, which leads to the startling conclusion that most of the mass in the Milky Way is invisible.

5.1 Differential rotation (CO p. 917)

5.1.1 Keplerian rotation

The velocity of a test mass m in circular motion around a mass M at distance R is

$$\frac{V_c^2}{R} = \frac{GM(< R)}{R^2}\,, \tag{5.1}$$

independent of m along as $m << M$. Mass M need not be a point mass: Newton's theorem guarantees this equation is also correct for an extended spherical mass distribution, as long as M is the mass enclosed[1] by the orbit

[1]We'll use the notation $M(< R)$ for the mass enclosed in a sphere of radius R.

R: mass outside R does not contribute to the gravitational force. This equation describes for example the motion of planets in the solar system, with M the mass of the Sun.

This equation also describes the circular motion of stars around the MW's centre: Newton's theorem also applies for motion in a disk[2] In the outskirts of the disk, for example at the position[3] $R_\odot$ of the Sun, we observe that most of MW's light is at $R \leq R_\odot$. This suggests that also most of the mass is within $R_\odot$, hence $M(< R) \approx M_{\rm MW}$, the total mass of the MW. For $M(< R) = M_{\rm MW}$ constant, Eq. (5.1) gives $V_c \propto R^{-1/2}$. The function $V_c(R)$ (circular velocity as function of radius) is called the **rotation curve**, and we expect the disk to be in *differential rotation*, with rotation curve $V_c \propto R^{-1/2}$. We can test this assertion by studying the motion of stars in the solar neighbourhood.

5.1.2 Oort's constants (CO p. 908-913)

Assume all disk stars are on circular orbits, with circular velocity $V_c(R)$ for a star at distance R from the MW centre. The observer (at radius R_0) is moving with circular velocity $V_{c,0} \equiv V_c(R = R_0)$ measures the following radial, V_r and tangential, V_t of a star at distance d and radius R, which has galactic coordinates $(b = 0, l)$ (see Fig.5.1)

$$\begin{aligned} V_r &= V_c \cos(\alpha) - V_{c,0} \sin(l) \\ V_t &= V_c \sin(\alpha) - V_{c,0} \cos(l)\,. \end{aligned} \tag{5.2}$$

In the indicated right-angled triangle

$$\begin{aligned} d + R\sin(\alpha) &= R_0 \cos(l) \\ R\cos(\alpha) &= R_0 \sin(l) \\ R_0 &= d\cos(l) + R\cos(\beta) \approx d\cos(l) + R \text{when } d \ll R_0\,, \end{aligned} \tag{5.3}$$

where β is the angle Sun-MW Centre-Star. Combining these equations gives

[2]Demonstrate this as an exercise.

[3]$R_\odot \sim 8$kpc denote here the distance of the Sun to the centre of the MW.

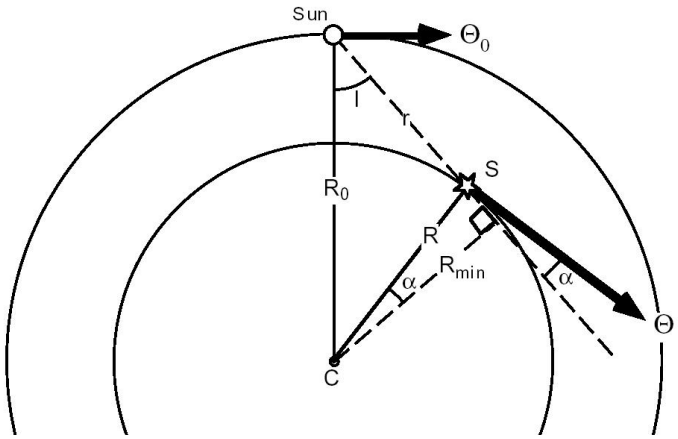

Figure 5.1: (Taken from http://www.csupomona.edu/˜jis/1999/kong.pdf) The observer is moving on a circular orbit with velocity Θ_0 and radius R_0, and observes a star at distance r, and galactic longitude l, on circular orbit with velocity Θ and radius R. In the text, r is denoted as d and the circular velocities are V_c and $V_{c,0}$ for the star and the Sun, respectively.

$$
\begin{aligned}
V_r &= (\Omega - \Omega_0) R_0 \sin(l) \\
V_t &= (\Omega - \Omega_0) R_0 \cos(l) - \Omega\, d\,, \qquad (5.4)
\end{aligned}
$$

where $\Omega_0 \equiv V_{c,0}/R_0$ is the *angular velocity* of the observer, and $\Omega \equiv V_c/R$ the angular velocity of the star. For *nearby stars*, $R \approx R_0$ and $\Omega(R) \approx \Omega_0 + (d\Omega/dR)(R - R_0)$. If we now define **Oort's constants** A and B as

$$
\begin{aligned}
A &\equiv -\frac{1}{2}\left[\frac{dV_c}{dR}|_{R_0} - \frac{V_{c,0}}{R_0}\right] \approx 14.4 \pm 1.2 \mathrm{km\,s^{-1}\,kpc^{-1}} \\
B &\equiv -\frac{1}{2}\left[\frac{dV_c}{dR}|_{R_0} + \frac{V_{c,0}}{R_0}\right] \approx -12.0 \pm 2.8 \mathrm{km\,s^{-1}\,kpc^{-1}}\,. \qquad (5.5)
\end{aligned}
$$

then

$$
\begin{aligned}
V_r &= A\, d\, \sin(2l) \\
V_t &= A\, d\, \cos(2l) + B d\,. \qquad (5.6)
\end{aligned}
$$

For example a star toward the galactic centre (or anti-centre; $l = 0$ and $l = 180^o$ respectively), has $V_r = 0$ and $V_t = (A + B)d$.

Jan Oort[4] measured (V_r, V_t) for stars as function of l and d, and inferred $A \approx 14.4 \pm 1.2 \mathrm{km\,s^{-1}\,kpc^{-1}}$ and $B = -12.0 \pm 2.8 \mathrm{km\,s^{-1}\,kpc^{-1}}$.

Using the results from section 5.1.1 we find that for a Keplerian disk, $V_c \equiv V_{c,0}(R_0/R)^{1/2}$, hence $dV_c/dR = -(1/2)V_c/R$. At the position of the Sun, $V_{c,0} \approx 220 \mathrm{km\ s^{-1}}$, with $R_0 \approx 8$kpc, hence we expect the values of Oort's constants to be

$$
\begin{aligned}
A_{\mathrm{Kepler}} &= \frac{3}{4}\frac{V_{c,0}}{R_0} = 19.4 \mathrm{km\ s^{-1}\,kpc^{-1}} \\
B_{\mathrm{Kepler}} &= -\frac{1}{4}\frac{V_{c,0}}{R_0} = -6.5 \mathrm{km\ s^{-1}\,kpc^{-1}}\,. \qquad (5.7)
\end{aligned}
$$

Our expected values are inconsistent with Oort's measured values. Assuming we measured V_c/R correctly, the measured and expected values for dV_c/dR are:

[4]Note that these are values appropriate for the Sun.

$$\begin{aligned}\frac{dV_c}{dR}|_{\rm measured} &= -(A+B) = -2.4 \pm 3.0 {\rm km\ s^{-1}\,kpc^{-1}} \\ \frac{dV_c}{dR}|_{\rm Keplerian} &= -\frac{1}{2}\frac{V_c}{R} = -13.0 {\rm km\ s^{-1}\,kpc^{-1}}\,. \end{aligned} \tag{5.8}$$

As expected, the Keplerian circular velocity drops $\propto 1/R^{1/2}$, hence $\frac{dV_c}{dR}| < 0$, but the *measured* value is consistent with zero: **the Mily Way's rotation curve is flat, *i.e.* $V_c(R) \approx$ constant**.

Of course in a real galaxy stars are not *exactly* on circular orbits, and each star has a small *peculiar* velocity with respect to the perfect circular motion $V_c(R)$. A standard of rest that moves on an exact circular orbit is called the 'local standard of rest' [5]: the speed of the Sun is ~ 16 km s^{-1} with respect to its local standard of rest.

Oort also discovered a small number of stars with very large deviations from the expectation given by Eqs. (5.6), which he called *high velocity stars*. He correctly identified these with stars belonging to the halo: the high velocity is because the halo does not rotate, whereas the disk, and the Sun with it, rotates with a speed ~ 220 km s^{-1}.

5.1.3 Rotation curves measured from HI 21-cm emission

The HI 21-cm emission line can be used to measure the velocity of the HI from its Doppler shift. This can be used to determine the rotation curve of the HI gas[6], if it were possible to determine R. Eqs. (5.2) show that V_r has a *maximum*

$$V_{r,\rm max} = V_c - V_{c,0}\sin(l)\,, \tag{5.9}$$

for any l with $|l| < \pi/2$, which occurs for $\alpha = 0$, at which point $d = R_0\cos(l)$. Therefore

$$\frac{dV_{r,\rm max}(l)}{dl} = \frac{dV_c(R)}{dR}\,\frac{dR}{dl} - V_{c,0}\,\cos(l) \tag{5.10}$$

[5] Note this is not an inertial system

[6] You can attempt this in L4, using the radio dish on the physics building

hence

$$\frac{dV_c(R)}{dR} = \frac{dV_{r,\max}(l)}{dl} \, /R_0 \, \cos(l) + V_{c,0}/R_0 \, . \tag{5.11}$$

The 21-cm analysis confirmed Oort's measurements: the MW's rotation curve near the Sun is essentially flat.

It is much easier though to measure rotation curves in other spiral galaxies, by simply measuring the Doppler shift as function of distance to the centre. Such measurements are now available for tens of spirals, and they all show flat rotation curves in their outskirts. The MW is definitely not unusual in this respect.

5.2 Rotation curves and dark matter (CO p. 914)

A flat rotation curve, instead of a $1/R^{1/2}$ falling rotation curve, implies the mass is not all concentrated within the solar circle, but is more extended. To find the shape of the density distribution that gives rise to a flat rotation curve, take the derivative[7] with respect to R of

$$V_c^2 \, R = GM \, , \tag{5.12}$$

for V_c is constant:

$$\begin{aligned} V_c^2 &= G\frac{dM}{dR} \\ \rho(R) &= \frac{V_c^2}{4\pi G R^2} \, . \end{aligned} \tag{5.13}$$

Hence a spherical distribution of mass, with $\rho(R) \propto 1/R^2$, gives rise to a flat rotation curve. But the observed light distribution in the MW is very different from this. This suggests three equally astonishing alternatives,

1. The mass-to-light ratio of stars in spirals conspires such that, although the light is very much centrally concentrated, the mass in stars is not. But stellar populations do not seem to vary significantly between the centre and the outskirts. However there may be unseen gas for example in the outskirts of the Milky Way providing the required $\rho(R) \propto 1/R^2$ density.

[7] Show that $dM/dR = 4\pi\rho(R)\, R^2$ in a spherically symmetric density distribution.

2. The Milky Way contains invisible matter, which does not emit, nor absorb light.

3. Gravity does not behave as $1/R^2$ on galactic scales. If this were true, then our reasoning above is simply not valid. The theory of **Mo**dified **N**ewtonian **D**ynamics (MOND) is able to provide very good fits to measured rotation curves with a small modification of gravity that cannot be probed in other regimes.

The currently favoured option is (2), namely that the MW, and other galaxies, contains invisible dark matter. More evidence for this later, including the fact that this matter cannot be baryonic[8] in nature.

5.3 Spiral arms (CO §25.3)

Before leaving the subject of spiral galaxies, we should address what is in fact probably the first question you'd like to know about them: *why* do they have spiral arms? So let's start by reviewing what we know about spiral arms.

Firstly, spiral arms are really evident when we look at massive stars and HII regions – these really delineate the spiral structure. But there is more: we also detect the arms in HI, and even better in molecular gas. In fact, GMCs are probably the best tracers of the pattern. So may be they have something to do with star formation?

However, they are also present in the K band where we are probing *old* stars. So first conclusion: it's really the whole galaxy that takes part in the spiral pattern. The *density contrast*[9] is not very large, probably less than a factor of two. The contrast in *surface brightness* can be quite a bit higher though, since the young stars in the arms are massive and hence bright.

The winding problem Given that the disk is in differential rotation, a spiral arm cannot be a material structure (meaning that it is always the same stuff in the arm going round and round) – because if it were, we would have a

[8]Baryons are subatomic particles made out of three quarks, such as protons and neutrons. The dark matter has to be composed of something else, hence cannot be in the form of faint stars, planets, rocks, or past exam papers.

[9]the relative difference in density at given r from the centre, within vs outside of the arm

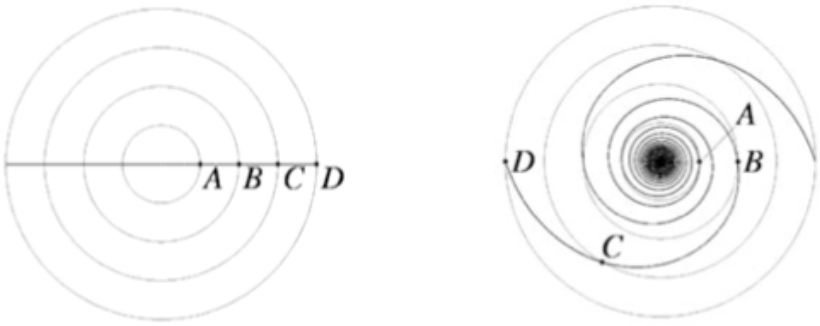

Figure 5.2: A spiral pattern made out of stars will rapidly wind-up in a disk undergoing differential rotation.

winding problem. To realise why this is so, consider the following thought experiment.

Suppose you paint all stars along a radius in the disk green, and follow how those green stars move (see figure (5.2). If the circular velocity is a constant, V_c, then the period of an orbit is proportional to its radius, $P \propto R$. Now concentrate on two green stars, one at distance R (star 1), the other at distance $2R$ (star 2), having periods $P_1 = P$ and $P_2 = 2\,P$. After a time P, star 1 will be at the original position, whereas star 2 will be at the other side of the galaxy. After time $2P$, both stars will be back at their original position, and so the green line of stars in between them will have circled the galaxy, i.e. *the initially straight line of green stars now encircles the galaxy*. Applying this to stars originally in a spiral arm, it is clear now that very quickly, the spiral arm will wind tighter and tighter. Considering how loosely wound some spiral arms are, this would imply they are all very recently formed, placing us at a peculiar instant in time where spiral structure forms.

In cases where we were are able to determine the sense of rotation of the pattern, it turned out that the spiral arms are *trailing*, that is, at least they are rotating in the same sense as the spiral pattern of our green stars.

So what's the solution? May be it's good to realise that there is quite a variety in spiral patterns. Grand Design spirals have two really well defined relatively open arms. Some spirals have *flocculent* arms, which are not very long (i.e. you can't trace them for very long), but often there are many in

the disk. So may be we're looking at more than one possible origin.

The theory of *spiral density waves* suggest that a density wave rotates with a constant pattern speed in the disk. You can think of such a wave as a natural mode of oscillation of the disk, much as you have sound waves in air, or harmonic waves in a violin string. If the rotation period of a star is shorter than of the pattern, then the star will occasionally overtake the wave. The gravitational force of the matter in the wave will make the star linger a bit near the pattern, before it leaves the arm again. An analogy often made is that of a slow lorry on the motor way causing a pile-up of faster cars behind it. Although most cars go fast, the speed with which *the pile-up* moves is determined by the slow lorry.

Another process which we *know* to occur, is the triggering of spiral arms by *galaxy encounters*. When two galaxies come close together, they will exert tidal forces on each other.[10] This effect can be convincingly demonstrated with numerical simulations. And so, although these arms may quickly disappear when left on their own (winding problem), the satellite galaxy may continually re-excite the spiral arms. Another hint comes from the fact that in barred galaxies, the spiral arms emanate from the ends of the bar (have a look at NGC 1365 if you don't believe me). It's is thought that Grand Design spirals are either triggered by a tidal encounter, or by the rotating bar.

Goldreich and Lynden-Bell said about flocculent spirals: 'a swirling hochpotch of spiral arms is a reasonably apt description' . So here we're probably faced by some kind of gas-dynamical instability in the disk.

So the conclusion about spiral arms is that there may be several processes that give rise to spiral arms, and depending on the particular spiral galaxy, one of these may dominate. So tidal encounters are probably responsible for the beautiful Grand Design spiral arms. The more messy pattern of flocculent spirals is probably due to a gas-dynamical instability in the disk. And once excited, a spiral pattern may live for a long time due to the spiral-density wave.

[10]The tidal force exerted by the moon causes the tides in the earth's oceans.

5.4 Summary

After having studied this lecture, you should be able to

- Derive the rotation curve for a Keplerian disk
- Derive the equations for the radial and tangential velocity of stars on circular orbits in a disk in differential rotation, and derive expressions for Oort's constants.
- Compute Oort's constants A and B for a Keplerian disk. Explain how A and B are measured in the MW.
- Explain how the 21-cm emission line can be used to estimate the rotation curve of the MW.
- Explain why both Oort's constants, and the rotation curve measured from 21-cm emission, suggest the presence of dark matter in the outer parts of the MW.
- Describe why spiral arms cannot all be material structures by explaining the winding problem.
- Discuss solutions to the winding problem.
- Explain the density wave theory of spiral arms.

Chapter 6

The Dark Halo

CO p. 896-897

Measurements of the rotation curve from HI 21-cm emission, analysis of the motions of stars in the solar neighbourhood with Oort's constants, and the Oort limit, all suggest the presence of a large amount of invisible 'dark matter' in the MW. Given such a startling conclusion, it may be a good idea to look for other evidence for dark matter in galaxy haloes.

6.1 High velocity stars

A number of high-velocity stars near the Sun have measured velocities[1] up to $v_\star \approx 500\text{km s}^{-1}$. Their existence provides us with a probe of the galaxy's mass, if we assume that these stars are still bound to the MW: it means that *the escape speed*[2] *at the solar circle,* $v_e > v_\star$.

[1]The quoted velocity is wrt to the centre of mass velocity of the MW. Do not confuse these with Oort's high velocity stars, which are typically low mass, low metallicity stars in the *Galactic Halo*. The velocities of Oort's stars are of order 200km s^{-1}. The present high velocity stars are typically *A*-type stars, presumably born in the disk, that have acquired their high velocity following a super nova explosion.

[2]Stars travelling at the local escape speed are just able to leave the potential well and escape to infinite.

6.1.1 Point mass model

If we assume there is no dark halo, then it is easy to find a relation between the circular velocity V_c and the escape speed v_e. If we assume all mass M of the MW is interior to the solar radius $R_\odot$ [3], then $V_c^2 = GM/R_\odot$, and the potential $\Phi = -GM/R_\odot = -V_c^2$. The velocity of a star just able to escape from the gravitational well is the *escape speed*, v_e. So since that star has zero total energy,

$$0 = E = \frac{1}{2}v_e^2 + \Phi = \frac{1}{2}v_e^2 - V_c^2\,. \tag{6.1}$$

So in this case, $v_e = 2^{1/2}\,V_c \approx 311\text{km s}^{-1}$ (Using $V_c = 220\text{km s}^{-1}$.) So for a point mass model of the MW, these high velocity stars cannot be bound to the MW – suggesting once more the presence of more mass in the outskirts of the MW than expected, given the rapid decrease in the distribution of light.

6.1.2 Parameters of dark halo

Given the failure of the point mass MW model, let's assume there to be a dark halo. In addition, let us assume the MW to be spherical, with a constant circular speed V_c out to some radius $R_\star$. Since $V_c^2 = GM/R = \text{constant}$, we have that

$$\begin{aligned} M(R) &= \frac{V_c^2\,R}{G} \qquad \text{when } R < R_\star \\ &= \frac{V_c^2\,R_\star}{G} \qquad \text{when } R \geq R_\star\,. \end{aligned} \tag{6.2}$$

Now the equation for the potential Φ is

$$\frac{d\Phi}{dR} = \frac{GM}{R^2} = \frac{V_c^2}{R}\,, \tag{6.3}$$

for $R \leq R_\star$. Integration gives $\Phi = \text{constant} - V_c^2 \ln(R_\star/R)$. We can determine the value of the constant at $R = R_\star$, since then $\Phi = -G\,M/R_\star = -V_c^2$. Hence

[3] $R_\odot$ is the radius of the circular orbit around the MW, at the position of the Sun – the solar galacto-centric radius.

$$\Phi(R) = -V_c^2 \, [1 + \ln(R_\star/R)] \, . \tag{6.4}$$

Using Eq.(6.1) for the escape speed, we obtain

$$v_e^2 = 2 \, V_c^2 \, [1 + \ln(R_\star/R)] \, . \tag{6.5}$$

For the Sun, $R \approx 8.5$kpc, $V_c = 220$km s^{-1}, $v_e \geq 500$km s^{-1}, implying $R_\star \geq 41$kpc, hence

$$M(R = R\star) \geq 4.6 \times 10^{11} M_\odot \, . \tag{6.6}$$

Since the total luminosity of the MW is of order $1.4 \times 10^{10} L_\odot$ (in the V -band), it means[4] that the mass-to-light ratio is at least 30. Given that the mass-to-light ratio of the MW *stars* is around 3 or so, our reasoning again suggests that a dominant fraction of the MW mass is not in stars.

Another estimate of the MW mass comes from the motion of neighbouring galaxies in the *Local Group*.

6.2 The Local Group (CO p. 1059-1060)

The MW is located in a rather average part of the Universe, away from any dense concentrations of galaxies. The 'Local Group' consist of the MW, Andromeda (M31), and about 40 small, irregular galaxies, gravitationally bound to each other.

6.2.1 Galaxy population

The MW has a couple of small galaxies gravitationally bound to it, for example the Large and Small Magellanic Clouds. The Magellanic stream is a stream of gas which originates from the Large Magellanic Cloud, which can be traced over a significant fraction of the whole sky. It may result from the tidal forces exerted by the MW.

The Sagittarius Dwarf galaxy is the neighbouring galaxy closest to the MW. It was discovered as recently as 1994, having eluded detection since it happens to be at the other side of the MW bulge and therefore is hiding

[4]Remember: we've only derived a lower-limit to the MW mass, hence a lower-limit to the mass-to-light ratio.

behind a large amount of foreground stars. Sagittarius has ventured so close to the MW that the tidal forces will probably tear it apart in the near future. Its discovery was actually hampered by its close proximity, since the large area on the sky ($\sim 8^o \times 2^o$) made it difficult to pick out against the bright MW foreground. Even away from the galactic plane (where dust obscuration limits our view), new members of the LG continue to be identified. The study of these small galaxies is exciting, since they allow us to constrain models for galaxy formation and evolution.

The Andromeda galaxy M31 is about twice as bright as the MW, and is the brightest member of the Local Group (LG). It is very similar to the MW, and so also has its own set of small galaxies orbiting around it. These galaxies, together with another 20 small galaxies, form the LG. M31 and the MW are by far the most massive galaxies in the LG.

The LG is almost certainly gravitationally bound to other nearby groups, and so does not really have a well defined edge. Galaxies in the outskirts of the LG may in fact belong to other groups.

The distribution of galaxies in the LG is rather untidy and lacks any obvious symmetry. Most of the galaxies are found either close to the MW, or close to M31. There is a third, smaller condensation of galaxies, hovering around NGC 3109.

The motion M31 can be used to estimate the mass of the Local Group, using the Local Group *timing argument*.

6.2.2 Local Group timing argument

The dynamics of M31 and the MW can be used to estimate the total mass in the LG. From the Doppler shifts of spectral lines, one can measure the radial velocity of M31 with respect to the MW[5],

$$v = -118\text{km s}^{-1}\,. \tag{6.7}$$

The negative sign means that Andromeda is moving *toward* the MW. This may be surprising, given that most galaxies are moving apart with the general Hubble flow. The fact that Andromeda is moving toward the MW is presumably because their mutual gravitational attraction has halted, and

[5]What one measures is the radial velocity wrt to the *Sun*. Since the Sun is on a (nearly) circular orbit around the MW, one needs to correct the measured heliocentric velocity to obtain the radial velocity of Andromeda wrt the MW.

eventually reversed their initial velocities. Kahn and Woltjer pointed out in 1952 that this leads to an estimate of the masses involved.

Since M31 and the MW are by far the most luminous members of the LG we can neglect in the first instance the others, and treat the two galaxies as an isolated system of two point masses. Since M31 is about twice as bright as the MW, and given that they are so similar, it is presumably also about twice as massive. If we further assume the orbit to be radial, then Newton's law gives for the equation of motion

$$\frac{d^2r}{dt^2} = -\frac{GM_{\rm total}}{r^2}\,, \tag{6.8}$$

where $M_{\rm total}$ is the sum of the two masses. Initially, at $t = 0$, we can take $r = 0$ (since the galaxies were close together at the Big Bang).

The solution can be written in the well known parametric form

$$\begin{aligned} r &= \frac{R_{\rm max}}{2}(1-\cos\theta) \\ t &= \left(\frac{R_{\rm max}^3}{8\,G\,M_{\rm total}}\right)^{1/2}(\theta-\sin\theta)\,. \end{aligned} \tag{6.9}$$

The distance r increases from 0 (for $\theta = 0$) to some maximum value $R_{\rm max}$ (for $\theta = \pi$), and then decreases again. The relative velocity

$$v = \frac{dr}{dt} = \frac{dr}{d\theta}\Big/\frac{dt}{d\theta} = \left(\frac{2\,G\,M_{\rm total}}{R_{\rm max}}\right)^{1/2}\left(\frac{\sin\theta}{1-\cos\theta}\right)\,. \tag{6.10}$$

The last three equations can be combined to eliminate $R_{\rm max}$, G and $M_{\rm total}$, to give

$$\frac{v\,t}{r} = \frac{\sin\theta\,(\theta-\sin\theta)}{(1-\cos\theta)^2}\,. \tag{6.11}$$

v can be measured from Doppler shifts, and $r \approx 710$kpc from Cepheid variables. For t we can take the age of the Universe. Current estimates of t are quite accurate[6], but even using ages of the oldest MW stars, $t \sim 15$Gyr gives an interesting result. Using these numbers, we can solve the previous

[6]From properties of the micro-wave background radiation.

equation (numerically) to find $\theta = 4.32$ radians, *assuming M31 is on its first approach to the MW*[7].

Substituting yields $M_{\rm total} \approx 3.66 \times 10^{12} M_\odot$, and hence for the MW mass, $M \approx M_{\rm total}/3$

$$M \approx 1.2 \times 10^{12} M_\odot \,, \tag{6.12}$$

comfortably higher than our lower limit Eq.(6.6).

Since the luminosity of the MW (in the V band) is $1.4 \times 10^{10} L_\odot$, the corresponding mass-to-light ratio for the MW is around $\Gamma = 100$. Furthermore, the estimate of M is increased if the orbit is not radial, or M31 and the MW have already had one (or more) pericenter passages since the Big Bang.

If all stars in the MW and M31 were solar mass stars, we would expect $\Gamma = 1$. Now even in the solar neighbourhood, most stars are less massive than the sun, and so the mass-to-light ratio for the *stars* is about 3 or so[8]. So the very large mass inferred from the LG dynamics strongly corroborates the evidence from rotation curves and Oort's constants, that most of the mass in the MW (and presumably also in M31) is dark.

From these numbers, we can also estimate the extent $R_\star$ of such a putative dark halo. If the the circular velocity $V_c = 220$km s^{-1} out to $R_\star$, then from $V_c^2 = GM/R_\star$ we find

$$R_\star = \frac{GM}{V_c^2} \approx \frac{G\, 10^{12} M_\odot}{(220\text{km s}^{-1})^2} \approx 100\text{kpc}\,. \tag{6.13}$$

If, as is more likely, the rotation speed eventually drops below 220km s^{-1}, then R is even bigger. Hence the extent of the dark matter halo around the MW and M31 is truly enormous. Recall that the size of the stellar disk is of order 20kpc or so, and the distance to M31 $\sim$ 700kpc. So the dark matter haloes of the MW and M31 may almost overlap.

[7]Equation (6.11) has no unique solution for θ, since it describes motion in a periodic orbit. On its first approach, θ should be the *smallest* solution to the equation.

[8]Recall that the luminosity of stars scales with their mass quite steeply, $L \propto M^\alpha$, with $\alpha \approx 5$, and hence $M/L \propto M^{1-\alpha}$. See your notes on stars, p. 34.

6.3 Summary

After having studied this lecture, you should be able to

- Show that in a point mass model of the MW, the high velocity stars are not bound.
- Estimate the parameters of a dark halo, assuming the high velocity stars are bound to the MW.
- Describe the properties of the Local Group in terms of the galactic content.
- Estimate the mass and extent of the dark halo of the MW from the Local Group timing argument.

Chapter 7

Elliptical galaxies.

CO S 25.1

Elliptical galaxies are spheroidal stellar systems with smooth luminosity profiles which contain old, metal rich stars. Unlike spirals, they have a large range in sizes, and rotation is generally unimportant. Their interstellar medium is very different from that of spirals, consisting of very tenuous, hot, X-ray emitting gas. Observations of this gas, and stellar dynamics, both suggest the presence of significant amounts of dark matter.

7.1 Luminosity profile (CO p. 892 & 950)

Elliptical galaxies have smooth surface brightness (SB) profiles, which in projection are ellipsoidal in shape (Fig.7.1). Note that the isophotes near the centre are well defined, becoming more noisy in the outskirts.

Average intensities as function of radius for these galaxies are shown in Fig. (7.2). The drawn line which fits the data well, is the de Vaucouleurs or '$r^{1/4}$' fit introduced previously in Eq. (3.2) for the MW's bulge:

$$I(r) = I_e \exp[-7.67(r/r_e)^{1/4} - 1]\,. \tag{7.1}$$

Here, $I(r)$ is the intensity at projected distance r from the centre. When surface brightness, $\mu = -2.5\log(I) + \text{const}$, is plotted as function of $r^{1/4}$ this profile is a straight line as in Figure (7.3). The intensity profiles of most elliptical galaxies can be fit with just the two parameters I_e and r_e.

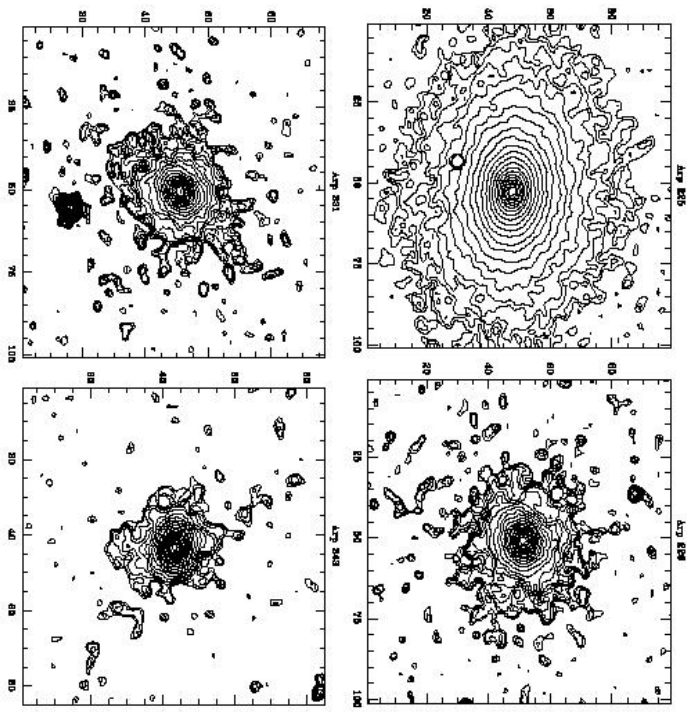

Figure 7.1: (Taken from astro-ph/0206097) Lines of constant surface brightness (isophotes) in the K-band for four elliptical galaxies. In successive isophotes, the surface brightness increases by 0.25 magnitudes.

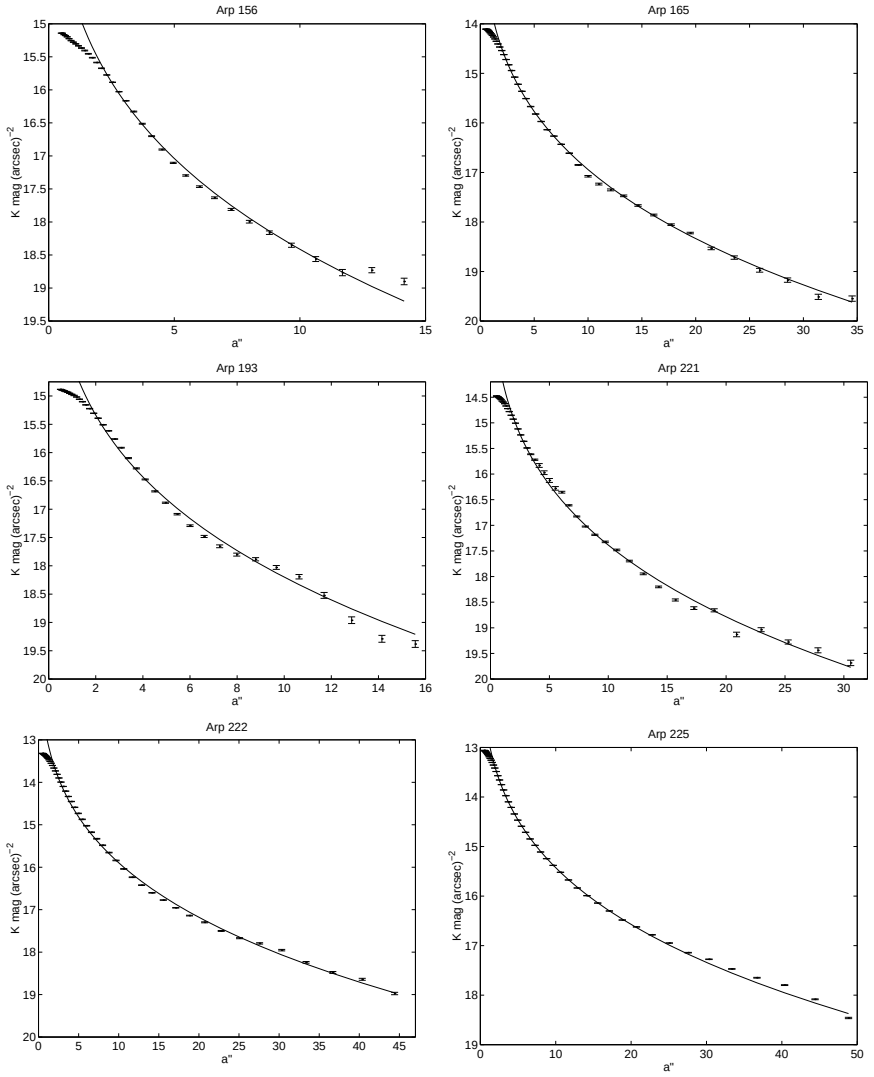

Figure 7.2: (Taken from astro-ph/0206097) Surface brightness as function of distance to the centre for the galaxies from Fig. 7.1. The drawn line is the best $r^{1/4}$ fit.

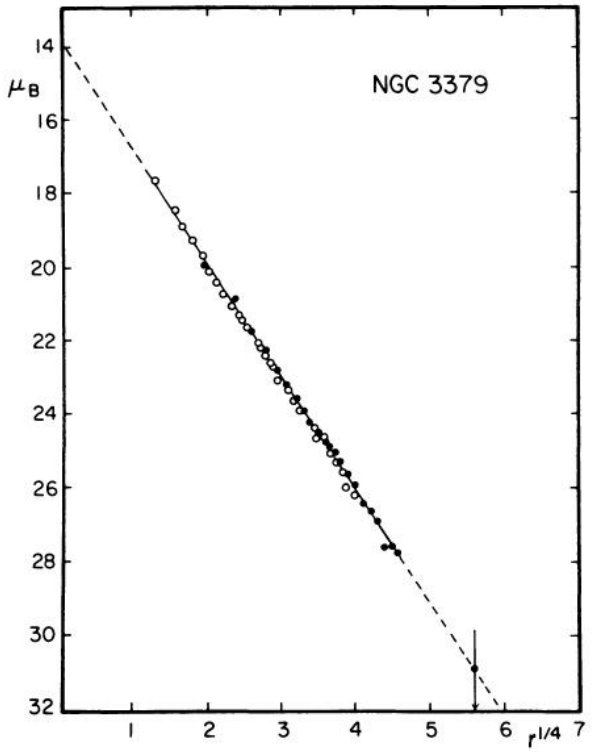

FIG. 2.—Mean E-W luminosity profile of NGC 3379 derived from McDonald photoelectric data. ●, Pe 4 data with 90 cm reflector; ○, Pe 1 data (M + P) with 2 m reflector. Note close agreement with $r^{1/4}$ law.

Figure 7.3: Luminosity profile for galaxy NGC 3379 (open symbols) and $r^{1/4}$ fit (drawn line). Taken from de Vaucoleurs & Capaccioli, ApJS 40, 1979.

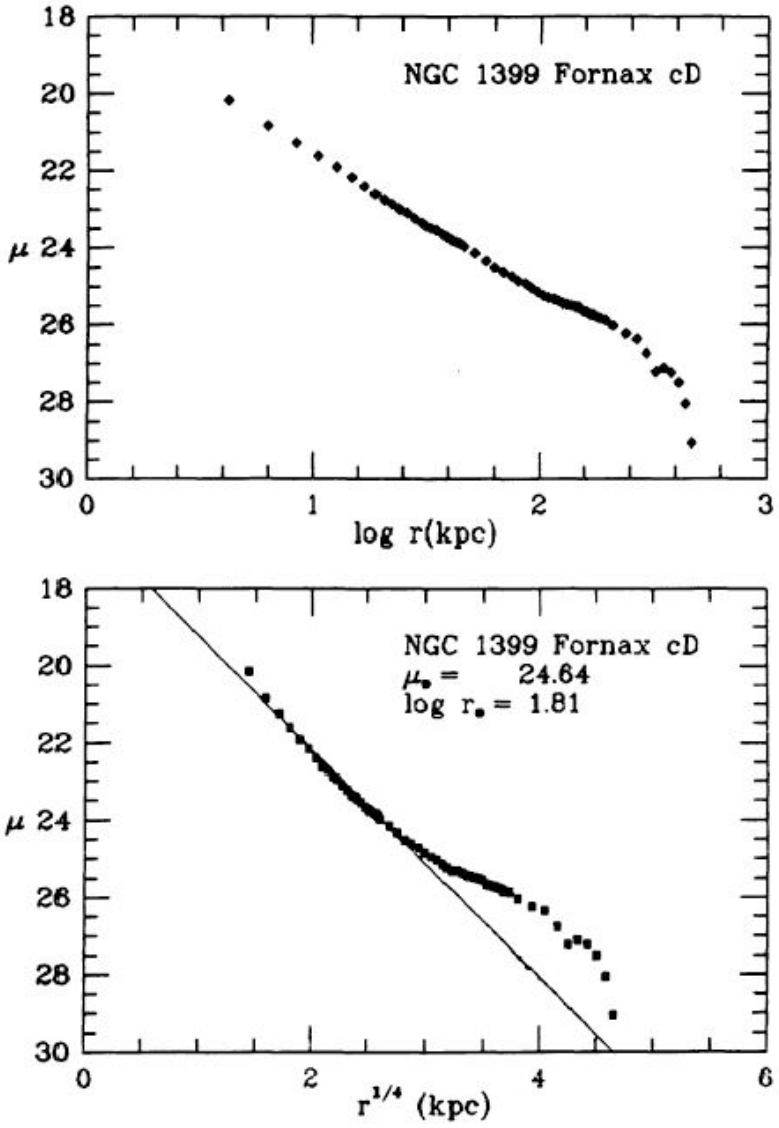

Figure 7.4: SB profile for NGC 1399 from Schombert (filled symbols; ApJS, 1989). The outer parts of the profile do not follow the $r^{1/4}$ fit (bottom panel), but are nearly a straight line in a SB-log(r) (i.e. a log $-$ log) plot (top panel), meaning the profile is close to a power-law.

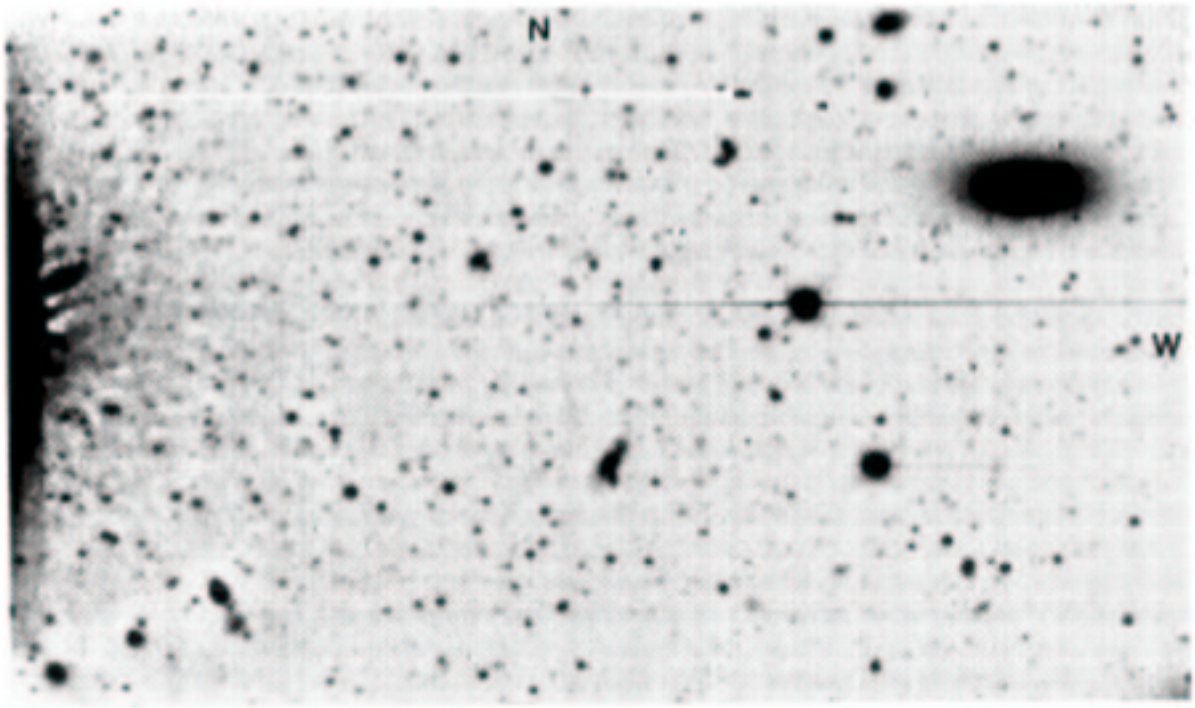

Figure 7.5: Image of NGC 1399 with smooth, best fit $r^{1/4}$ profile subtracted (Bridges et al., AJ 101, 469 (1991). The centre of NGC 1399 is at the left, the object toward the top right is another galaxy in the galaxy cluster. The other extended objects in the image are other galaxies. Clearly seen are hundreds of high SB unresolved objects, which are GCs in the halo of NGC 1399.

Some of the giant elliptical galaxies that are invariably found in the centres of big clusters of galaxies have an extended stellar halo not fit well by the de Vaucouleurs profile. Such galaxies are called cD galaxies. An example is NGC 1399, the cD galaxy in the nearby Fornax cluster of galaxies (Fig. 7.4). The extent of such a halo can be truly enormous and be traced to around a Mpc , making the size of NGC 1399 on the night sky about the size of the moon, even though Fornax is at a distance of ~ 20 Mpc.

Ellipticals also have many globular clusters (CO p. 962). Figure (7.5) is an image of NGC 1399, where an $r^{1/4}$ fit to the SB-profile of the galaxy has been subtracted. Clearly visible are 100s of high surface brightness objects, indistinguishable on this plate from foreground stars, which are in fact GCs in the halo of the galaxy.

What is the origin of the $r^{1/4}$ profile? Numerical simulations of of collisions between two spiral galaxies produce objects with surface brightness profiles resembling the $r^{1/4}$ profile. Since elliptical galaxies are found in dense environments where such collisions are frequent, it seems plausible that elliptical galaxies form from collisions between spirals galaxies. However the stellar populations of ellipticals and spirals differ: ellipticals contain mostly old and metal rich stars (see below), whereas spirals contain younger and more metal poor stars. So ellipticals may still have formed from collisions, but not collisions between *todays* spiral galaxies.

7.2 Stellar populations and ISM

The redder colours of stars in elliptical galaxies is due to

1. the absence of star formation: the blue light in spirals is partly due to young and massive stars, but these massive stars are not present in ellipticals

2. the higher metallicity of stars in ellipticals. The presence of heavy elements ('metals') in stars leads to redder colours, both because of changes in the stellar structure, and because the metals in the stellar atmosphere redden the emitted light.

The fact that a stellar population is blue either because it is young (and the blue light is emitted by massive and hence young stars), or because it

is metal poor, or both, is called the *age-metallicity degeneracy*: the colour of the population is not enough to tell a young but metal rich population, from an old metal poor one. Metallicity measurements of stars in elliptical galaxies have shown that both effects, absence of star formation, and high metallicities, cause the redder colours of ellipticals.

Dust and gas Whereas the ISM in spirals consists of dust and cold gas, these are generally absent in ellipticals. Sometimes though a large galaxy accretes a smaller one and this may lead to a large dust lane strung across the face of the large galaxy: the Sombrero galaxy (Fig. 7.6) is an example. Such recent mergers may be quite common: a number of ellipticals have faint rings of stars around them (see for example Fig. 7.7), probably a result of such 'galactic cannibalism'.

7.3 X-rays

X-rays are absorbed by the Earth's atmosphere hence are observed from rockets or satellites. They are focussed onto a detector by placing a set of nearly parallel plates in the beam: the X-rays ricochet off these plates onto the detector[1].

The emission of X-rays from elliptical galaxies is due to two unrelated sources: hot gas in their interstellar medium (thermal bremsstrahlung), and binary stars. Binary stars may emit X-rays due to mass transfer (see your notes on stars). Subtracting such point sources from the X-ray image of the galaxy reveals extended X-ray emission from *thermal bremsstrahlung*.

Thermal bremsstrahlung[2] is the process whereby high energy radiation (X-rays) is produced in a plasma of ions and electrons, due to the electromagnetic deflection of a high-speed (thermal) hot electrons passing close to a positively charged ion. The deflection of the electron means it is accelerated, and an accelerating charge emits electromagnetic dipole radiation: this is the radiation that we observe[3] . The plasma is highly ionised because it is so

[1]See additional images on the web-page or http://chandra.harvard.edu/xray_astro/.

[2]German for 'braking radiation'.

[3]Note that the detected radiation is **not** blackbody radiation from the hot gas: the spectrum of thermal bremsstrahlung is not the same as that of a black body. Also other

Figure 7.6: Image of the ‘CenA’ galaxy, with its striking dust lane.

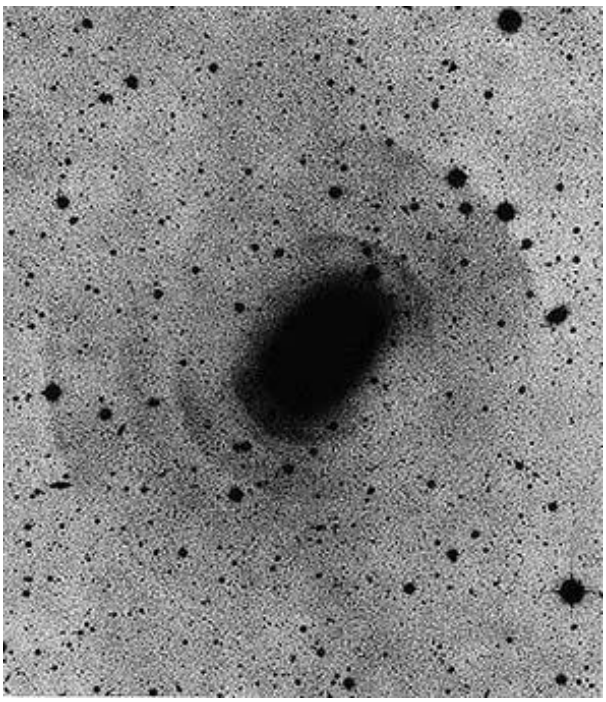

Figure 7.7: Image of NGC 3923 taken by David Malin. Several faint shells of stars appear as ripples in the outer parts of the galaxy, probably resulting from the merger of the central galaxy with a much smaller system. (see http://www.ast.cam.ac.uk/AAO/images/general/ngc3923.html)

hot, and the electrons are not bound to any particular ion. For this reason, thermal bremsstrahlung is sometimes called 'free-free' radiation.

The *emissivity* ϵ (the amount of energy radiated per unit volume) is

$$\epsilon \propto n_e \, n_i \, T^{1/2} \, , \tag{7.2}$$

where n_e and n_i are the electron and ion number densities respectively, and T is the temperature of the plasma.

Thermal bremsstrahlung produces a power-law spectrum up to some cut-off frequency, but the observed X-ray spectra of elliptical galaxies also show *spectral lines*, where electronic transitions in some highly ionised elements present in the hot plasma contribute to the spectrum. This makes it possible to measure *abundances* of elements in the ISM.

It is often possible to detect several different transitions of Iron. The relative strength of these transitions depends only on the temperature T of the gas, and not on the abundance of Iron: this makes it possible to measure T from the X-ray spectrum.

7.4 Evidence for dark matter from X-rays (CO p. 1063)

It is possible to constrain the density distribution of the elliptical galaxy by assuming the hot X-ray emitting gas is in *hydrostatic equilibrium*, much in the same way as one can derive the equations for stellar structure. Gravity pulls the gas inward, whereas the pressure of the gas pushes it outward. In hydrostatic equilibrium these two forces balance. We can determine the temperature T of the gas from its X-ray spectrum, its density ρ from the emissivity, $\epsilon \propto n_e \, n_i \, T^{1/2}$ and hence infer its pressure, p, as function of radius. Hydrostatic equilibrium then allows us to measure the gravitational potential and hence the total density distribution. Assume for simplicity that the galaxy is spherical.

ions undergo electromagnetic deflections, but since they are much more massive than the electrons, their contribution to the emission is negligible.

Let M_s be the mass inside the shell of radius r (consisting of stars, gas and dark matter: $M = M_\star + M_{\rm gas} + M_{\rm dm}$), dr its thickness, and $M(r)$ the mass of the sphere with radius r. The gravitational force F_g on the shell is due to this total enclosed mass

$$F_g(r) = \frac{GM(r)M_s}{r^2}\,, \tag{7.3}$$

where $M_s = 4\pi r^2 \rho_{\rm gas}(r) dr$ is the mass of the shell.

Let $p(r)$ be the pressure in the hot gas. The pressure force on a surface is $p(r)$ times the surface area, $4\pi r^2$. The net outward force is the difference between the outward and inward pressures:

$$F_p(r) = 4\pi r^2 (p(r) - p(r+dr)) = -4\pi r^2 \frac{dp}{dr}\, dr\,, \tag{7.4}$$

where the pressure was expanded in a Taylor series, assuming $dr << r$. Expressing hydrostatic equilibrium, $F_g = F_p$, yields

$$\frac{GM(r)}{r^2} 4\pi r^2 \rho_{\rm gas}(r) dr = -4\pi r^2 \frac{dp}{dr} dr\,, \tag{7.5}$$

hence

$$\frac{GM(r)}{r^2} = -\frac{1}{\rho_{\rm gas}(r)} \frac{dp}{dr}\,, \tag{7.6}$$

or in terms of the gravitational potential Φ

$$\nabla\Phi = -\frac{\nabla p}{\rho_{\rm gas}}\,. \tag{7.7}$$

This should look familiar from hydrostatic equilibrium in stars!

The X-ray observations can be used to determine the right-hand-side: the X-ray spectrum yields T, and the emissivity ρ. Application of Eq. (7.6) then yields $M(r)$. The value of this 'dynamical mass' can be compared to the mass of the elliptical in stars and gas, $M_\star + M_{\rm g}$. The fact that $M_\star + M_{\rm g} < M$ is evidence for the presence of dark matter in ellipticals.

The temperature T is observed to remain approximately constant, in which case we can obtain an approximate expression for the density profile. The pressure p in an ideal gas depends on T and ρ as

$$p = \frac{\mathrm{k_B}\, T}{\mu\, m_\mathrm{p}}\, \rho_\mathrm{gas}\,, \tag{7.8}$$

where $\mu\, m_\mathrm{p}$ is the mean molecular weight per particle. Substituting this into Eq. (7.6) and assuming T to be constant yields

$$GM(<r) = -\frac{\mathrm{k_B} T}{\mu\, m_\mathrm{p}} r^2 \frac{d\ln \rho_\mathrm{gas}}{dr}\,. \tag{7.9}$$

Finally taking the derivative of both sides with respect to r, gives

$$G4\pi r^2 \rho_\mathrm{tot} = -\frac{\mathrm{k_B} T}{\mu\, m_\mathrm{p}} \frac{d}{dr}\left(r^2 \frac{d\ln \rho_\mathrm{gas}}{dr}\right), \tag{7.10}$$

where ρ_tot is the *total mass density*, *i.e.* due to stars, gas and dark matter.

If the total density and gas density were proportional, $\rho_\mathrm{gas} \propto \rho_\mathrm{total}$, we could solve Eq. (7.9) by trying a solution of the form $\rho_\mathrm{total} = \rho_0\,(r_0/r)^\beta$. Substitution shows this is indeed a solution provided $\beta = 2$, and yields

$$\rho_\mathrm{tot}(r) = \frac{\mathrm{k_B}\, T}{2\pi\, G\mu m_\mathrm{p}}\, r^{-2}\,. \tag{7.11}$$

Even if total and gas density do not trace each other it is possible to infer ρ_total from the X-ray data. We can then compare the inferred total density ρ_total with that from stars, $\rho_\star$, and gas, ρ_gas combined: this analysis demonstrates that elliptical galaxies also contain dark matter, since $\rho_\mathrm{total} > \rho_\star + \rho_\mathrm{gas}$.

7.5 Summary

After having studied this lecture, you should be able to

- describe the surface brightness profiles of Es in terms of the de Vaucouleurs profile.
- explain why we think that this profile results from galaxy encounters
- recall that Es have typically hundreds of GCs.
- explain why dust lanes in ellipticals and shells of stars around them are thought to be evidence for galactic cannibalism.
- contrast the stellar population and ISM of ellipticals with those of spirals
- describe how X-rays are detected, and explain the process with which X-rays are produced in the hot gas in ellipticals
- explain how X-ray observations can be used to infer the gravitational potential and derive the equation for hydrostatic equilibrium, relating gas properties to the total density

Chapter 8

Groups and clusters of galaxies

CO §27.3

Galaxies are not distributed homogeneously in the Universe. Galaxies such as the Milky Way huddle together in small groups (the Local Group), voids are very large regions of space where galaxies are very rare, and *clusters* of galaxies are regions where the galaxy density is very high. Galaxy groups and clusters themselves are clustered in super clusters (i.e. clusters of clusters). But there are no clusters of super clusters: on sufficiently large scales the Universe is not a fractal but becomes homogeneous.

8.1 Introduction

The Milky Way, Andromeda, and some 40 small irregular galaxies within 2Mpc or so from the MW, are part of a gravitationally bound system, called the Local Group (see Sect. 6.2). Most spiral galaxies are found in such loose groups.

Galaxy clusters are gravitationally bound systems of 10s-100s of elliptical galaxies and 1000s of smaller dwarf galaxies. Fornax and Virgo are two clusters of galaxies within $\sim 20\,\mathrm{Mpc}$ of the Milky Way. The galaxy M 87, which has a super massive black hole (see Sect 11) with mass $\sim 10^9\,M_\odot$ lurking in its centre, is the central object in the nearby *Virgo* cluster of galaxies. The Local Group, including the Milky Way, is falling toward Virgo. The large cD galaxy NGC 1399 (see Sect.7.1) is at the centre of the *Fornax* clus-

ter of galaxies. The *Coma* cluster of galaxies, at a distance of 90Mpc, has a mass as large as $10^{15} M_\odot$. Clusters such as Coma contain the most massive galaxies known.

George Abell and collaborators eye balled photographic plates in the 1950s to identify galaxy clusters as over dense concentrations of galaxies. He discovered some 4500 clusters, ranking them from poor to rich, according to the number of galaxies they had. Distant clusters are still identified with the number Abelll allocated.

Clusters of galaxies are the most massive virialised structures in the Universe. Their crossing time[1] is sufficiently small that each galaxy has had the opportunity to cross the system several times, and hence these systems are thought to be in dynamical equilibrium.

8.1.1 Evidence for dark matter in clusters from galaxy motions (CO p. 960)

The Swiss astronomer Fritz Zwicky measured Doppler velocities of galaxies to infer the dynamical mass of galaxy clusters in the 1930s. Inferring the mass in stars from the observed luminosity, he decided that clusters must contain dark matter: this was the first time that the need for dark matter arose. Zwicky's mass measurement was based on the following argument.

Assume all cluster galaxies have the same mass m, and that the cluster contains N galaxies. The kinetic energy of the system is

$$K = \frac{1}{2} \sum m\, v^2 = \frac{1}{2}\, M\, \sigma^2 \,, \tag{8.1}$$

where $M = N\, m$ is the total mass of the cluster galaxies, and the velocity dispersion, σ, is defined by

$$\sigma^2 = \frac{\sum m\, v^2}{M} \,. \tag{8.2}$$

[1] If v is the typical velocity of a galaxy in a cluster of galaxies, and R is the radius of the cluster, then the crossing time $T_{\rm cr} = R/v$, i.e. it is the typical time a galaxy takes to cross the cluster once.

Note that these velocities are measured with respect to the *mean* velocity of the cluster. The potential energy in the system is of order[2]

$$U = -\frac{G\,M^2}{R}\,, \tag{8.3}$$

where R is a measure of the size of the system. When the system is in *virial equilibrium*, $2K = |U|$ hence M can be determined from measuring σ and R from

$$M = \frac{R\,\sigma^2}{G}\,. \tag{8.4}$$

This allowed Zwicky to estimate the dynamical mass, M, of the cluster, from the observed velocities and size of the system.

Note that the velocity inferred from the Doppler shift, $\lambda = \lambda_0\,(1 + v_r/c)$, is only the *radial component* of the velocity, but the kinetic energy employes the *total* velocity, $v^2 = v_r^2 + v_t^2$, the sum of radial and tangential components. Since we cannot measure v_t, Zwicky assumed[3] that $v_t^2 = 2v_r^2$, since we (the observers) are presumably not in a special position.

Zwicky estimated the masses of the galaxies as inferred from their luminosities, $M_L = \Gamma\,L$, where $\Gamma_L \sim 3\,M_\odot/L_\odot$ is the stellar mass-to-light ratio, and compared the result with the dynamical mass, M. He found that, not only was the dynamical mass much larger, $M \gg M_L$, the velocities of the cluster galaxies was so high that, given the amount of mass inferred to be in the galaxies, the cluster was not even a gravitationally bound system: $K + U > 0$. Left on its own, it would cease to be a high density region of galaxies on a short time scale because the galaxies would fly apart very rapidly. So either clusters were just chance superpositions of galaxies, or there was much more mass in them than was inferred from just the galaxies. Zwicky concluded that most of the mass in clusters must be invisible, hence introducing *dark matter*.

[2]CO's value is 3/5 of this – here we simply look at the order of magnitude.

[3]The extra factor 2 arises because the tangential velocity has two Cartesian components. To see this, choose a Cartesian system of axes with z along the radial direction, then $v_r^2 = v_z^2$, whereas the tangential velocity $v_t^2 = v_x^2 + v_y^2$. Assuming isotropy, $v_x^2 = v_y^2 = v_z^2$, hence $v_t^2 = 2v_r^2$.

8.2 Evidence for dark matter from X-rays observations

The hot gas[4] in clusters emits X-rays due to *thermal bremsstrahlung*, which can be used to determine their mass assuming the hot gas is in hydrostatic equilibrium. We did the same for elliptical galaxies in Section 7.3. The (total) mass of the cluster in a sphere of radius r, relates to gas density, $\rho_{\rm gas}$, and pressure, p, as (see Eq. 7.6)

$$\frac{GM(<r)}{r^2} = -\frac{1}{\rho_{\rm gas}(r)}\frac{dp}{dr}\,. \tag{8.5}$$

As for ellipticals, the X-ray data can be used to measure the right hand side, allowing a determination of the encloded mass, $M(<r)$. Comparing this to the mass in stars and gas, $M_\star = \Gamma\, L$, and $M_{\rm gas}$ inferred from the X-ray emissivity, yields $M \gg M_\star + M_{\rm gas}$: X-rays strongly indicate the presence of dark matter in clusters.

What is the origin of the gas, and why is it so hot? A high-mass cluster will suck gas in from its surroundings due to its large gravitational pull. The accreting gas slams into the gas already there, and the rapid compression of the gas converts kinetic energy into thermal energy in an *an accretion shock*.

Assume a parcel of gas starts at infinity has velocity $v = 0$, and is accreted by a cluster with mass M. It slams into the gas already present at distance R (the radius of the cluster). Expressing energy conservation yields

$$E = 0 = \frac{1}{2}v^2 - \frac{G\,M}{R}\,, \tag{8.6}$$

since the energy of the parcel at infinity is zero. When the gas converts its kinetic energy $(1/2)\,v^2$, into thermal energy, it gets heated to temperature T given by

$$\frac{3}{2}\frac{{\rm k_B}T}{\mu\, m_p} = \frac{1}{2}\,v^2\,. \tag{8.7}$$

[4]Note that the emission is extended, and not just due to the elliptical galaxies themselves: most of the hot gas is between the galaxies, not associated with any particular galaxy.

Here, μ is the mean molecular weight of the gas. These equations relate the cluster's mass and radius to the **virial temperature** T of the gas:

$$\frac{G\,M}{R} = \frac{3}{2}\,\frac{\mathrm{k_B}T}{\mu m_\mathrm{p}}\,. \tag{8.8}$$

Clusters have such high values of T that all the hydrogen atoms are fully ionised, hence[5] $\mu = 1/2$.

8.3 Metallicity of the X-ray emitting gas.

The X-ray spectra of clusters consists of a power-law component due to thermal bremsstrahlung, with additional emission lines mostly from inner-shell transitions of the Fe ion, see Figure 8.1. Recall that the ratio of emission lines can be used to determine T, whereas the emissivity $\epsilon \propto \rho_\mathrm{gas}^2\,T^{1/2}$ then determine ρ_gas. The first surprise is that most of the baryonic mass in the cluster is in the X-ray gas: $M_\star \ll M_\mathrm{gas}$. Although we identified galaxy clusters as regions with a high density of galaxies, most of the baryons in the cluster have not actually collapsed to form stars.

Once T and ρ_gas are known, the strength of the lines allows one to determine the *amount* of Fe in this intra-cluster medium. Comparison with the total amount of gas gives a mean metallicity $M_\mathrm{Fe}/M_\mathrm{gas} \approx 1/3$ of the solar value[6].

The high metallicity of the cluster *gas*, and the enormous amount of metals outside of galaxies, is an even bigger surprise. Note that metal abundance is higher than that of *stars* in most globular clusters and dwarf galaxies. Presumably these metals were produced in stars, and subsequently ejected from their parent galaxy into the intra-cluster gas. This demonstrates that galaxies are far from closed boxes: a large fraction of the products of stellar evolution are blown out of the galaxy. Current models suggest that this is due to the combined effect of many super nova explosions.

[5] A more accurate expression for μ takes into account the presence of Helium and other elements, giving $\mu \approx 0.6$.

[6] Recall that the Sun contains a mass fraction of 0.02 of metals.

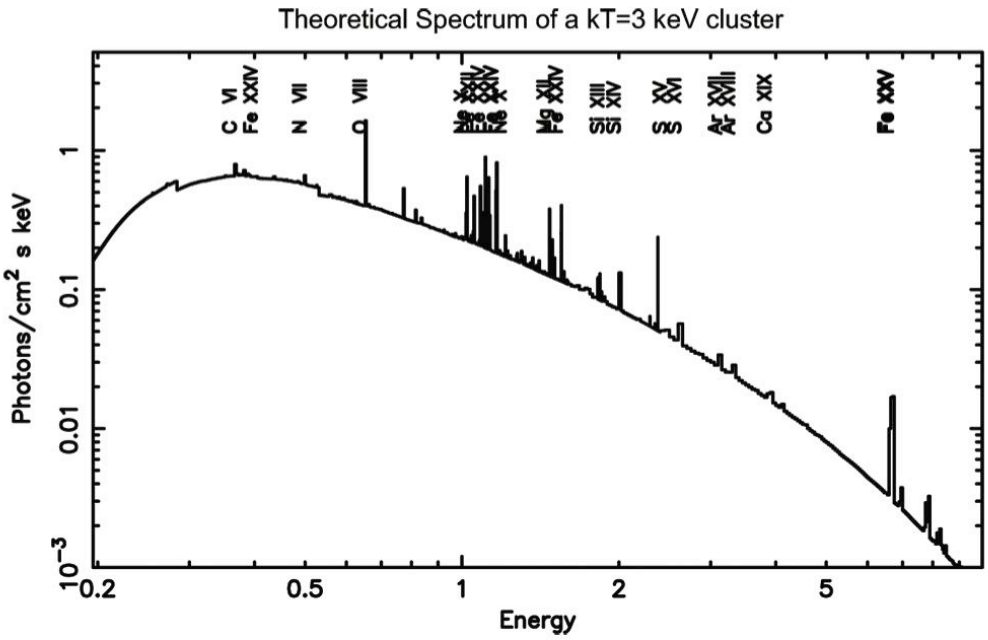

Figure 8.1: Theoretical emission spectrum of a hot plasma. Emission lines due to a range of elements (indicated) appear on top of a smooth continuum caused by thermal bremsstrahlung.

8.4 The dark matter density of the Universe

Clusters can be used to determine the dark matter density of the Universe as a whole. Assume the Universe starts-out smooth, with a (nearly) constant ratio ω of dark matter to baryons:

$$\omega = \frac{\rho_{\rm dm}}{\rho_{\rm b}} \,. \tag{8.9}$$

The forming cluster grows through accretion of dark matter and baryons, and so the density of both components increases. As the potential well of the cluster deepens, it is probably a good approximation to assume that eventually neither dark matter, nor baryons, can ever escape from the cluster, meaning the ratio of dark matter to baryons, *in the cluster as a whole*, $M_{\rm dm}/M_{\rm b}$, equals the primordial value:

$$\omega \approx \frac{M_{\rm dm}}{M_{\rm b}} \,. \tag{8.10}$$

Therefore we can determine ω by measuring the dark matter mass of a cluster, $M_{\rm dm} = M - M_{\rm b}$, and the baryonic mass, $M_{\rm b}$. Recall that we could determine M from either galaxy motions (Eq. 8.4) or X-ray observations, with $M_{\rm b} = M_\star + M_{\rm gas}$ from combining the stellar mass (from the observed stellar luminosity) and the gas mass from the X-ray emissivity. Doing so for a range of clusters yields $\omega \approx 6$.

An estimate for the mean baryon density, $\rho_{\rm b}$, follows from the *abundance* of Deuterium[7] relative to normal Hydrogen, $\rho_{\rm D}/\rho_{\rm H}$. Deuterium is produced during nucleosynthesis in the first three minutes after the Big Bang, and destroyed during nuclear burning in stars. Therefore any Deuterium found[8] is primordial and left over from Big Bang. Crucially, *the Deuterium abundance depends on the baryon density* (Figure 8.2). The inferred mean baryon density is $\rho_{\rm b} \approx 2.2 \times 10^{-7}$ hydrogen atoms per cm^{-3}. This is approximately 30 orders of magnitude lower than the density of the paper that these notes are printed on (or the density of the screen if you read them on your computer).

[7]Recall that the nucleus of a Deuterium atom differs from that of ordinary Hydrogen in that it has a proton and a neutron.

[8]Deuterium abundance measurements use quasar spectra (see Chapter 11 for a discussion of quasars) to probe nearly primordial gas in between the galaxies.

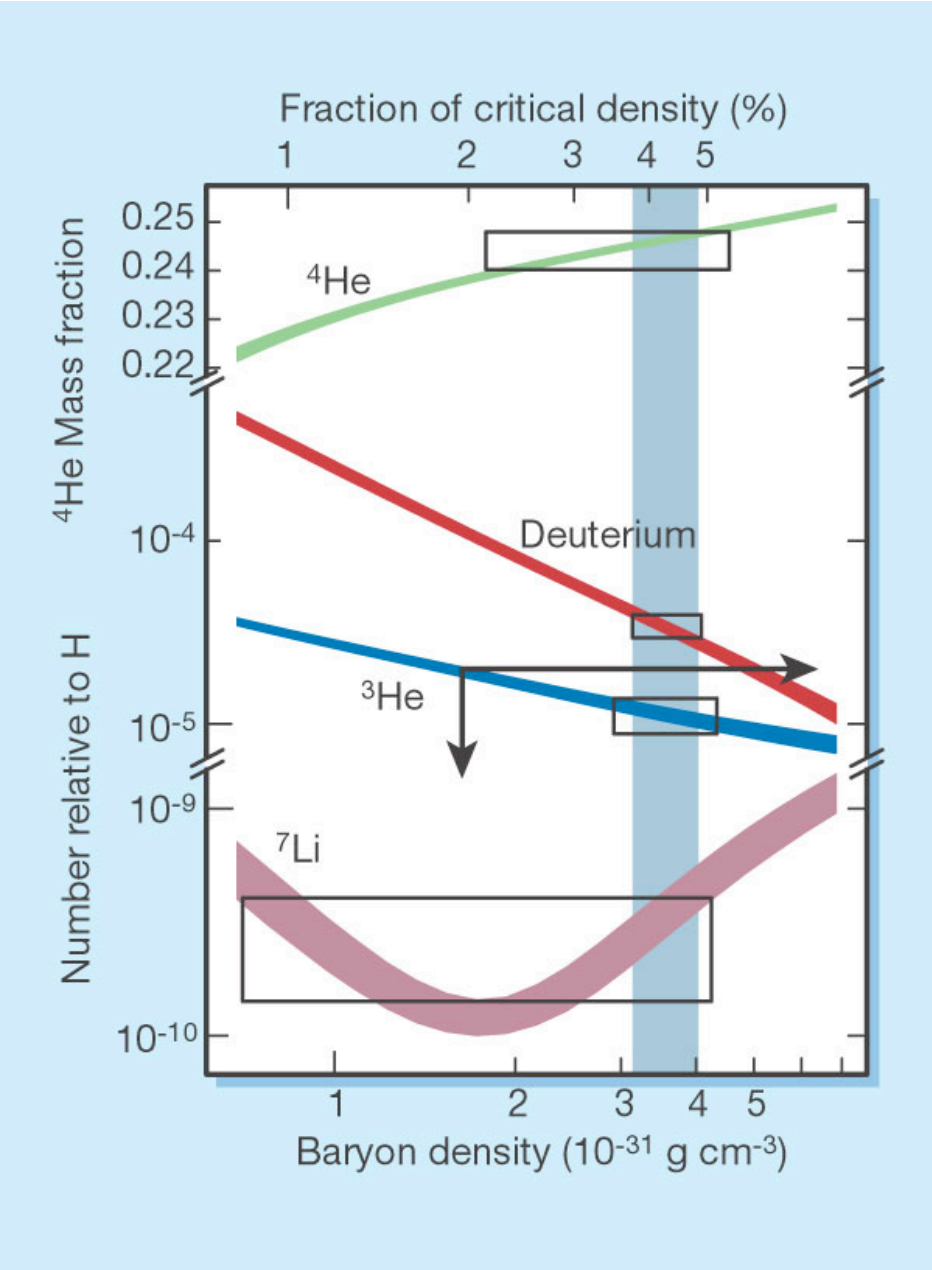

Figure 8.2: The production of various elements during Big Bang nucleosynthesis as a function of the baryon density. (*Nature* **415**, p. 27, 2002)

Combining the mean baryon density with $\omega = 6$ yields $\rho_{\rm dm} \approx 2.2 \times 10^{-30}$ g cm^{-3} for the mean dark matter density of the Universe.

8.5 Summary

After having studied this lecture, you should be able to

- Define what is a cluster and a group of galaxies by listing some of their properties.
- Explain how galaxy motions suggest the presence of dark matter in clusters.
- Explain how X-ray observations suggest the presence of dark matter in clusters.
- Explain the origin of the high temperature of the cluster gas.
- Explain how we know that most of the baryons in a cluster are in hot gas, and not in stars.
- Explain why the high observed metallicity of the cluster gas suggests that a large fraction of the products of stellar evolution are blown out of galaxies
- Explain how clusters have been used to estimate the mean dark matter density of the Universe.

Chapter 9

Galaxy statistics

Galaxies surveys select objects on the night sky based on size, luminosity and colour to distinguish galaxies from stars or other foregrounds. Distances are inferred to relative nearby galaxies using standard candles such as Cepheid variables, or assuming the globular cluster luminosity function to be universal, or using colours or redshifts for more distant galaxies[1]. The survey then provides the three dimensional position of each galaxy (two angles and a distance), as well as a large sample of object for which the *physical* (as opposed to apparent) properties are known. The recent **2dF** ('two degree redshift survey'; an Anglo-Australian collaboration with an extensive Durham contribution; see the movie!) collected a spectroscopic sample of 250k galaxies, the more recent and larger **Sloan redshift survey** used a dedicated telescope to both image the sky and obtain spectra, and collected about a million galaxies.

Inferences about the galaxy population need to take into account observational *biases*: whether or not a galaxy makes it past the selection criteria and ends-up in the survey sample depends on external factors, such as its distance (since surveys collect galaxies with flux brighter than some minimum magnitude), its surface brightness, and its position on the sky (nearby bright stars, foreground extinction due to the Milky Way, and other effects may affect the selection). The galaxy's intrinsic properties themselves may bias the sample: for example it is much easier to measure the redshift of an emission line galaxy (*e.g.* a spiral with recent star formation) than of

[1]Recall the L1 lab on the Hubble constant

a galaxy without emission line (an old elliptical galaxy, say). Consequently emission line galaxies may be over-represented with respect to galaxies without emission lines.

The visible Universe contains around 10^{11} galaxies more massive than the Milky Way, with approximately half of all stars in spirals, half in ellipticals. Galaxies are not homogeneously distributed, with groups lining-up along *filaments*, and rich clusters of galaxies at the intersection of filaments. The filaments themselves delineate large under dense regions (nearly) devoid of galaxies called *voids*. Cosmological numerical simulations that follow the gravitational amplification of small fluctuations, as seen in the Cosmic Microwave Background, are able to produce a pattern very similar to this 'cosmic web' (see movies). This chapter discusses the statistical properties of galaxies, as inferred from such surveys.

9.1 The density-morphology relation

Once galaxies are identified it may be possible to classify them according to the Hubble sequence[2]. When Hubble type is plotted against galaxy density (*i.e.* the density of galaxies per unit volume), it appears that *low density regions (*e.g. groups*) are mostly populated by spiral galaxies, whereas high density regions (*e.g. clusters*) are mostly populated by S0s and Es (see Fig.9.1)*: this is called the **density-morphology relation**.

The origin of this relation has long been debated, but it seems plausible that galaxies in high-density regions suffer more tidal encounters with other galaxies, and this may destroy the fragile disk (recall the movie of a collision between two spirals), hence converting spirals into S0s or Es. Another possibility is that the hot gas associated with clusters (Chapter 9) removes the gas from spiral galaxies that fall into a cluster (by *ram-pressure stripping*), thereby suffocating the galaxy (descriptively termed *strangulation*).

[2]This is only possible for relatively nearby galaxies: at high redshifts, galaxies are so small on the sky that a morphological classification becomes impractical.

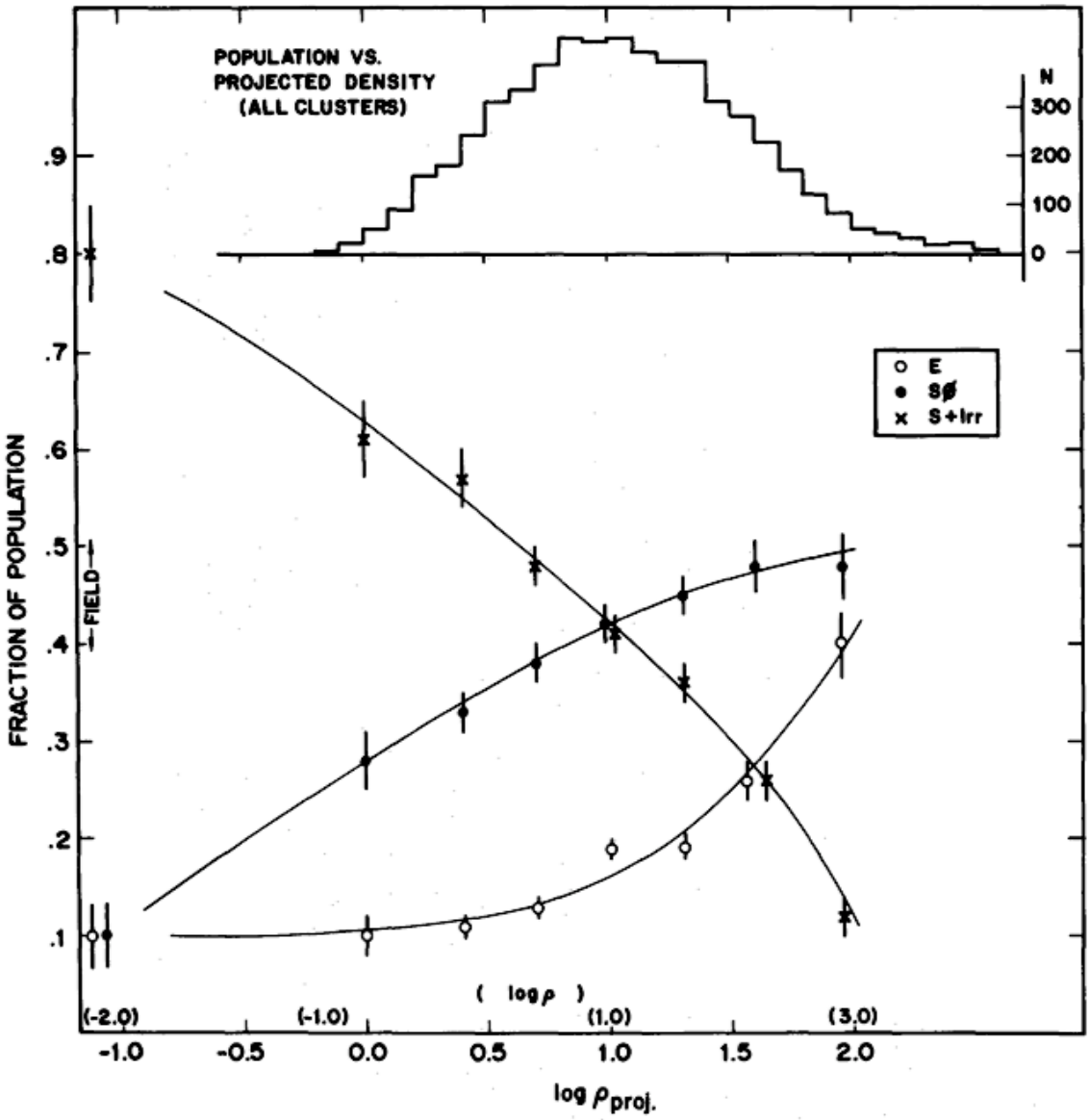

Figure 9.1: The fraction of Elliptical (E), S0, and Spiral + Irregular (S+I) galaxies as function of the logarithm of the projected density($\rho_{\rm proj}$, in galaxies Mpc^{-2}). At low density (small $\rho_{\rm proj}$), most galaxies are type S or Irr, whereas at high densities, most galaxies are S0 or E: there appears to be a relation between density of galaxies, and galaxy type: this is the 'density-morphology' relation. From Dressler, ApJ 236, p. 351 (1980).

9.2 Galaxy scaling relations

9.2.1 The Tully-Fisher relation in spirals (CO p. 952-956)

Spiral galaxies have flat rotation curves: the circular velocity is independent of radius away from the centre. The *Tully-Fisher* relation $L \propto V_c^4$ relates the luminosity L of the spiral to its circular velocity V_c: bright spirals (high L) spin faster (higher V_c), see Fig 9.2.

To measure this relation we need to determine L, and the circular velocity[3] V_c. L is inferred from the apparent magnitude, once the distance to the galaxy is known. V_c is inferred from measuring velocities of stars or gas in the interstellar medium, for example using Hα as emission line, or more usually using the HI 21-cm line.

Consider a galaxy at distance r, which is edge-on (so we need not correct for inclination). On average, such a galaxy will be moving away from us at speed $v = H_0\, r$ due to the expansion of the Universe, where $H_0 \approx 72\,\mathrm{km\,s^{-1}\,Mpc^{-1}}$ is the Hubble constant. This will redshift the measured wavelength of the HI-21cm line from its laboratory value, $\lambda_0 = 21.106\,\mathrm{cm}$, to $\lambda = \lambda_0\,(1+v/c)$. If V_c is the rotation speed of this galaxy, the gas on one side (the right-hand side, say) will move with speed $v + V_c$, while on the left-hand side the speed is $v - V_c$. Consequently the measured wavelength right and left are $\lambda_\mathrm{r} = \lambda_0\,(1 + (v + V_c)/c)$ and $\lambda_\mathrm{l} = \lambda_0\,(1 + (v - V_c)/c)$, respectively. The *difference* $(\lambda_\mathrm{r} - \lambda_\mathrm{l})/\lambda_0 = 2V_c/c$ yields the rotation speed.

What is the origin of this relation? The circular velocity depends on enclosed mass $M(< R)$ as

$$V_c^2 = \frac{\mathrm{G}\, M(< R)}{R}\,. \tag{9.1}$$

Let

[3]The circular velocity of spirals rises from the centre, then remains nearly constant. This maximum of the 'circular velocity' is denoted V_c below. Note also that the *measured* value depends on the inclination of the disk: V_c below is assumed to have been corrected for this.

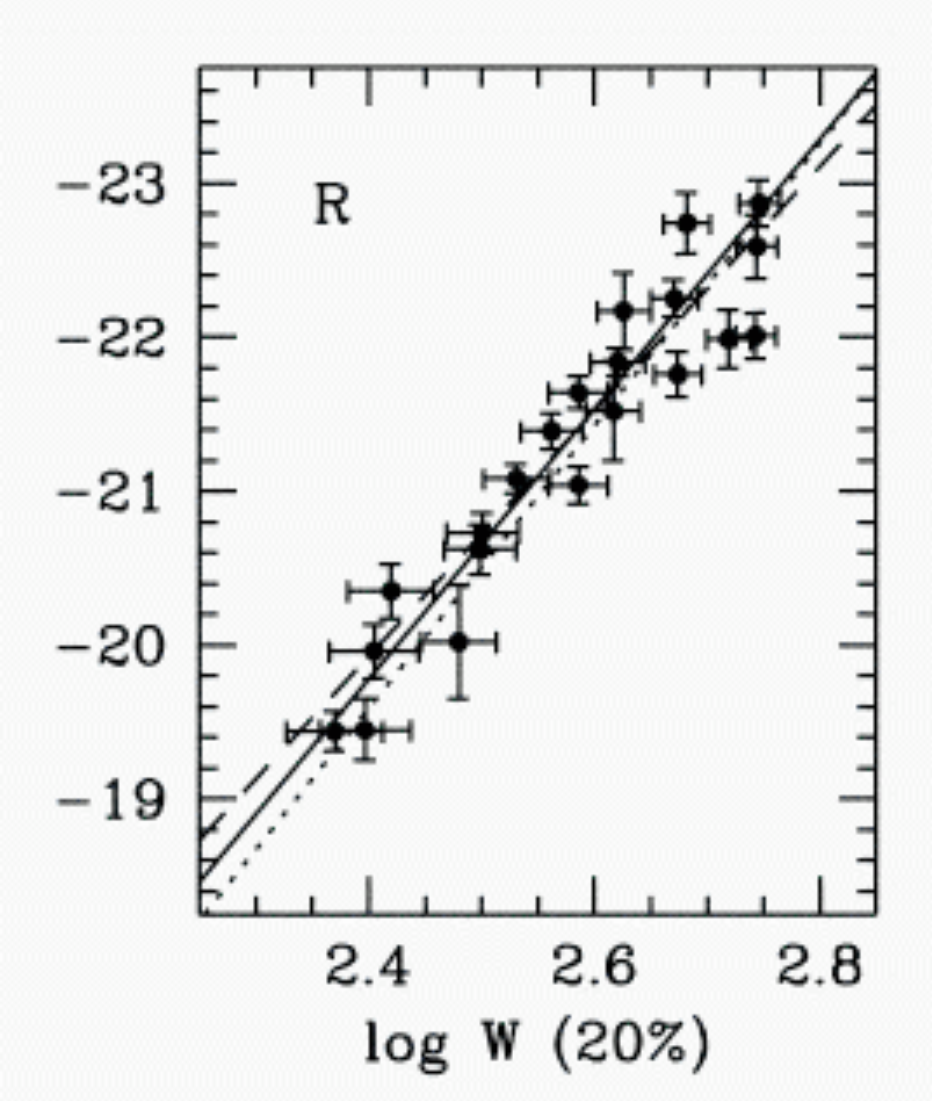

Figure 9.2: R-band absolute magnitude $R = -2.5 \log(I_R)$ of a set of spiral galaxies as function of their circular velocity $W \equiv V_c$ (in km s^{-1}). *Brighter* spiral galaxies (more negative R) rotate *faster* (higher W).

$$\Gamma \equiv \frac{M(< R)}{L}\,, \tag{9.2}$$

denote the global mass-to-light ratio, then

$$V_c^2 = \mathrm{G}\Gamma\,\frac{L}{R}\,. \tag{9.3}$$

.

The mass-to-light ratio Γ will depend on the type of stars in the galaxy (which determines L), and the amount of dark matter (which mainly determines M). The intensity I is the luminosity per unit area, $I = L/(\pi\,R^2)$, or solving for R

$$R = \left(\frac{L}{\pi\,I}\right)^{1/2}\,. \tag{9.4}$$

Therefore

$$L = \frac{1}{\mathrm{G}^2\,\Gamma^2\pi\,I}\,V_c^4\,. \tag{9.5}$$

This reproduces the Tully-Fisher relation *assuming* intensity I and mass-to-light ratio Γ are *independent* of the luminosity of the galaxy. Notice that this is not a *derivation* of the Tully-Fisher relation: we are just trying to understand what is required for spirals to follow this relation. The fact that Γ and I are independent of L implies that somehow stars and dark matter are closely linked, or in other words: the star formation history is largely determined by the mass of the dark halo of the galaxy.

The exponent α in the *observed* Tully-Fisher relation, $L \propto V_c^\alpha$, depends on colour (*i.e.* the broad-band filter through which L is measured: clearly our argument is not complete.

9.2.2 The Faber-Jackson relation in ellipticals (CO p. 987)

The Faber-Jackson law, Figure 9.3, relates the velocity dispersion σ of the stars in an elliptical galaxy with its luminosity L,

$$L \propto \sigma^4\,. \tag{9.6}$$

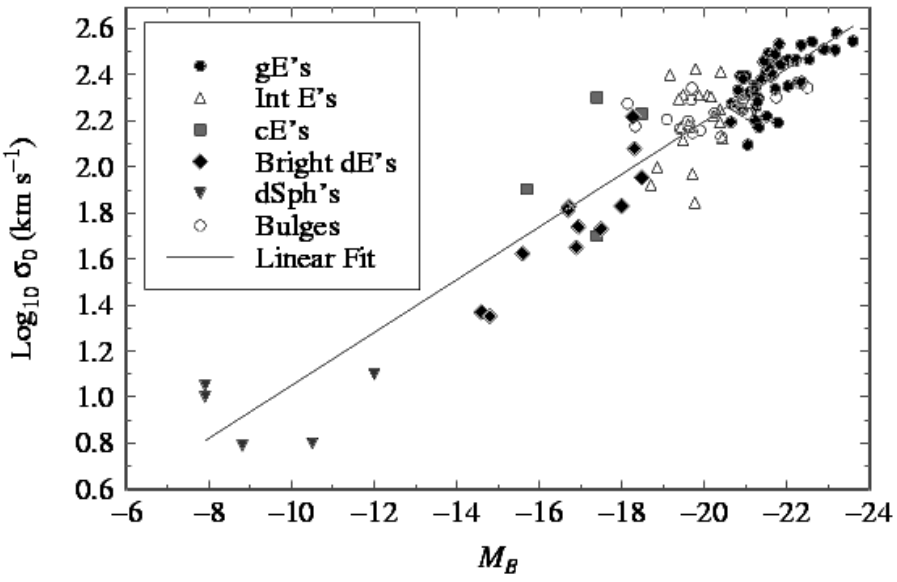

Figure 9.3: B-band absolute magnitude M_B for a sample of elliptical galaxies plotted versus their stellar velocity dispersion σ (in km s^{-1}). *Brighter* ellipticals galaxies (more negative $M_{\rm B}$) have a *larger* velocity dispersion: the **Faber-Jackson** relation

This is similar to the Tully-Fisher, but replaces V_c by σ. Measuring this relation again requires determining distances to a sample of elliptical galaxies, and measuring σ from line-widths in spectra.

Comparison of Figure 9.3 with Figure 9.2 shows that the *scatter* in the Faber-Jackson relation is significantly larger that that in the Tully-Fisher relation: spirals follow the TF relation much better than ellipticals follow the FJ relation. Following a similar reasoning that lead to the TF relation, we can improve on FJ.

Suppose an elliptical galaxy has luminosity L, stellar velocity dispersion σ, radius R, intensity I and mass-to-light ratio Γ. Assuming virial equilibrium,

$$\sigma^2 = \frac{\mathrm{G}M}{R} = \frac{\mathrm{G}\,\Gamma\,L}{R}\,. \tag{9.7}$$

Now *assume* Γ depends on L as

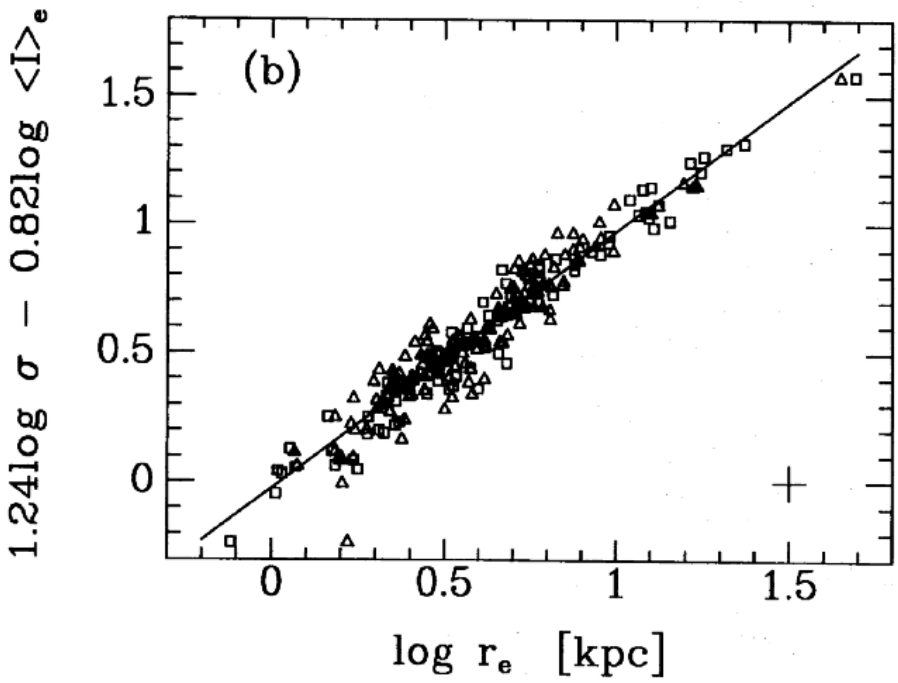

Figure 9.4: **The Fundamental plane relation** for elliptical galaxies between radius r_e, (central) intensity I_e and velocity dispersion σ, $r_e \propto \sigma^{1.24}\, I_e^{-0.82}$ (drawn line). Data points refer to the same sample of Es plotted in Figure 9.3. The galaxies follow this relation with significantly less scatter than in the Faber-Jackson relation in Fig.9.3.

$$\Gamma = \Gamma_\star\, (L/L_\star)^\alpha\,, \tag{9.8}$$

for some value of $\Gamma_\star$, $L_\star$ and α to be determined. Using $I = L/\pi R^2$ to eliminate L yields

$$\sigma^2 \propto \frac{L^{1+\alpha}}{R} \propto \frac{(R^2\, I)^{1+\alpha}}{R} \propto I^{1+\alpha}\, R^{1+2\alpha}\,, \tag{9.9}$$

or

$$R \propto \sigma^{2/(1+2\alpha)}\, I^{-(1+\alpha)/(1+2\alpha)}\,. \tag{9.10}$$

Figure 9.4 shows that the same galaxies plotted in Figure 9.3 follow the relation

$$R \propto \sigma^{1.24}\, I^{-0.82}\,, \tag{9.11}$$

very well. Choosing $\alpha = 0.25$ in Eq. (9.10) yields $R \propto \sigma^{1.33}\, I_e^{-0.82}$, close to what is observed. Put differently, *if* the mass-to-light ratio of ellipticals depends on luminosity as $\Gamma \propto L^{0.25}$, then we can understand why ellipticals follow the relation plotted in Figure 9.4 so tightly.

Relation Eq. (9.11) is called the **fundamental plane**: in the 4D space with axes L, R, σ and I, galaxies are close to the plane defined by this relation, hence 'fundamental plane'. Note that once more we have not *derived* this equation: we used simple arguments to understand what is needed for galaxies to follow the observed relation. In contrast to spiral galaxies, we had to assume that Γ depends on L: somehow stars and dark matter in an elliptical galaxy conspire to have a mass-to-light ratio that depends on total luminosity as $M/L \propto L^{0.25}$.

9.3 Tully-Fisher and Fundamental plane relations as standard candles

The Tully-Fisher relation in spirals , $L \propto V_c^4$ (Eq.9.5), and the fundamental plane relation, $R \propto \sigma^{1.24}\, I^{-0.82}$ (Eq. 9.11), both relate quantities independent of distance (V_c, respectively, σ and I) to intrinsic quantities (luminosity L and size R, respectively). This makes both relations useful as *standard candles*.

Suppose we were to determine the proportionality constant A in the Tully-Fisher relation, $L = A\, V_c^4$, by inferring luminosity L from flux F and distance r from Cepheid measurements for local spirals (using $F = L/4\pi r^2$). For spirals too distant for Cepheid measurements, we can determine their distance from measurements of V_c (distance independent) and flux, by applying the Tully-Fisher relation.

Similarly we can use local ellipticals to determine the proportionality constant B in the fundamental plane relation, $R = B\, \sigma^{1.24}\, I^{-0.82}$. For more distant ellipticals we can determine the distance independent quantities σ and I, apply the fundamental plane relation to infer R, and get the galaxy

distance by measuring its angular size $\theta = R/r$.

Both methods are widely used, since measuring velocities is relatively easy from a good quality spectrum, and can be done even for faint and/or distant galaxies. And since the scatter in the relations is small, we can obtain a relatively accurate distance estimate.

9.4 Galaxy luminosity function (CO p. 991)

The galaxy luminosity function is simply a histogram of the number of galaxies per unit volume, binned as function of their luminosity (Fig. 9.5). This requires knowing distances r to the galaxies, for example using the Tully-Fisher or fundamental plane relation, or simply assuming $r = v/H_0$. The shape of the luminosity function is well captured by the **Schechter** function

$$\frac{dN}{dL/L_\star} = N_\star \left(\frac{L}{L_\star}\right)^\alpha \exp(-L/L_\star)\,, \tag{9.12}$$

which has three parameters: $L_\star$, $\alpha \sim -1$ and $N_\star$. At low luminosities $L \ll L_\star$, the number of galaxies increases $\propto L^\alpha \sim 1/L$. At high luminosities $L \geq L_\star$, the number of galaxies drops exponentially. Finally, $N_\star$ is a normalisation constant, which determines the mean number density of galaxies.

Observed values are $N_\star \approx 0.007\mathrm{Mpc}^{-3}$, $-1.3 \leq \alpha \leq -0.8$, and $L_\star \approx 2 \times 10^{10} L_\odot$ in the B-band. From Tables 3.1 and 3.2, we find that the total B-band luminosity of the MW is about $1.8 \times 10^{10} L_\odot$, so the MW is just slightly fainter than an $L_\star$ galaxy.

When the faint-end slope is steeper than $\alpha = -1$ the total number of galaxies per unit volume, $N = \int_0^\infty (dN/dL)\, dL$, diverges, because there are so many faint galaxies. In reality, this does not happen of course: there must be a *finite* number of small galaxies. The mean luminosity follows from integrating

$$\langle L \rangle = \int_0^\infty L \frac{dN}{dL}\, dL/N\,. \tag{9.13}$$

$N \langle L \rangle$ is the mean luminosity per unit volume. Combining this with the mean density of the universe as obtained in section 8.4, we can estimate the

mass-to-light ratio for the Universe as a whole!

Finally, Figure 9.6 shows how different galaxy types contribute to the total luminosity function, and how this depends on environment.

9.5 Epilogue

The classification of galaxies that we have used so far, in terms of spirals and ellipticals, is based largely on how these galaxies appear in pictures. With several 10^5 galaxies in modern surveys, it is not really possible to eye-ball all of them in order to classify them. In addition, it is not even necessarily the best way, and certainly not the only way, of classifying galaxies and identifying different types. With so many spectra and images available, new statistical techniques are presently being developed, where computer programs which do not suffer from human prejudices, such as principle component analysis and neural networks, decide how galaxies should be grouped and classified.

9.6 Summary

After having studied this lecture, you should be able to

- describe the density-morphology relation for galaxies
- describe the Tully-Fisher relation, and explain how it is used as a distance indicator
- describe the Faber-Jackson and fundamental plane relations, and explain how they are used as a distance indicator
- explain what the luminosity function is, and sketch it.

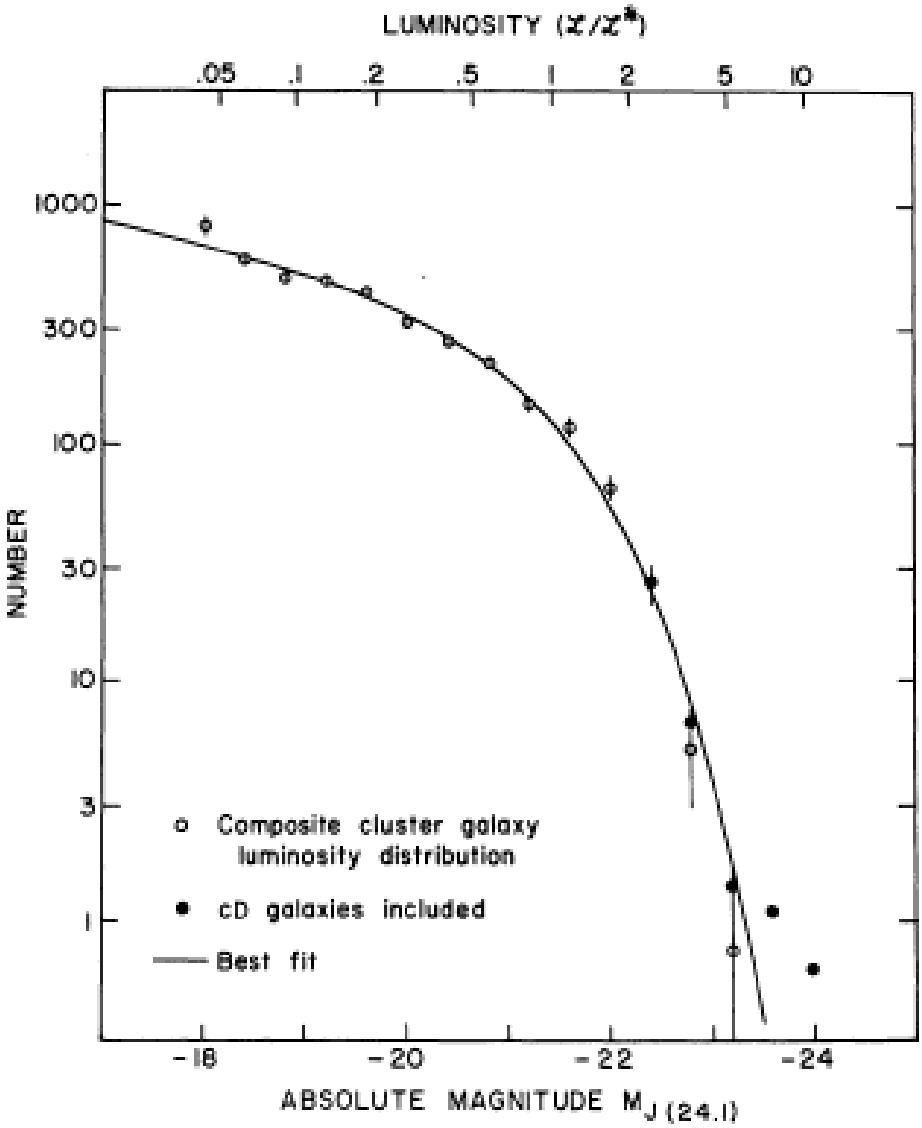

Figure 9.5: Galaxy luminosity function (symbols) together with best-fit Schechter function (drawn line).

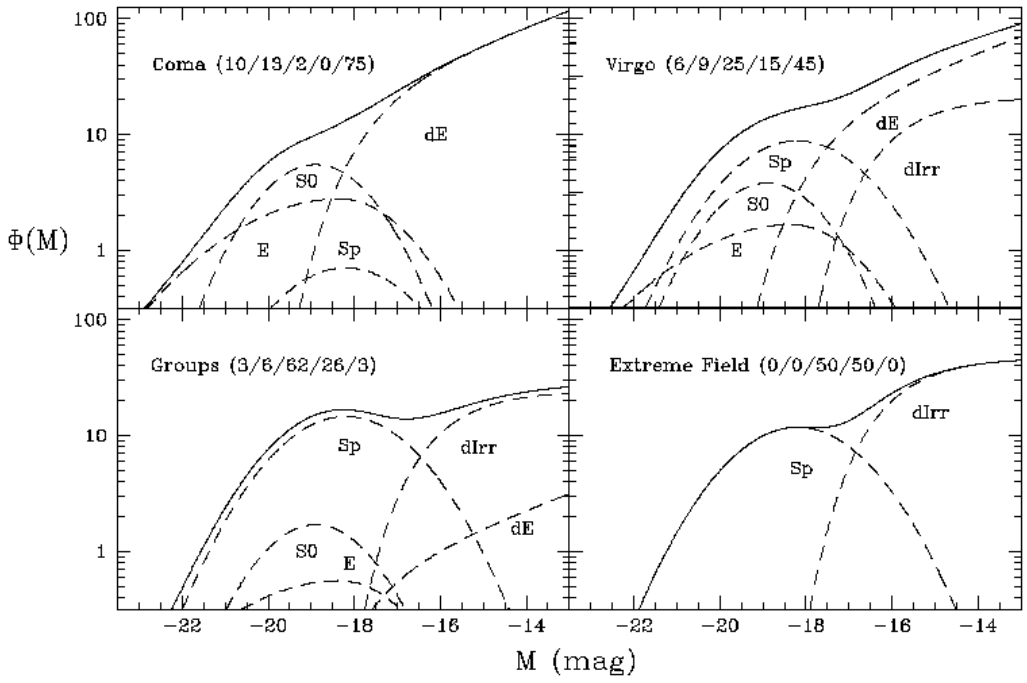

Figure 9.6: Contribution of different galaxy types to the total galaxy luminosity function, $\Phi \equiv dN/dL$. The different panels illustrate how the luminosity function depends on environment: note the predominance of types E and S0 in the Coma galaxy cluster (top left), how spirals contribute more in groups, and the almost complete absence of E and S0 types in low density regions ('extreme field'). Figure taken from Dr Helmut Jerjen at the Australian National University

Chapter 10

Active Galactic Nuclei - or AGN

CO §28

Quasars are the most luminous objects in the known Universe, with the most extreme objects outshining the combined star light of a bright galaxy by a factor 10^5 or more. They are one of the many observational manifestations - such as strong X-ray emission, radio emission, emission of energetic particles, jets - of an *active galactic nucleus*, *i.e.* of a powerful energy source lurking in the centres of $\approx$ 1 per cent of massive galaxies. AGN are thought to be powered by accretion of gas onto a central super massive black hole, with masses $10^6 - 10^9 M_\odot$. There is strong observational evidence that most massive galaxies contains such a massive black hole, the Milky Way harbours a super massive black hole of mass $\sim 4 \times 10^6 M_\odot$. The small fraction of AGN amongst massive galaxies results most likely from the massive black hole being starved of mass to accrete.

10.1 Discovery and observational properties

The discovery of AGN and the realisation that a variety of curious observational phenomena were all due to mass accretion onto a central supermassive black hole, had quite a checkered history.

Seyfert reported in 1943 that a small fraction of galaxies have a very bright and unresolved nucleus, emitting radiation characterised by emission lines produced by gas atoms in a wide range of ionisation stages. These are turned out to be feeble members of the AGN family, where the light and ionising radiation are both originating from very close to the central black hole.

Radio surveys in the 1950s uncovered many sources not obviously associated with optical counterparts. The radio radiation itself is produced due to a process called *synchrotron radiation*: EM radiation produced by electrons spiralling along magnetic field lines. This results in a nearly power-law spectrum, and the absence of any emission or absorption lines in such a spectrum makes it impossible to determine the redshift of the source. Identification of the radio source then requires matching up the position of the radio source with that of an optical counterpart - *e.g.* the host galaxy. The third brightest radio source on the sky, Cygnus A, was found to be coincident with a peculiar-looking cD galaxy, whose centre is encircled by a ring of dust, at a redshift of $\Delta\lambda/\lambda_0 = 0.057$. This implies a large distance to the source, and a very high radio luminosity, around 10 times the total bolometric luminosity of the Milky Way.

In 1960, Matthews and Sandage attempted to identify the optical counterpart to the radio source 3C 48[1]. The radio source was coincident with a faint 16th magnitude star-like object (*i.e optically unresolved*), with a very curious optical spectrum featuring broad emission lines that they could not identify with any known element or molecule. Sandage put it very scientifically: 'This thing is exceedingly weird'. Another such weird object was found in 1963, associated with the radio-source 3C 273. Given these objects looked like stars, they were dubbed quasi-stellar objects - *QSO* - or quasi-stellar radio sources - *quasar*.

The Dutch astronomer Maarten Schmidt realised in 1963 that the pattern of lines in 3C 273 was similar to that of the Balmer series[2] of the Hydrogen atom – but only if they were redshifted to the (improbably large ?) value of $\Delta\lambda/\lambda = 0.16$, implying a recession velocity of $0.16c$ and a distance of $\sim$

[1]The third Cambridge radio-survey.

[2]The Balmer series is the series of electronic transitions which end at $n = 2$.

660Mpc. The distance to 3C 48 was even greater: a recession velocity of $0.367c$ and a distance of 1800Mpc.

Such large distances imply exceedingly bright sources: a distance of $r = 660$Mpc implies a distance modulus of $m - M = -5\log(r/10) \approx 39$, therefore the measured apparent magnitude of $m = 12$ of 3C 273 yields an absolute magnitude of $M = -26$, compared to $M = 5$ for the Sun. The luminosity of this source is therefore $L = 10^{31/2.5}\, L_\odot = 2.5 \times 10^{12} L_\odot$, or about 100 times the luminosity of the entire Milky Way. What kind of object can be so small - because unresolved - yet so tremendously powerful?

Current quasar surveys contain $\sim 10^5$ sources, with the current redshift record held by a source[3] at $z = 7.1$. The luminosity of the brightest quasars can range up to 10^5 times the luminosity of the MW.

AGN may be detected from radio, over optical and UV, to X and gamma-rays, and the most energetic cosmic rays are also suspected to be produced by AGN. However confusingly, not all AGN are visible over this entire wavelength range. QSOs by definition are bright in the optical, but some powerful AGN are only detected in the radio, or in X-rays, but are not detected or very faint in the optical, say. Other observational manifestations of AGN include jets, radio lobes, and cavities filled with high-energy particles carved-out in the hot X-ray gas of clusters. Although the ultimate source of energy is presumably mass accretion onto a super massive black hole, it is still not very clear why this results in such a large variety of AGN phenomena.

10.2 Accretion onto super massive black holes

The basic model for energy generation by an AGN is accretion of gas onto a super massive black hole. Similarly to stellar mass black holes ('Stars' lectures), accreting gas will form an accretion disc, and gas needs to lose angular momentum to spiral in. As the gas moves in, the disc becomes

[3]When interpreted as a Doppler shift, the velocity of this source $v = z\,c = 7.1\,c$. A proper description applies the Friedmann-Robertson-Walker metric to the Universe, and the redshift is not interpreted as a velocity: the photons from the quasar always move with just the speed of light. Note that it is incorrect to attempt to 'correct' this seemingly superluminal motion by using special relativity.

progressively hotter, and so we expect that X-rays from the AGN will be produced in the inner parts of the disc, potentially close to the event horizon.

10.2.1 Why AGN variability hints at black hole accretion

The luminosity of AGN fluctuates in time, on a range of time scales that depend on wavelength. Variability in the X-rays occurs on the scale of minutes[4]. This implies that the extent of the region that produces the X-rays is of the order of light minutes - *i.e.* of order of the distance Earth-Sun. Indeed to get large variations in X-ray luminosities the whole emitting region needs to take part - and that can only be orchestrated if information can travel across the region[5] - which it does at speeds not larger than c. The extreme small size of the AGN engine, combined with its extreme power, rules out most alternative to the hypothesis that black hole accretion powers AGN.

10.2.2 Eddington limited accretion

Consider an object with mass $M_{\rm BH}$ (a super massive black hole) accretion mass at a rate $\dot{M}$. If all the rest mass of the accreting gas were converted into radiation, then the luminosity of the object would be $\dot{M}c^2$ (using Einstein's famous $E = Mc^2$ equation). It is thought that AGN come close to radiating at this maximum efficiency, with accretion luminosities of

$$\begin{aligned} L &= \eta \dot{M} c^2 \\ \eta &\approx 0.1 \,. \end{aligned} \tag{10.1}$$

The efficiency η is estimated from considerations of the last stable orbit around a black hole[6]. The value of $\eta = 0.1$ is much higher than the energy efficiency of *stars* since Hydrogen fusion only manages a meagre efficiency of 0.007.

[4]The variability is not periodic, more like flickering.

[5]Think of it in terms of a *Mexican wave* in a sports stadium: spectators need to be able to see the wave approaching if they want to take part.

[6]In Newton mechanics, circular orbits around a point mass are stable - but this is no longer the case in general relativity when the radius of the orbit is close to the event horizon. The value of $\eta = 0.1$ quoted in the text applies to a Schwarzschild - or non-spinning - black hole.

Curiously, the mass of the black hole does *not* increase as $\dot{M}_{\rm BH} = \dot{M}$ - because the extreme luminosity that is radiated by the black hole represents a mass-loss term. The correct relation is then

$$\dot{M}_{\rm BH} = \dot{M} - \frac{L}{c^2} = (1-\eta)\,\dot{M} = \frac{1-\eta}{\eta}\frac{L}{c^2}\,. \tag{10.2}$$

The steady state accretion rate is limited by the *Eddington limit*. Indeed, consider a spherical shell of gas of radius r, and thickness, dr, containing Hydrogen with number density n. This shell feels gravity exerted (mostly) by the black hole pulling the gas inward. But radiation streaming through the shell pushes the shell away due to radiation pressure. If the radiation pressure is too large, the net force is outward, and the black hole can no longer accrete mass. To compute this 'Eddington luminosity' we equate the gravitational force to the force exerted by the radiation pressure[7].

For simplicity we consider a shell consisting of Hydrogen (neglecting other elements) which is fully ionised (by the ionising radiation of the black hole). Its mass density $\rho = m_{\rm H}\, n$ and so the (inward) gravitational force (neglecting self gravity) is

$$F_{\rm G} = \frac{G\, M_{\rm BH}\, 4\pi r^2\, dr\, \rho}{r^2}\,. \tag{10.3}$$

The (energy)flux impinging on the shell is $F_{\rm E} = L/(4\pi r^2)$. Since a photon of energy E has momentum E/c, this corresponds to a momentum flux of $F_{\rm p} = L/(4\pi r^2\, c)$. To calculate the radiation pressure we need to know the interaction cross section of the radiation with the matter. One interaction process is Thomson scattering of photons off electrons, with the wavelength independent Thomson cross section, $\sigma_T = 6.625 \times 10^{-29}$ m^2. The force on a single electron is thus $F_{\rm p}\,\sigma_T$, which mulitplying with the number of electrons in the shells yields the radiation force on the shell as

$$F_{\rm L} = \frac{L}{4\pi r^2\, c}\,\sigma_T\,(4\pi\, r^2\, dr\, n)\,. \tag{10.4}$$

Setting $F_{\rm G} = F_{\rm L}$ yields the expression for the Eddington luminosity,

$$\begin{aligned} L_{\rm Edd} &= \frac{4\pi G\, M_{\rm BH}\, c\, m_{\rm H}}{\sigma_T} \\ &= 3.3 \times 10^{12}\, \frac{M_{\rm BH}}{10^8\, M_\odot}\, L_\odot\,. \end{aligned} \tag{10.5}$$

[7]Recall the identical derivation in the *Stars* part of this course

Comparing this with the values of the QSO luminosity inferred for 3C 273 above immediately suggests that the black holes in QSOs are indeed extremely massive, of order $10^8\,M_\odot$.

10.2.3 Growth of black holes

Once a seed black hole exists, it can grow in mass through accretion and merging with other black holes. How black hole seeds form is unclear: they may simply be remnants of massive stars ending their lives as black hole remnants, or may form through a completely different route, for example direct collapse of a gas cloud.

The Eddington luminosity implies a maximum rate at which a black hole can grow through accretion, which follows from replacing L in Eq. (10.2) with $L_{\rm Edd}$ from Eq. (10.5):

$$\begin{aligned} \dot{M}_{\rm BH} &\leq \frac{M_{\rm BH}}{\tau_{\rm S}} \\ \tau_{\rm S} &\equiv \frac{\eta}{1-\eta}\,\frac{\sigma_T\,c}{4\pi\,G\,m_{\rm H}} = \frac{\eta}{1-\eta}\,4.5\times10^8{\rm yrs}\,. \end{aligned} \tag{10.6}$$

This time scale is called the *Salpeter time*. When growing at its fasted rate through accretion, the mass of the black hole increases exponentially,

$$M_{\rm BH}(t) = M_{\rm BH}(t=0)\,\exp(t/\tau_{\rm S})\,, \tag{10.7}$$

where $M_{\rm BH}(t=0)$ is the seed mass. Although this is quite fast, it is still difficult to understand how to form the $\sim 10^9 M_\odot$ redshift $z=7.1$ black hole mentioned before, since the age of the Universe was only $t\sim 0.79$ Gyr at this redshift. Even if the seed were in place at the time of the Big Bang, it would have to have had a mass of $M_{\rm BH}(t=0)\sim 100 M_\odot$.

10.2.4 Unification schemes

If mass accretion powers AGN, why is there such a variety of observational manifestations? Angular momentum ensures that gas accreting onto a black hole forms an *accretion disc*, and it may be that the orientation of the observer with respect to the disc explains part of the variety - for example see

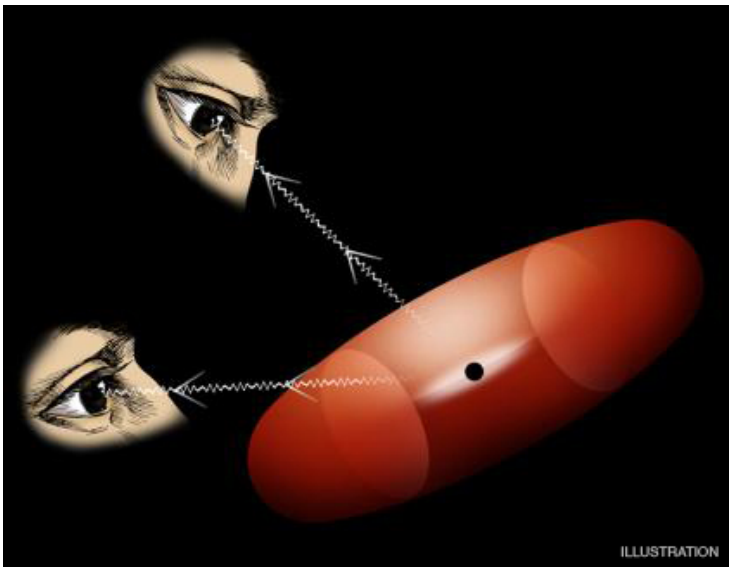

Figure 10.1: Depending on the orientation of the observer with respect to the torus of gas surrounding the black hole, the AGN may look different. Seen from above, the observer sees very close to the centre and may see an optically bright source - a QSO. Seen from the side, optical/UV light gets obscured and the observer does not see a QSO. Figure credit: Chandra observatory.

the disk nearly pole on and you detect the optical/UV light emitted and infer the presence of a QSO, but see it edge on and the disk absorbs all optical/UV light - so no QSO. However that does not explain why some AGN have huge extended radio lobes and others don't. A *unification scheme* tries to explain the variety of phenomena in terms of properties of the accretion disc.

10.3 Evidence for super massive black holes

Some of the best evidence for the presence of super massive black holes (SMBH) in galaxies is for systems in which the black hole is not active - *i.e.* for galaxies without an AGN. The evidence derives from observations indicating the presence of a very massive but small object in the centre - but there is as of yet no really convincing evidence that this object has an event horizon. The dynamical evidence is based on properties of stars, and of gas, in the very centres of galaxies.

10.3.1 Evidence from stellar dynamics

Central cusps

The Jeans equations relate stellar density and stellar velocity dispersion to enclosed mass. For a spherical system (see Eq. **??**):

$$\frac{G\,M(<r)}{r^2} = -\frac{1}{\rho_\star}\frac{\partial}{\partial r}(\frac{1}{3}\rho_\star\sigma_\star^2)\,. \tag{10.8}$$

Away from the SMBH, the enclosed mass, $M(<r)$, is dominated by stars and dark matter. However very close to the SMBH it's mass dominates $M \approx M_{\rm BH}$, the left hand side $\propto 1/r^2$, and the black hole requires a sharp increase in $\rho_\star$ - a *cusp* - an increase in stellar velocity dispersion $\sigma_\star$, or both.

The expected angular extent of such a cusp is of order

$$\begin{aligned} r_c &\approx \frac{GM_{\rm BH}}{\sigma_\star^2} \\ &= 1{\rm arcsec}\frac{M_{\rm BH}}{2\times10^8 M_\odot}\,(\frac{\sigma_\star}{200{\rm km\ s^{-1}}})^{-2}\,\frac{R}{5{\rm Mpc}}\,, \end{aligned} \tag{10.9}$$

for an object at distance R. This is small, even for a very massive BH in a relatively nearby galaxy. HST did show that some nearby ellipticals are

consistent with having a cusp. However this still does not *require* the presence of an SMBH, because stellar orbits need not be isotropic near the black hole. If they're not, then the spherical Jeans equation is not valid. Hence the evidence is suggestive, but not unambiguous.

Motions of stars near the centre of the Milky Way

The Milky Way centre coincides with the radio source Sagittarius A* - a very weak AGN. Recent *Fermi* satellite measurements found evidence for a pair of giant gamma-ray bubbles (sizes ~ 20 kpc), which might be due to increased activity of the central black hole, several millions of years ago.

More direct evidence for the presence of an SMBH in the MW comes from observations of the motions of stars near the centre. Infrared[8] astrometry of stars near the centre performed over several years allowed Genzel and collaborators to measure *orbits* of these stars. Some move at very high speeds (several 1000s km s^{-1}) around a central object, and the mass of this object, $M \sim 4 \times 10^6 M_\odot$, is calculated simply using Kepler's laws[9]. This high mass, combined with the small extend in which it is contained, makes the conclusion this really is a black hole, almost - but not quite - unavoidable.

10.3.2 Evidence from gas kinematics

Inferring masses using *gas dynamics* as opposed to stellar dynamics, is general more assumption free, because we do not need to know or measure velocity anisotropy. However there is a caveat in that there may be non-gravitational forces acting on the gas, magnetic fields or radiation pressure for example.

Optical emission lines HST found several examples of nuclear gas disks, some of which are in Keplerian rotation with rotation speeds of up to 1000 km s^{-1} at a distance of 19 pc from the centre. Applying Kepler's law yields masses of $\approx 10^9 M_\odot$ for the central object - again very suggestive for the presence of an SMBH in these galaxies.

[8]Infrared observations allow observations of the centre, as the IR light is not obscured by dust.

[9]Kepler's law provide the 3D orbit - whereas we only see the projected 2D orbit. Comparison allows us to infer the distance to the centre of the Milky Way as well.

Maser emission Some AGN containing *masers*[10] in orbit around the centre of the galaxy. Doppler shift measurements, combined with applying Kepler's law, again allows us to infer the presence of a very massive central object - consistent with the presence of an SMBH.

Reverberation mapping An elegant way to determine the extent of an AGN is *reverberation mapping*. Many of the emission lines seen from an AGN are due to the light from the central source being reprocessed by the surrounding material. As the central source varies in luminosity, the emission lines vary as well, but with a time-lag that corresponds to the light-travel time between the central source and the line-emitting gas. An estimate for the size of the light-emitting region follows from measuring the time lag.

10.3.3 Profile of X-ray lines

The Fe Kα line at 6.4keV is a common feature in the X-ray spectra of AGN. It is thought to arise from fluorescence in the colder material in the surroundings of the source, irradiated by the X-rays from the source.

This line is produced very close to the SMBH, and it exhibits Doppler motions approaching relativistic speeds, $\sim 10^5$km s$^{-1} \approx 0.3c$. Now crucially, the line-profile displays asymmetries consistent with a *gravitational redshift*. The photons lose energy as they climb out of the deep potential well near the black hole. In doing so, their wavelengths become longer – a 'gravitational redshift'.

For the AGN galaxy MCG-6-30-15, the best fitting accretion disk has an inner radius of 6 Schwarzschild radii, i.e. *very* close to the event horizon. A similar analysis has now been performed for other AGN as well. **The shape of the line probably provides the best evidence to date for the existence of SMBHs.** However, other mechanisms for generating the line profile are possible, but implausible. With better data, detailed modelling of the profile even has the potential to determine the spin of the SMBH, by measuring another general relativistic effect called frame-dragging.

[10] A *maser* is a laser that operates in the microwave regime.

10.4 Epilogue

A small fraction of galaxies contains an immensely luminous source of radiation in their centres: these are called active galactic nuclei. These sources display a large variety of observational manifestations, and are thought to be powered by accretion onto a black hole.

We have evidence that probably most, if not all, galaxies with masses of order the MW mass or higher, have a SMBH in their centres, although the evidence that this is really a black hole (as opposed to a very massive dense object) is weaker. Most of these SMBHs are starved of fuel: this explains why most galaxies have a SMBH yet are not AGN.

And finally: a star venturing too close to a SMBH may be torn apart as a result of the tidal forces. This could lead to a very bright flare lasting for of order months. The realisation that SMBHs may be quite common provides fresh motivation to search for such flares. Upcoming missions designed to detect SNe will find these flares – if they exist.

10.5 Summary

After having studied this lecture, you should be able to

- describe observational manifestations of AGN.
- describe briefly the current paradigm for energy generation in AGN (mass accretion through a disk onto a SMBH)
- related the mass accretion rate to luminosity for AGN, and apply the concept of Eddington limited accretion to the maximum growth rate of black holes
- describe three arguments that suggest the presence of SMBHs in galaxies.

Chapter 11

Gravitational lensing

CO §28.4

A massive object distorts space-time around it, as described by General Relativity. The distortion due to the presence of the Sun makes the planets orbit around it on ellipses. When light travels through a curved space-time due to the presence of mass it also gets deflected. The deflection is in general small, therefore our view of the near and distant Universe is generally not greatly affected.

The gravitational field generated by a mass distribution, for example due to stars, galaxies, or clusters of galaxies, distorts the image from background objects. A good analogy is how hot air (above a road in summer, say), distorts the view behind it, because the index of refraction of air depends on temperature. Similarly, the gravitational distortion of space-time acts as if the index of refraction varies in space. This effect is called 'gravitational lensing', although 'gravitational miraging' might be a better description since the distortion is more 'blurring' (like the hot air) than focusing (like a proper lens).

A very good introduction to the subject is the recent review by Joachim Wambsganss[1], who claims that a German physicist in 1804 was the first to suggest that gravitational lensing might be observable, for example in terms of the deflection of star light passing close to the Sun.

[1] see http://www.livingreviews.org/Articles/Volume1/1998-12wamb

Just as with any lens, there are several possible observable effects of gravitational lensing:

1. *deflection*: the image position is displaced from the source position,
2. *amplification*: the image may be become brighter or fainter,
3. *distortion*: if the source is extended (for example lensing of a galaxy by a galaxy cluster), then lensing may distort the image,
4. *multiple images*: in general a single source will be imaged in multiple images.

All these effects have been observed.

Even though gravitational lensing is generally weak, it has become a powerful tool in Astronomy: this chapter discusses some of the applications.

11.1 The lens equation

11.1.1 Bending of light

Suppose a particle with mass m and velocity v flies with impact parameter b past an object with mass M. The gravitational pull of M will deflect m, and give its velocity a component $v_\perp$ perpendicular to its initial v. For the case $m = M$ we derive the expression for the deflection angle α in the Appendix, see Eq. 12.4. Convince yourself that this is the correct result also in case $m \neq M$, the result is

$$\alpha = \frac{2GM}{b\,v^2}\,. \tag{11.1}$$

We use a trick to infer the deflection due to gravitational lensing: the expression for α does not depend on the mass m of the particle being reflected, only on the mass M of the deflector. So we might be tempted to put $m = 0$, $v = c$ and claim this is the angle by which light will be deflected as well.

Applying this to starlight grazing the surface of the Sun, we can use $M = M_\odot$, $R = R_\odot = 7 \times 10^5$km, which yields $\alpha = 0.83$arcsec – so $\alpha \ll 1$

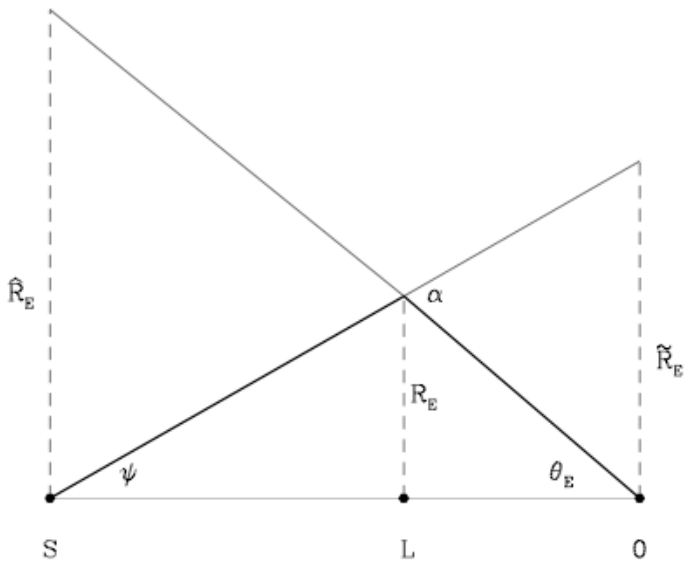

Figure 11.1: Gravitational lensing when source (S), lens (L) and observer (O) are all aligned. Light from S is deflected by an angle α toward O. Because of symmetry, O sees the source S as ring of radius R_E centred around L.

is certainly satisfied. This was actually the value Einstein found in 1911, though *Johann Soldner* already obtained it almost a century earlier.

Curiously, the answer is wrong! Once Einstein formulated his theory of General Relativity, he did the problem again, and found that the deflection angle is *twice* our 'Newtonian' value. So the correct deflection angle for light is

$$\alpha = \frac{4GM}{b\,c^2}\,, \tag{11.2}$$

and it was great vindication for GR when Eddington verified this during a solar eclipse in 1920. Note that the deflection angle increases with M and decreases with b – the closer you pass to the more massive an object, the bigger is the deflection.

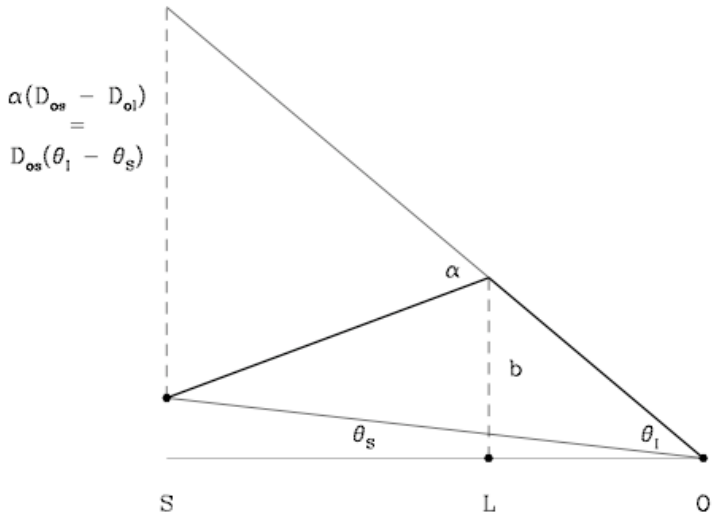

Figure 11.2: Gravitational lensing of point sources when source (S), lens (L) and observer (O) are not aligned. O sees two images of S, one of which is depicted here while the other one lies on the other side of L.

11.1.2 Point-like lens and source

Suppose light source (S), lens (L) and observer (O) are exactly aligned, as in Fig.11.1. Also assume they are point like (i.e. not extended like for example a galaxy). Light rays from S are deflected by L over an angle α toward O. Because of symmetry of the situation, O sees a ring of light around L: an Einstein ring[2].

Introducing the distances between observer and lens D_{OL}, observer and source D_{OS}, and lens and source D_{LS}, we can compute R_E and the angle θ_E under which O sees the ring. Since $\psi + \theta_E = \alpha$ we get, using the lensing equation and the figure,

[2]The figure is not to scale: α should be small if we want to apply the lensing equation.

$$\begin{aligned} \theta_E &= \frac{R_E}{D_{OL}} \\ \psi &= \frac{R_E}{D_{SL}} \\ \alpha &= \frac{4GM}{R_E\, c^2}\,, \end{aligned} \tag{11.3}$$

and hence

$$R_E^2 = \frac{4GM}{c^2}\,\frac{D_{OL}(D_{OS}-D_{OL})}{D_{OS}}\,. \tag{11.4}$$

If O, L and S are not aligned, as in Fig.11.2, O does not see a ring, but *two* images. Denote the angular position of S from the line OL by θ_S, and the angle between S and its image I by θ_I. Then $\alpha(D_{OS}-D_{OL}) = D_{OS}(\theta_I-\theta_S)$. A bit of juggling and using the lensing equation yields:

$$\theta_I^2 - \theta_I\theta_S = \theta_E^2\,. \tag{11.5}$$

This is a quadratic equation for θ_I for a given θ_S and so there will be *two* images, at positions $\theta_{I,\pm}$.

Often the change in position is too small to be unobservable (and in fact, we don't usually *know* the unlensed position!). But in addition to being lensed, images will also be *magnified* (or de-magnified). So when the displacement is too small to see two images, you'll only see one but magnified by total magnification $A = A_+ + A_-$ of each image separately. Interestingly, for a small fraction of peculiar alignments A formally *diverges*, in practice yielding potentially very large amplifications.

11.1.3 More realistic lensing

An extended lens yields an odd number of multiple images (3,5,7,...), depending on impact parameter and density distribution. If the *source* is extended as well, then different parts of the source may be deflected and amplified in various ways, and so the image may be highly deformed. We are now in a position to look for applications.

Figure 11.3 shows an example of an *Einstein ring*: a distant spiral galaxy gets lensed by an intervening elliptical, with a fortuitous alignment resulting

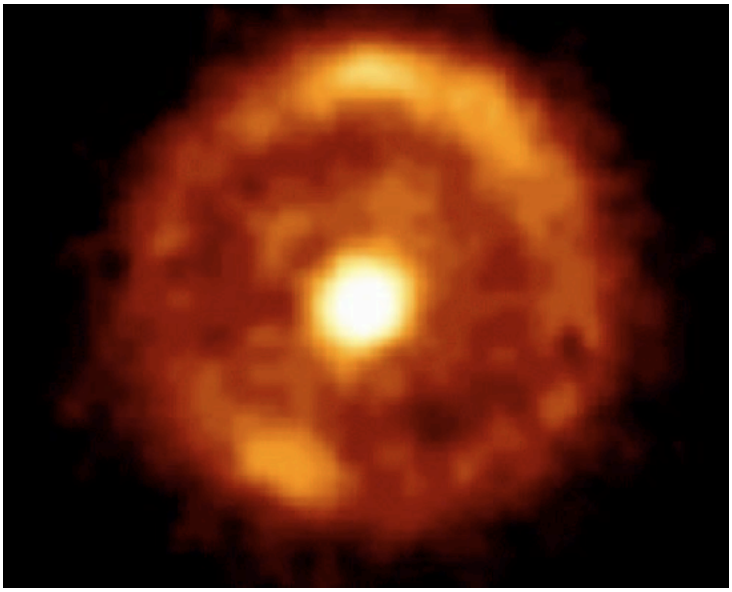

Figure 11.3: Hubble Space Telescope image of an Einstein ring, where a fortuitous alignment has caused an intervening elliptical galaxy (the central spot) to lens a background spiral galaxy into a ring.

in an almost perfect ring.

Figure 11.4 shows how a nearby spiral galaxy has lensed a very distant background quasar into multiple images, in this case five images.

11.2 Micro-lensing

A distant star may be lensed by an intervening star[3], a situation where we may apply the results for point source and point lens. We expect very small deflections, but potentially large magnifications for chance alignments.

Fortuitous alignment of a foreground Milky Way star with a star in the bulge, or the LMC, will brighten that star by a relatively large amount (up to

[3]I took this part, including the figures, from W Evans' 2003 review, see astro-ph/0304252

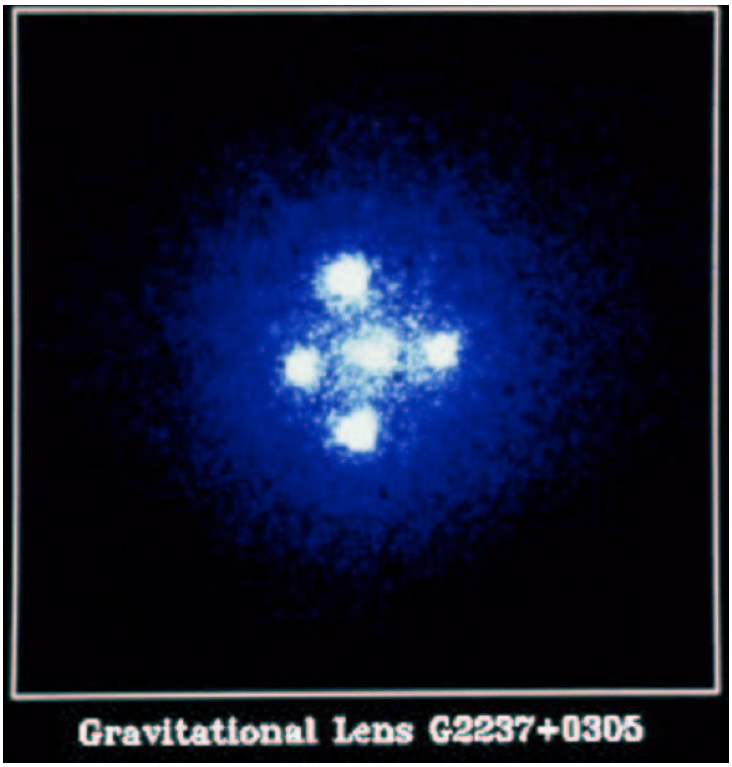

Figure 11.4: Hubble Space Telescope image of the 'Einstein cross', where a distant quasar has been lensed into multiple images by an intervening spiral galaxy.

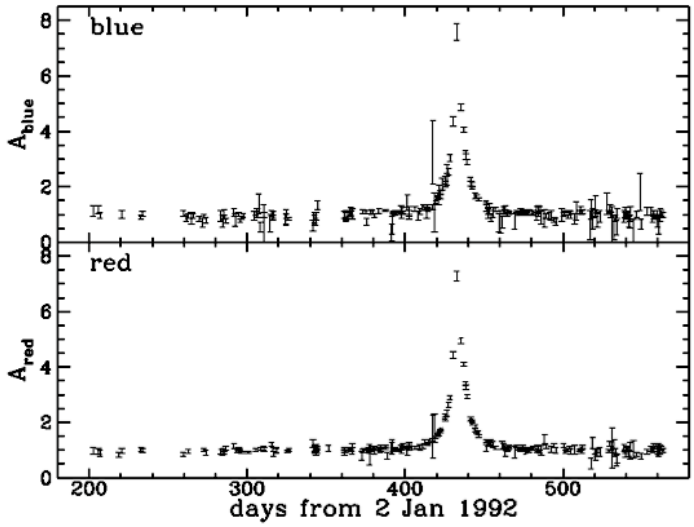

Figure 11.5: Luminosity of a star in the LMC in the blue (top) and red (bottom) as a function of time. Lensing causes it to brighten around day 420.

a factor of 30), during the few days where the alignment is very good. This phenomena is called *micro-lensing* (because the deflection angle is so small, $\sim 10^{-6}$arcsec). The alignment needs to be so good that only a very small fraction, around 1 in 10^7, of bulge or LMC stars, is brightened significantly at any time. Movements of the stars breaks the good alignment, which is why the duration of the lensing event is so short.

How can we be sure that the variation in flux is due to lensing, and not simply because we found a variable star? The deflection angle is independent of wavelength, as so is the amount of amplification. This is quite crucial, since luminosity variations in variable stars are usually colour dependent. In addition, the *shape* of the light curve is well defined, and because lensing is so unusual, a star brightened by gravitational lensing is expected to be lensed only once. If the flux detected from a star varies only once, with amplitude independent of wavelength, and with amplitude as function of time as well-fit by micro-lensing, then we can be confident we have indeed detected lensing. Figure 11.5 shows an example of micro-lensing of a star in the LMC, which brightens considerably around day 420, equally much in the blue as in the red.

Although we so far only considered lensing by stars, in fact any massive object will produce lensing. This has been exploited by the **MACHO collaboration**[4] to constrain the nature of the dark matter in the halo of the Milky Way. Indeed, suppose dark matter consisted of some type of massive objects, like black holes, or Jupiter-like objects, or any other type of **MA**ssive **C**ompact **H**alo **O**bject. Since we know that the outer parts of the Milky Way halo are dominated by dark matter, there should be many such objects between the Sun and the LMC. If they exist, then we should be able to detect them by their lensing signal.

The MACHO collaboration imaged millions of stars in the LMC every night for four years, and indeed found several lensing events like the one pictured in Fig.11.5. However, it is now believed that in each case, the lens is actually a normal star in the LMC, and *not* a dark matter clump in the Milky Way's halo. As a consequence, this experiment has now ruled-out a wide range of dark matter candidates. If the dark matter is some type of elementary particle, it will not lens LMC stars (well, it will, but $M \to 0$!), so that is still an option.

The future of micro-lensing is very bright. Suppose for example that the lens is a binary star – then the light curve of the lensed object may be much more complicated, as the source may be lensed by each component of the binary in turn. Such events have already been detected toward the bulge. This is also a very promising way for detecting *planets* around distant stars, and planned satellite missions will undoubtedly detect planets in this way.

11.3 Strong lensing

The effect of lensing increases with the mass of the lens. So can we use galaxy clusters with masses $\sim 10^{15} M_\odot$ as lens? Yes we can, and we do get large deflections of several tens of arc seconds up to several arc minutes.

Figure 11.6 is an HST image of a rich cluster of galaxies, containing many red ellipticals as expected. Because of the superb image quality of HST you

[4] http://wwwmacho.mcmaster.ca/

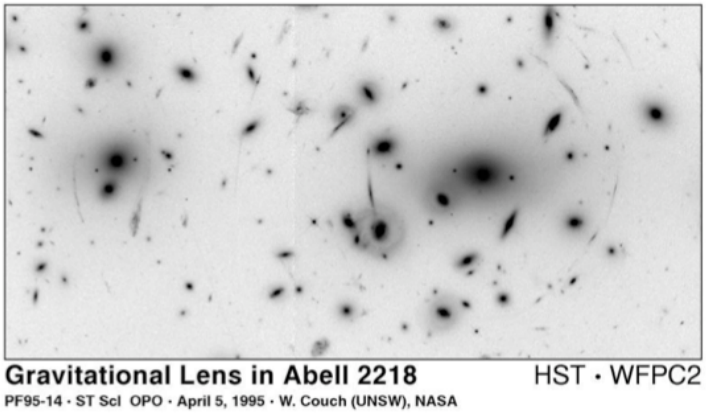

Figure 11.6: Hubble Space Telescope image of the rich cluster of galaxies Abell 2218. The large galaxies in the image are all massive elliptical galaxies in this galaxy cluster. The tens of arcs are images of *background* galaxies that have been lensed and distorted by the cluster's gravitational potential.

also notice tens of *tangential arcs*, centred on the cluster centre[5] These arcs are the distorted images of background galaxies lensed by the gravitational potential of the cluster. Such lensing can be used to determine the mass of the cluster, and also to study distant galaxies.

The locations and amplification factors of the lensed galaxies depend on the shape of the gravitational potential of the cluster, and hence lensing can be used to constrain the density distribution and also the total *mass* of the cluster. Note that the signal depends on the *total mass*, sum of baryonic and dark matter mass. In addition, the signal does not depend on the dynamical state of this mass. This makes gravitational lensing ideal for mass measurements[6]. Fortunately different mass measurements of clusters (dynamics, X-ray gas, gravitational lensing) agree reasonably well. All result in a mass considerably higher than can accounted for in stars or gas, hence suggesting large amounts of dark matter. Recent observations of the *bullet cluster* even

[5]Lack of resolution in ground-based observations makes it impossible to see these arcs.

[6]Previously we used the motion of galaxies, *assuming virial equilibrium*, or the properties of X-ray gas, *assuming* hydrostatic equilibrium, to determine the mass of clusters. Gravitational lensing does not need any such assumptions: the signal depends only on the mass.

suggest that the centre of mass, and the centre of the X-ray emission, do not coincide, even more suggestive for the presence of dark matter.

Several lensed galaxies are *multiply imaged*, i.e. you see the same lensed galaxy at various positions in the cluster. In addition, some have been magnified by a lot, sometimes as much as a factor of 30, and their angular size dramatically increased. The cluster acts as a giant telescope, allowing the study of faint and distant galaxies. The intervening lens makes distant small and faint galaxies appear bright and big, and so they can be studied in much more detail[7]. Astronomers deliberately target clusters in order to study better the faint galaxies behind it.

11.4 Weak lensing

The arclets seen in clusters arise because the image of the background galaxy is strongly deformed. Equation (11.2) shows that as we look at galaxies further from the projected centre of the cluster – hence with increasing impact parameter b – the distortion will become smaller and smaller. Eventually, we won't be able to detect the deformation for a single galaxy any more, but we could look at many galaxies in a given small patch of sky, and try to determine whether perhaps they are all slightly elongated in the same direction, as would be the case if there were a lot of mass nearby. This is called *weak lensing*: you try to identify the presence of a large mass in a given direction, from the fact that galaxies nearby in projection, tend to be elongated due to their distortion, in the *same* direction. This makes it possible to directly trace the mass distribution, without prejudice of requiring there to be light associated with the mass.

[7]The cluster also distorts the images of the galaxies: we need a good lens model to infer the intrinsic shape of these galaxies.

11.5 Summary

After having studied this lecture, you should be able to

- derive the Newtonian lensing equation (11.1)
- explain why alignment produces an Einstein ring, and derive its radius.
- explain how micro-lensing works and has been used to search for massive compact halo objects in the Milky Way halo
- explain how gravitational lensing has been used to estimate the mass of galaxy clusters, and hence infer that they contain dark matter.

Chapter 12

Appendix: Gravitational deflection of a test mass

Consider two stars with masses m flying past another at large speed v and impact parameter b, see Fig. 12.1. We want to compute the deflection angle α in case the deflection is small. To do so we approximate the orbit as a straight line, traversed with constant velocity v and calculate the velocity $v_\perp$ induced on the test star along the orbit. The deflection angle is then $\alpha = v_\perp/v$.

The component of the gravitational force perpendicular to the orbit is

$$\mathbf{F}_\perp = \frac{Gm^2}{b^2+(vt)^2}\,\cos(\theta) = \frac{Gm^2}{b^2}\,\left[1+(\frac{vt}{b})^2\right]^{-3/2}\,. \tag{12.1}$$

Combining this with Newton's law,

$$m\dot{\mathbf{v}}_\perp = \mathbf{F}_\perp\,, \tag{12.2}$$

yields

$$v_\perp = \frac{Gm}{bv}\int_{-\infty}^{\infty}(1+s^2)^{-3/2}\,ds\, = \frac{2Gm}{b\,v}\,, \tag{12.3}$$

and hence

$$\alpha \equiv \frac{v_\perp}{v} = \frac{2Gm}{bv^2}\,. \tag{12.4}$$

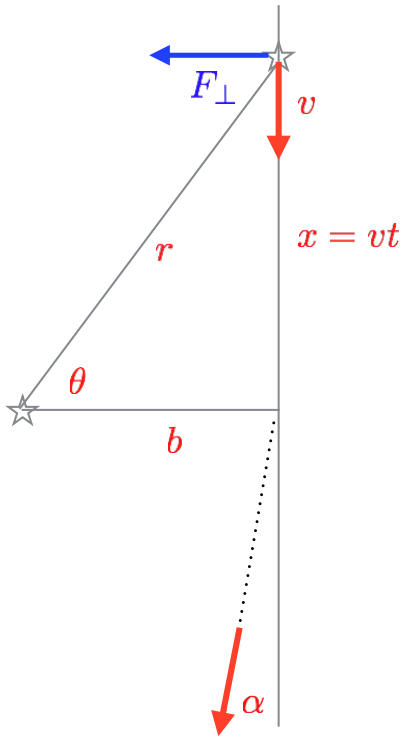

Figure 12.1: Deflection of test stars passing at velocity v and impact parameter b.

Chapter 13

Workshop questions

13.1 Stars & Galaxies, Workshop I

Question 1.

1. Describe the Hubble sequence.
   Answer: tuning fork with elliptical galaxies (red, roundish, no star formation little ISM) arranged along the handle of the tuning fork, from round (E0) to flattened (E7), where in En, $n = 10(1 - b/a)$ with a (b) the semi-major (semi-minor) axis. Spiral galaxies are dived into barred (SB) and unbarred (S), and further divided in S(B)a-c with a having a bigger bulge relative to the disk, and c having a smaller bulge.

2. Spiral galaxies have blue stars, whereas those in ellipticals are red. What does this imply for the different stellar populations?
   Answer: Massive stars are blue and also short lived. If the blue colour is due to massive stars, then it implies that the stars in Es are old, whereas Ss have recent star formation. The presence of metals in stars also affects colours: so stars in ellipticals tend to be more metal rich.

3. Define surface brightness, and demonstrate that it is independent of distance.
   Answer: surface brightness is the amount of flux dF detected per unit solid angle $d\Omega$, so SB=$dF/d\Omega$. Since the flux received decreases as $dF \propto 1/r^2$ whereas the surface area seen under a solid angle increase $\propto r^2$, the SB is independent of r (see notes)

4. Why can't you see the Milky Way's bulge in the optical? In which wavelength might you may able to see it? Why?
   Answer: In the optical the bulge is obscured by dust in the MW's disc. IR photons have longer wavelengths than the sizes of the dust grains and hence are much less absorbed.

5. Give the definition of a parsec, and compute its value in metres. Use 1 AU = 149.60×10^6 km.
   Answer: A parsec is that distance at which 1 AU has an angular extent θ of 1 arc second (1"). Therefore using the small angle approximation $1\text{pc} = 1\text{AU}/\theta$. hence $1\text{pc} = 1\text{AU}/(\pi/(180 \times 3600)) = 3.085 \times 10^{16}$ m. The factor $\pi/(180 \times 3600)$ converts arc seconds to radians.

6. Derive the equation $m - M = 5\log(r) - 5$ that relates the apparent magnitude, m, the absolute magnitude, M, and the distance r to a star in parsecs, when obscuration is neglected.

   Answer: Magnitudes are a relative scale, such that two stars with fluxes F_1 and F_2 have a magnitude difference of $m_1 - m_2 = -2.5\ \log(F_1/F_2)$. The flux of a star with luminosity L depends on distance r as $F = L/(4\pi r^2)$ in the absence of absorption.
   By definition, the absolute magnitude M of a star equals its apparent magnitude m at a distance of $r = 10$ pc.
   Therefore for a star at distance r,

$$\begin{aligned} m - M &= -2.5 \log\left((L/4\pi r^2)/(L/4\pi(10\text{ pc})^2\right) \\ &= -2.5 \log\left((\frac{10\text{ pc}}{r})^2\right) \\ &= 5\log(r/\text{pc}) - 5\,. \end{aligned}$$

Question 2
The absolute magnitude of the Sun in the B-band is $M_{\rm B} = +5.48$, and its luminosity $L_{\rm B} = 3.86 \times 10^{26}$ W.

1. Compute the flux from a solar type star in the Andromeda galaxy, at distance $r = 710$ kpc. Compute its apparent magnitude in the B-band.

2. Assume that the density of stars in Andromeda falls exponentially with height above the disk, $n(z) = n_0 \, \exp(-|z|/z_0)$, with $n_0 = 1$ pc^{-3}, where the scale-height $z_0 = 0.1$ kpc. Compute the surface density (σ) of stars (the number of stars seen per unit area), when the disk is seen face on.

3. Consider the flux, F, received from Andromeda from a square with side-length $\theta = 1$ arc seconds, assuming all its stars are like the Sun. Convert this to magnitudes. Assume Andromeda's disk is seen face-on.

4. Assume Andromeda has an exponential disk, where the number density of stars in cylindrical coordinates (R, z) follows

$$n(R, z) = n_0 \, \exp(-R/R_0) \, \exp(-|z|/z_0) \, , \tag{13.1}$$

with the disk scale-length $R_0 = 3$ kpc. Compute and plot the surface brightness in the B-band, $\mu_{\rm B}(R)$. Use the same values for n_0 and z_0 as above, and assume the disk to be face-on.

Answers:

1.

$$\begin{aligned} F &= L_{\rm B}/4\pi r^2 = 6.4 \times 10^{-20} \, {\rm W \, m^{-2}} \\ m &= 5.48 - 5 + 5 \log(r/{\rm pc}) = +29.7 \, . \end{aligned} \tag{13.2}$$

2. $\sigma = 2 \int_0^\infty \exp(-z/z_0) \, dz = 200$ pc^{-2}.

3. The surface area of the square is $(r\theta)^2$, when θ is expressed in radians, since $\theta \ll 1$. The number of stars in the square is $N = \sigma \, S$, so the flux

$$F = N \, L_{\rm B}/4\pi r^2 = \sigma \theta^2 \, L_{\rm B}/4\pi \, . \tag{13.3}$$

is distance independent.

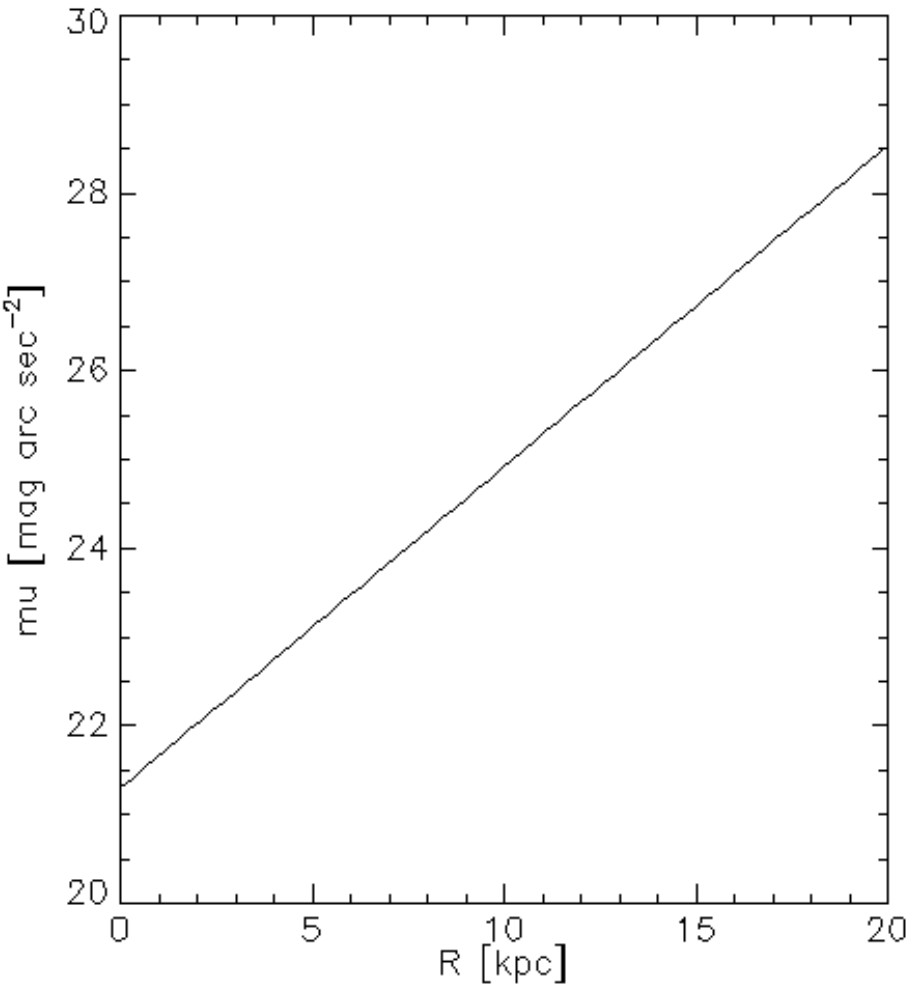

Figure 13.1: Surface brightness as function of radius.

Using the definition of magnitudes, and using the Sun at 10 pc as reference,

$$\begin{aligned} \mu_{\rm B} - M_{\rm B} &= -2.5 \log \left(\frac{F}{L_{\rm B}/4\pi 10^2} \right) \\ &= -2.5 \log(10^2 \, \sigma\theta^2) \end{aligned}$$

hence $\mu_{\rm B} = M_{\rm B} - 5 - 2.5 \log(\sigma\theta^2) = 21.3$.

4. We just need to replace n_0 by $n_0 \exp(-R/R_0)$ in the previous analysis, yielding $\mu_{\rm B} = 21.3 + 2.5 \log_{10}(e) \, \frac{R}{R_0}$.

13.2 Stars & Galaxies, Workshop II

Question 1.

1. What are Cepheid variables? Explain how they can be used to estimate distances to galaxies.

   Answer: Cepheids are variables stars for which there is a well defined relation between luminosity (L) and period (P) of the luminosity variations (a Period-Luminosity or $P-L$ relation. For a Cepheid variable in a distance galaxy, we can measure the period (P) and flux $F = L/(4\pi d^2)$. Given P we obtain L from the $P-L$ relation, and given F and L we can infer d, the distance to the galaxy.

2. What are *globular clusters?*

   Answer: Globular clusters are dense stellar systems of $10^5 - 10^6$ old stars in orbit around galaxies. Some of them can orbit at radii R considerably larger than the size of the galaxy.

3. What are roto-vibrational transitions in molecules? What is the nature and origin of the light emitted by the dust in spiral galaxies?

   Answer: the atoms in a molecule can vibrate, and the molecule as a whole can spin. The energy stored in these variations and rotations is quantised. When a molecule transitions between rotational or vibrational states, it can emit (or absorb) a photon.
   When dust absorbs mostly short-wavelength radiation, the energy of the absorbed photons heats the dust grain. The dust grain then starts to radiate it heat into space, in the form of infra-red and longer wavelength radiation.

4. How are the galactic coordinates (l, b) defined? **Answer:** In the plane of the Milky Way, the galactic longitude l is the angle between the projection of an object in the galactic plane and the direction to the MW centre, and the galactic latitude b the height of the object above the galactic disc (see Fig. 3.1 in the notes). Full details, see the original paper

5. What is HI, HII and H_2 gas? What is CII?

Answer: HI is atomic (neutral) hydrogen, HII is ionised hydrogen, and H_2 is molecular hydrogen; CII is single ionised Carbon. In general, the notation Xn refers to the (n-1)-times ionised state of element X.

Question 2. HII regions

1. A gas cloud has uniform density of $n = 5$ hydrogen atoms per cm^3. A central O stars emits $\dot{N}_\gamma = 10^{48}$ ionising photons per second. Compute the radius (location) in parsecs and speed of the ionisation front in km s^{-1} after time $t = 10^4$ yrs.

   Answer: Let R be the radius of the ionisation front. The total number of hydrogen atoms to ionised within R is

   $$N = \frac{4\pi}{3} R^3 n \,. \tag{13.4}$$

   The total number of ionising photons emitted by the source up to t is

   $$N_\gamma = \dot{N}_\gamma t \,. \tag{13.5}$$

   For all HI to be ionised within R requires $N_\gamma = N$, therefore

   $$\begin{aligned} R &= \left(\frac{3\dot{N}_\gamma\, t}{4\pi n} \right)^{1/3} = 8.0 \text{ pc} \\ \dot{R} &= \frac{\dot{N}_\gamma}{4\pi R^2\, n} = 260. \text{ km s}^{-1} \,. \end{aligned} \tag{13.6}$$

2. Compute the Strömgren radius in parsecs in this cloud. Take $\alpha = 3.1 \times 10^{-13}$ cm^3 s^{-1} as the value of the recombination coefficient.

   Answer: When $R = R_S$ recombination balance photo-ionisations,

   $$\frac{4\pi}{3} R_S^3\, \alpha\, n^2 = \dot{N}_\gamma \,, \tag{13.7}$$

   therefore

   $$R_S = \left(\frac{3\dot{N}_\gamma}{4\pi\alpha n^2} \right)^{1/3} = 10 \text{ pc} \,. \tag{13.8}$$

3. Taking into account recombinations, demonstrate that the speed of the ionisation front is given by

$$\dot{N} = 4\pi R^2\, n\, \dot{R} + \frac{4\pi}{3}\, \alpha\, n^2\, R^3\,. \tag{13.9}$$

Answer: If R is the current position of the ionisation front, then there are $(4\pi/3)\alpha\, n^2 R^3$ recombinations per unit time in the already ionised region. To advance R to $R+\dot{R}\,dt$ in a time dt requires ionising a further $4\pi\, nR^2\dot{R}\,dt$ neutral atoms. Equating the number of required ionisations per unit time, $(4\pi/3)\alpha\, n^2 R^3 + 4\pi\, nR^2\dot{R}$, with the number of photons emitted by the source, $\dot{N}$, yields the required relation.

4. Show that $R(t) = R_0\,(1-\exp(-t/t_0))^{1/3}$ is the general solution to this equation. Obtain expressions for t_0 and R_0. Show this general solutions reverts to the solution at early times (when recombinations are negligible) as well as the solution at late times (when the ionisation front stalls at the Strömgren radius).

Answer: The time derivative of $R(t) = R_0\,(1-\exp(-t/t_0))^{1/3}$ is

$$\begin{aligned}
\dot{R} &= \frac{R_0}{3t_0}\exp(-t/t_0)/(1-\exp(-t/t_0))^{2/3} \\
&= \frac{R_0}{3t_0}\,\frac{1-(1-\exp(-t/t_0))}{(R/R_0)^2} \\
&= -\frac{1}{3t_0}\,R + \frac{R_0^3}{3t_0}\,\frac{1}{R^2} \\
&= -\frac{\alpha n}{3}\,R + \frac{\dot{N}}{4\pi n}\,\frac{1}{R^2}\,,
\end{aligned} \tag{13.10}$$

where the last line follows from Eq. (13.9). Comparing the last two lines shows that

$$\begin{aligned}
t_0 &= \frac{1}{\alpha n} \\
R_0^3 &= \frac{3\dot{N}}{4\pi\alpha n^2}\,.
\end{aligned} \tag{13.11}$$

Comparison with Eq. (13.7) shows that R_0 is the Strömgren radius, which is also the value of $R(t)$ for $t \gg t_0$.
For small times, $t \ll t_0$, the solution is $(R/R_0)^3 = (t/t_0)$, hence the speed of the front is $\dot{R} = (R_0^3/3R^2)\,1/t_0 = \dot{N}/4\pi\, nR^2$

$[1\ \mathrm{pc} = 3.09 \times 10^{16}\ \mathrm{m},\ M_\odot = 2.0 \times 10^{30}\ \mathrm{kg},\ G = 6.67 \times 10^{-11}\ \mathrm{m^3\ kg^{-1}\ s^{-2}}]$

13.3 Stars & Galaxies, Workshop III

Question 1.

1. What is the *rotation curve* in a galaxy?

   Answer: The rotation curve is the run of circular velocity as function of radius.

2. What are the main assumptions of the *local group timing argument*? How can we estimate the mass of the Milly Way based on the local group timing argument? Which observations are needed, and how were they obtained?

   Answer: The timing argument assumes that the mass of the local group is concentrated in two galaxies - Milky Way and Andromeda - and that these two point masses move on a radial orbit. These galaxies starting moving apart at the Big Bang, and their mutual gravity is the cause that they are moving towards each other now.
   An estimate of the mass follows from describing their motion as a Newtonian two-body problem, and given the masses of the two galaxies $M_{\rm MW}$ and $M_{\rm A}$ we can compute the orbit. Assuming $r = 0$ at $t = 0$, we can determine $M_{\rm MW} + M_{\rm A}$ given t (time since the Big Bang), r current distance, and v_r (current radial velocity). r follows from Cepheid distant measurements, t from the ages of globular clusters, and v_r from the Doppler shifts of known spectral lines in the spectrum of Andromeda.

Question 2.

1. Consider a spherical density distribution $\rho(R) = \rho_0\,(R_0/R)^\alpha$, with ρ_0, R_0 and α constants. Calculate and sketch the circular velocity as function of radius for the cases $\alpha = 0$, 1 and 2.
   Answer: The enclosed mass for these distributions is

$$M(<r) = 4\pi \int_0^r \rho(r)\, r^2\, dr = 4\pi\rho_0\, \frac{r_0^3}{3-\alpha}\, (r/r_0)^{3-\alpha}\ .$$

   and the corresponding circular velocity $V_c = (GM/r)^{1/2}$ is sketched in Fig. 13.4

2. Observed rotation curves of galaxies are typically constant in their outskirts, and fall towards the center as in Figure 1. However the shape in their inner parts can differ, typically the rotation curves of massive spirals rise quickly (e.g. NGC 5533) and those of smaller (dwarf) galaxies rise much more slowly (e.g. IC 2574). Sketch the density distribution that you infer for NGC 5533, UGC 128 and IC 2574.

   Answer: Comparing the rotation curves to those in Fig. 13.4 we notice that a $1/r^2$ profile gives rise to constant V_c, a $1/r$ profile to a curving $V_c \propto r^{1/2}$ and a r^0 profile to a linearly rising $V_c \propto r$.
   For NGC 5533 we find $V_c \sim$ constant and hence $\rho \propto r^{-2}$.
   For UGC 128 we find approximately $V_c \propto r^{1/2}$ and hence $\rho \propto r^{-1}$.
   For IC 2574 we find approximately $V_c \propto r$ and hence $\rho \propto r^0$.

3. Estimate the enclosed mass in those 3 galaxies (i.e. NGC 5533, UGC 128 and IC 2574) at 10 kpc, and for the two most massive of those, at $r = 50$ kpc

   Answer: The enclosed mass is $V_c^2 r/G$, where V_c is the circular velocity at $R = 10$ kpc
   For NGC 5533 we find $V_c \sim 300$ km s^{-1} and hence $M(r < 10 \text{ kpc}) \sim 2 \times 10^{11} M_\odot$
   For UGC 128 we find $V_c \sim 130$ km s^{-1} and hence $M(r < 10 \text{ kpc}) \sim 3.9 \times 10^{10} M_\odot$
   For IC 2574 we find $V_c \sim 80$ km s^{-1} and hence $M(r < 10 \text{ kpc}) \sim 1.5 \times 10^{10} M_\odot$

   At the larger radius of $R = 50$ kpc, we find:
   for NGC 5533 we find $V_c \sim 240$ km s^{-1} and hence $M(r < 50 \text{ kpc}) \sim 6.7 \times 10^{11} M_\odot$
   for UGC 128 we find $V_c \sim 130$ km s^{-1} and hence $M(r < 50 \text{ kpc}) \sim 1.9 \times 10^{11} M_\odot$

4. The Milky Way hosts a super massive black hole with mass $M_{\rm BH} \sim 10^6 M_\odot$ in its centre. How close to the black hole do you expect to notice its effect on the circular orbits of stars?

   Answer: We know that in the absence of a BH, the MW has nearly constant circular velocity, $V_{c,0} \approx 220$ km s^{-1}. In the presence of a

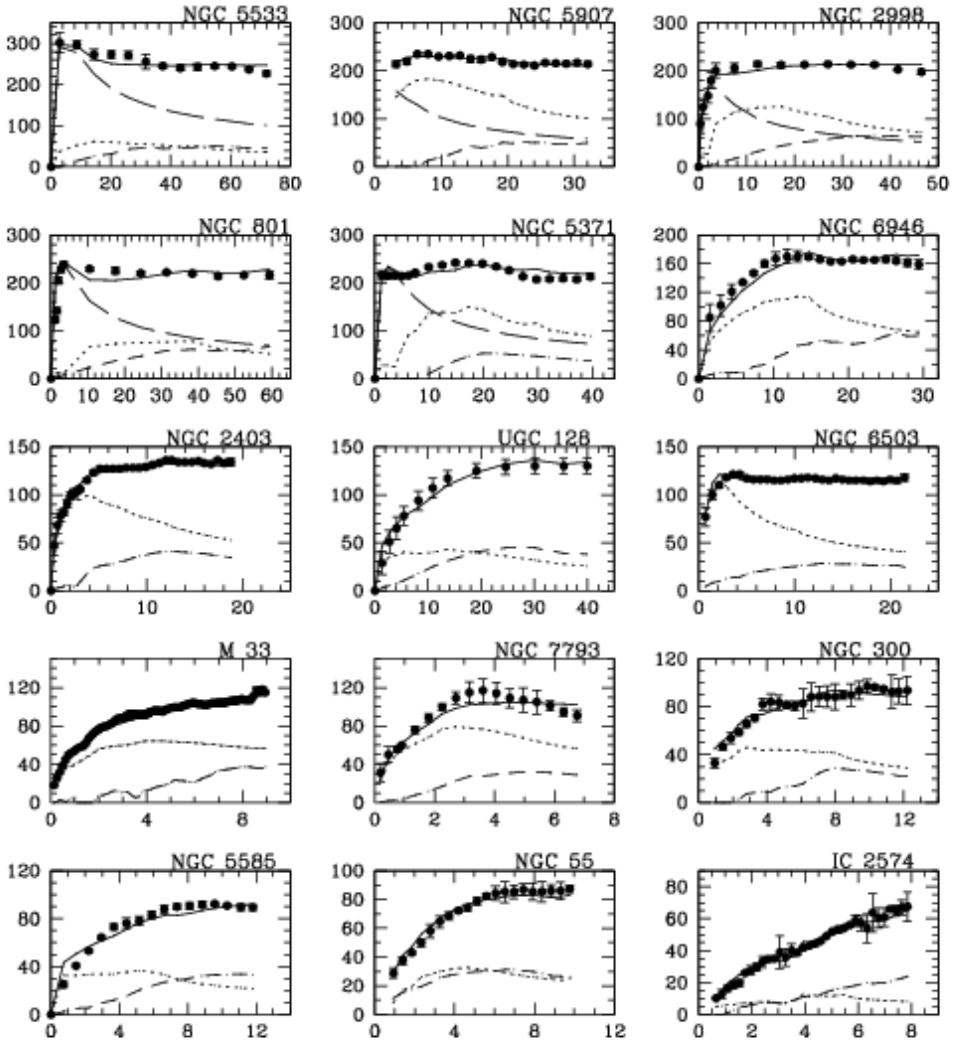

Figure 13.2: Observed rotation curves for a set of spiral galaxies.

BH, the circular velocity increases to $V_c^2 = GM_{\rm BH}/r + V_{c,0}^2$. Say we want to measure an increase more than 1 per cent above $V_{c,0}$, so that $V_c^2 = (1.01 \times V_{c,0})^2$. This occurs at a radius

$$R = \frac{G\,M_{\rm BH}}{(1.01^2 - 1^2)\,V_{c,0}^2} = 4.4 \text{ pc}\,.$$

5. Demonstrate that the gravitational force on a point mass due to an infinity sheet is independent of the distance to the sheet. Use this to make a simple model of how stars move perpendicular to the galactic disc.

   Answer: Let b be the distance to the sheet, and σ its surface density. The force due to a ring of mass (radius x, thickness dx) perpendicular to the sheet is

   $$dF = G\,\sigma\,\frac{2\pi x\,dx}{b^2 + x^2}\,\cos(\theta)\,, \tag{13.12}$$

   where θ is the angle between the vertical and the ring (see Fig.13.3). Making a change of variables from x to θ yields $dF = G\,\sigma 2\pi\,\sin(\theta)\,d\theta$ which integrates to $F = 2\pi G\,\sigma$.

   Let the star start at $t = 0$ with height $b = 0$ and (upwards speed) $\dot{b}_0$. Its motion is $b(t) = \dot{b}_0 t - (g/2)t^2$, where $g \equiv 2\pi G\,\sigma$. It comes back to hit the disc at time $t_0 = 2\dot{b}_0/g$ moving down at speed $-\dot{b}_0$. Therefore it oscillates with period $P = 2t_0$, and observing the star allows us to measure the surface density (called the Oort limit).

[1 pc $= 3.09 \times 10^{16}$ m, $M_\odot = 2.0 \times 10^{30}$ kg, $G = 6.67 \times 10^{-11}$ m^3 kg^{-1} s^{-2}]

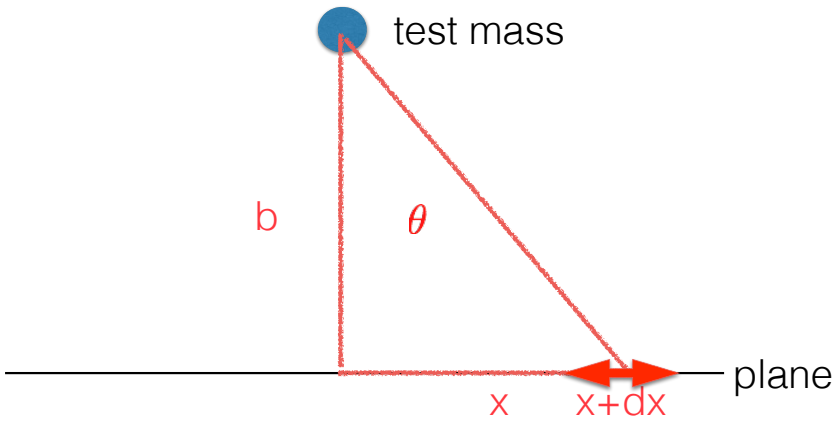

Figure 13.3: Infinitesimal force due to ring in a uniform sheet.

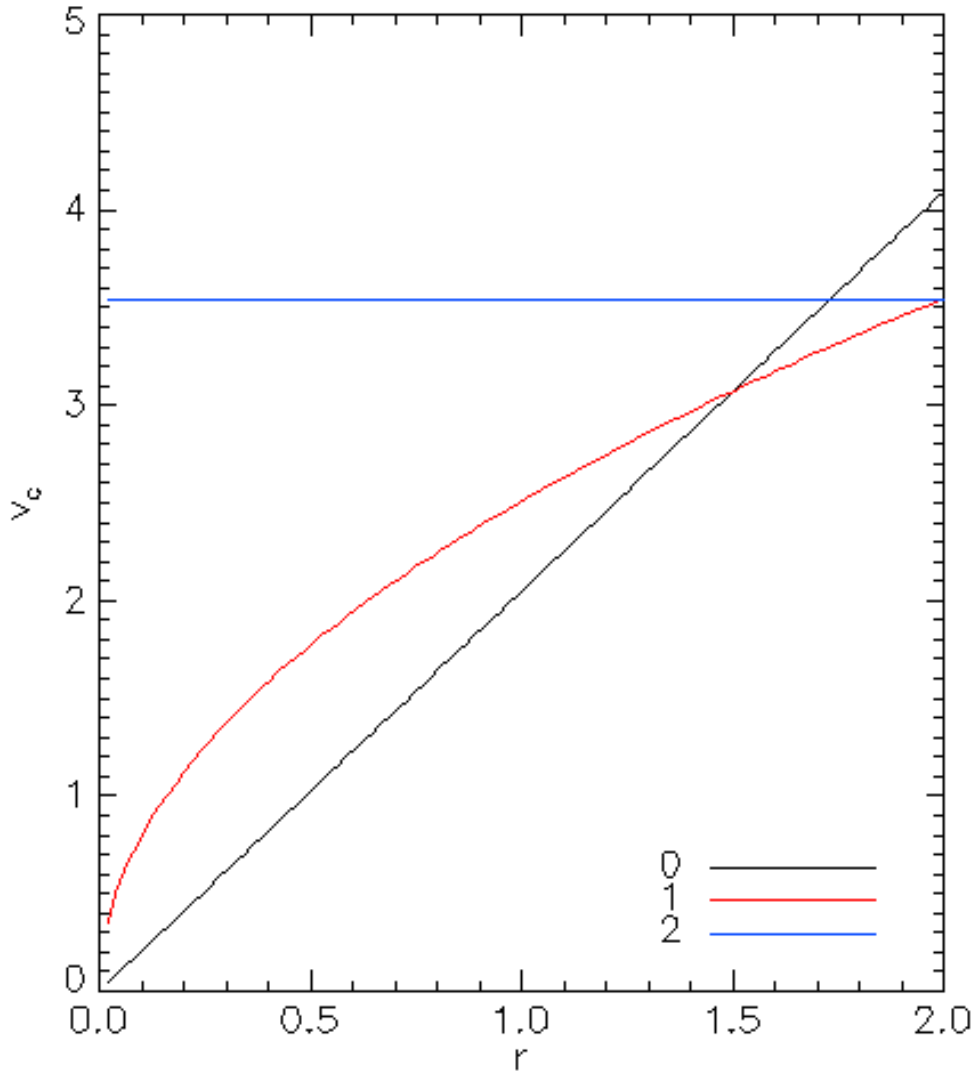

Figure 13.4: Shapes of rotation curve for power-law densities.

13.4 Stars & Galaxies, Workshop IV

Question 1.

1. Which physical process produces the diffuse X-ray emission detected in ellipticals and clusters of galaxies?

   Answer: This *thermal bremsstrahlung* is due to the acceleration of electrons that are moving fast due to the high temperature in the hot plasma that fills ellipticals and clusters of galaxies, when passing close to nucleons. The accelerating electrons (being charged particles) emit EM radiation - these are the X-rays we detect.

2. How can the motions of galaxies in a cluster of galaxies be used to infer its mass? Why did this suggest the presence of dark matter in clusters?

   Answer: By measuring the line-of-sight velocity of galaxies with respect to the mean, we can determine the velocity dispersion σ of galaxies in the clusters assuming isotropic orbits. Given σ and assuming the cluster to be in virial equilibrium yields its dynamical mass. The dynamical mass if much larger than the mass in stars and gas combined. The invisible missing mass is thought to be dark matter.

3. How have clusters of galaxies been used to determine the mean dark matter density of the Universe?

   Answer: From dynamical measurements (e.g. motions of galaxies) we can determine the total mass M_T (in baryons plus dark matter) of the cluster. From X-ray measurements we can determine the baryons mass M_b (the baryon mass in stars is small), Since the potential well of clusters is so deep, we can assume that the ratio M_b/M_T is the same as the ratio ρ_b/ρ_m of baryons over total mass density for the Unverse as a whole. We can infer ρ_b from Big Bang nucleosynthesis by measuring isotope ratios of the light elements produced in the BB. Given ρ_b, and ρ_b/ρ_m from clusters, yields the mean dark matter density, $\rho_m - \rho_b$.

Question 2. The Coma cluster of galaxies is at a distance of $d = 90$ Mpc. It contains 1000s of galaxies in a radius of $R = 3$ Mpc.

1. The observed radial velocity dispersion of galaxies in Coma is $\sigma_{1D} = 850\text{km s}^{-1}$. Use the virial theorem to estimate its total mass M.

2. Compute the virial temperature of Coma, assuming a pure hydrogen gas. Compare your answer to the binding energy of the hydrogen atom, 13.6 eV. Do you expect the gas to be mostly neutral, or mostly ionised? Use this to decide what is the appropriate mean molecular weight to use.

3. Assume that the ratio of dark matter to gas mass in the cluster, $M_{\text{dark matter}}/M_{\text{gas}} = 6$. Compute the total gas mass, and the mean electron density n_e.

4. The X-ray emissivity per unit volume, $L_x = 1.42 \times 10^{-27} n_e^2 T^{1/2}$ erg s^{-1} cm^{-3}, where n_e is the electron density in particles per cm^3, and T is the gas temperature in Kelvin. Use this to compute the total X-ray luminosity of Coma.

5. The Chandra X-ray telescope has a collecting area of $S = 800$ cm^2. Assuming all X-rays have energy 10 keV, estimate how many X-ray photons per second Chandra detects when pointing at Coma.

6. The metal abundance inferred from the X-ray spectrum is 1/3 of the solar value, $Z_\odot = 0.02$ (This is the fraction by mass of elements heavier than Helium over the total mass.) Compute the total mass in metals in Coma. The typical stellar yield, $y = M_{\text{metal}}/M_{\text{star}} \approx 0.02$, *i.e.* nuclear fusion in a stellar population of mass $M_\star$, will produce $y\,M_\star$ metals before the stars die. Use this to estimate the total mass that once was in stars. What fraction of the total gas mass is this?

7. Most of these metals are produced in Super Nova (SN) explosions. There is typically 1 SN per 100 solar masses of stars. Compute the total number of SNe explosions that took place in Coma. If they occur equally spaced in time, what is the current rate? Assume $t_0 = 13$ Gyear for the age of Coma.

8. The explosion energy of a SN is $E_{\text{SN}} = 10^{51}$ erg. Compare the total energy input of SN with the thermal energy of the gas. Can SNe be responsible for heating the gas to the observed temperature?

Answer:

1. The 3D velocity dispersion $\sigma = 3^{1/2}\,\sigma_{1D}$ (assuming isotropy). Virial theorem, Eq. (8.4), then gives $M = R\sigma^2/G = 1.5 \times 10^{15} M_\odot$.

2. Eq.(8.7) gives $T = (2/3)(\mu m_p/k_B)\,(GM/R) = 8.75 \times 10^7$K=7.54 keV, for $\mu = 0.5$. Temperature is much higher than H binding energy, hence fully ionised, hence $\mu = 0.5$ for hydrogen gas.

3. Total gas mass $M_g = M/7 = 2.16 \times 10^{14} M_\odot$, mean electron density $n_e = M_g/(4\pi\, R^3 m_p/3) = 0.77 \times 10^{-4}$ electrons per cm^3.

4. $L_x = 1.42 \times 10^{-27} n_e^2 T^{1/2}\,(4\pi R^3/3) = 2.64 \times 10^{44}$ erg s^{-1}.

5. Energy of 1 photon $E_x = 10$ keV $= 1.6 \times 10^{-8}$ erg, hence total photon flux is $N_x = L_x/E_x$. Count rate in Chandra $= C = N_x * (S/4\pi d^2) =$ 13.6 photons per second.

6. Metal mass $M_z = Z_\odot \times M_g/3 = 1.44 \times 10^{12} M_\odot$, where $Z_\odot = 0.02$ is the metal abundance of the Sun (e.g. page 79, footnote 6). For yield $y = 0.02$, mass once in stars, $M_\star = M_z/y = Z_\odot M_g/3/y = M_g/3 = 7.20 \times 10^{13} M_\odot$,*i.e.* 1/3 of the total gas mass.

7. Number of SNe $N = M_\star/100 M_\odot = 7.20 \times 10^{11}$, currently $N/t_0 = 55$ per year.

8. Total SN energy is $E_{\rm SN} = N \times 10^{51}$ erg=7.20×10^{62} erg. Thermal energy of gas per unit mass is $u = (3/2)({\rm k_B} T/\mu m_{\rm h}) = (GM/R)$. Hence total thermal energy is $U = u\, M_g = 9.31 \times 10^{63}$ erg, hence $E_{\rm SN}/U = 7.7\%$, so SNe may have had a small effect on heating the gas.

[$G = 6.67 \times 10^{-11}$ m^3 kg^{-1} s^{-2}, $M_\odot = 1.99 \times 10^{30}$ kg,
1pc $= 3.09 \times 10^{16}$ m, ${\rm k_B} = 1.38 \times 10^{-23}$ J K^{-1}, $m_{\rm h} = 1.67 \times 10^{-27}$ kg]

13.5 Stars & Galaxies, Workshop V

Question 1.

1. What is the 'density-morphology' relation of galaxies?

   Answer: The 'density-morphology' relation relates the number density n of galaxies to their type. With increasing n the fraction of spirals decreases, and the fraction of Es and S0s increases.

2. The stellar mass-to-light ratio $\Gamma = M_\star/L_\star$ depends on the properties of the stellar population of a galaxy. Is Γ higher or lower for an elliptical galaxy compared to a spiral galaxy?

   Answer: Elliptical do not harbour the massive stars that are very bright, but typically contain lower mass star with higher metallicities. Both contribute to them generating less light for the same mass, hence Γ is higher for Es than for Ss.

3. What are the Tully-Fischer and the Faber-Jackson relations? How can these be used as standard candles?

   Answer: The TF relation relates galaxy luminosity L to circular velocity V_c in spirals, approximately $L \propto V_c^4$. The FB relation relates L to velocity dispersion σ of the stars in Es, approximately $L \propto \sigma^4$.

   The proportionality constant L_c (as in $L = L_c(V_c/220\text{km s}^{-1})^4$ for the TF relation for example) in these relation can be found by measuring distance d to nearby galaxies using Cepheids for example, enabling the determination of L from the measured flux, $F = L/(4\pi d^2)$. This makes these relations standard candles: measuring V_c gives L from TF, which combines by the measured value of F, yields the distance d.

4. What is the Eddington limit of an object? Are there any objects with luminosity higher than their Eddington limit?

   Answer: The Eddington limit is that luminosity L_{Edd} at which the radiation pressure equals the gravitational pull.
   A system not in equilibrium can have luminosity $L > L_{\text{Edd}}$, for example a super nova explosion.

5. What observational evidence do we have that the MW harbours a super massive black hole?
   Answer: Stars near the centre of the MW are observed to be on Keplerian orbits, from which we can infer that mass of the central object. The extent of this massive object ($M \sim 10^6 M_\odot$) is small as inferred from the fact that stars can pass very close to it. Combined this suggest the central object is a black hole.

Question 2.

1. The observed rotation speed of a distant galaxy is $V_c = 180$ km s^{-1} and its flux is $F = 4.8 \times 10^{-11}$ W m^{-2}. Estimate the¡ distance to the galaxy in Mpc assuming it lies on the Tully-Fisher (TF) relation. Assume the Milky Way, with luminosity $L_{\rm MW} = 3 \times 10^{10} L_\odot$ and circular velocity $V_{c,\rm MW} = 220$ km s^{-1} also lies on the TF relation.

   Answer: The luminosity of the galaxy is $L = L_{\rm MW}\,(V_c/V_{c,\rm MW})^2$, and giving its flux F we can calculate the distance $d = (L/(4\pi F))^{1/2} = 3$ Mpc.

2. The Schwarzschild radius of a black hole with mass M is

$$R_S = 2GM/c^2\,. \tag{13.13}$$

   Gas on a circular orbit with radius $R = 2R_s$ emits an emission line with energy $E = 6.38$ keV - the Iron K-α line. Assume the disk is seen edge on so light on one side is Doppler shifted to the red and on the other side is shifted to the blue. Calculate the wavelength you observe this line on either side, assuming the black hole is lurking in the centre of a galaxy that moves away from us at speed $v = 12000$ km s^{-1}.

   Answer: The circular speed at radius $R = 2R_S$ is

$$V_c^2 = \frac{GM}{2R_S} = \frac{c^2}{4}\,, \tag{13.14}$$

   so we need to use the equation for relativistic Doppler shift, with observed (λ_o) and emitted (λ_e) wavelengths related by

$$\lambda_o = \lambda_e \left(\frac{1+\beta}{1-\beta}\right)^{1/2} (1 + v/c)\,, \tag{13.15}$$

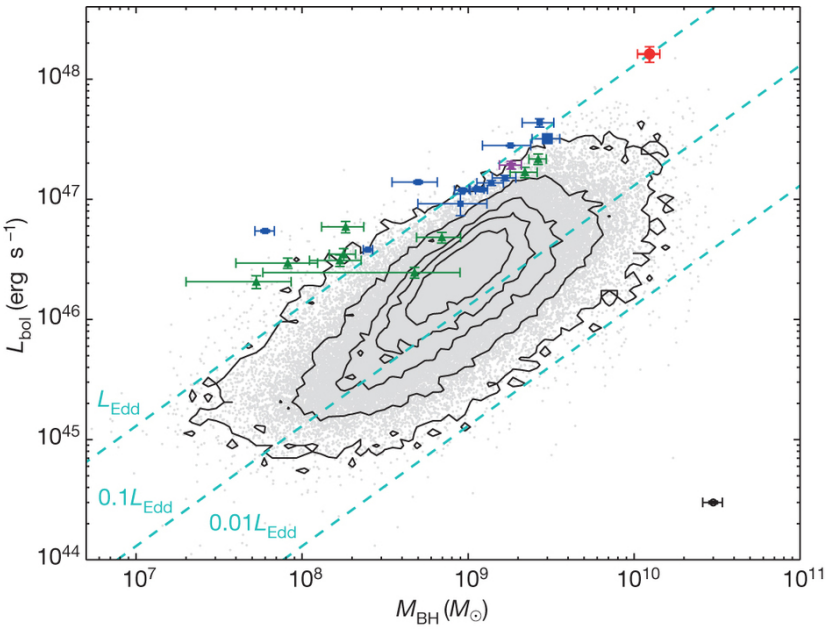

Figure 13.5: Bolometric (total) luminosity versus mass for a set of quasars from the SDSS survey (contours), a set of $z > 6$ QSOs (blue squares) and the recently discovered QSO J0100+2802, red. (from Wu et al, *Nature* 512, February 2015)

where $\beta = \pm V_c/c = \pm 1/2$ and the extra factor $(1 + v/c)$ is due to the non-relativistic motion of the galaxy. The ratios λ_o/λ_e are then 1.73 and 0.58 for the redshifted/blue shifted line, where $\lambda_e = hc/E$ is the laboratory wavelength of Fe-Kα.

3. Figure 13.5 relates black hole mass to luminosity for a set of QSOs. Calculate the Eddington luminosity for QSO J0100+2802 (black hole mass is $1.2 \times 10^{10} M_\odot$). This QSO is seen when the Universe was only $t = 0.884$ Gyr old. Assume the BH grew from a seed-mass of $M_{\rm seed} = 500 M_\odot$ and has been accreting at the Eddington rate ever since. Calculate when the seed formed. Assume the luminosity of the QSO depends on the accretion rate as $L = 0.1\dot{M}c^2$.

   Answer: The Eddington luminosity from Eq. (10.5) is

$$L_{\rm Edd} = 3.3 \times 10^{12} \, \frac{M_{\rm BH}}{10^8 M_\odot} \, L_\odot \, . \tag{13.16}$$

Substituting $M_{\rm BH} = 1.2 \times 10^{10} M_\odot$ for QSO J0100+2802 yields $L_{\rm Edd} = 1.5 \times 10^{48}$ erg s^{-1}, consistent with QSO J0100+2802 currently accreting at the Eddington rate.

The mass of the BH increases exponentially when accreting at the Eddington rate (Eq. 10.7)

$$M_{\rm BH}(t) = M_{\rm BH}(t=0)\, \exp(t/\tau)\,, \tag{13.17}$$

where the Salpeter time $\tau = 5 \times 10^7$ yr (for $\eta = 0.1$). Taking $M_{\rm BH}(t = 0) = 500 M_\odot$ then yields $t = \tau \log(1.2 \times 10^{10}/500) = 8.5 \times 10^8$ yrs, which is only *just* below the age of the Universe at that time.

4. The presence of a point mass M distorts (curves) space-time around it so that light rays passing near M at distance b appear to be deflected by an angle.

$$\alpha = \frac{4GM}{bv^2}\,, \tag{13.18}$$

where $v = c$ is the speed of light. Show this is *twice* the angle under which a test mass moving at speed v is deflected in case the deflection angle is small. Consider a situation under which observer, lensing mass M and source are exactly aligned. Demonstrate the observer sees the source images in a ring and calculate the angle θ_E ('Einstein radius') under which the observer sees this ring (Fig. 13.6). Calculate θ_E in arc seconds, for the case where the distance observer-lens=500 Mpc, the distance lens-source=500 Mpc, and the mass of the lens $M = 10^{13} M_\odot$.

Answer: The first part of the exercise appears in the Appendix of the notes.
The second part combines Eqs.(11.3) and (11.4) in the notes.
This yields $\theta_E = 9$ arc sec.

[$G = 6.67 \times 10^{-11}$ m^3 kg^{-1} s^{-2}, $M_\odot = 1.99 \times 10^{30}$ kg,
1pc $= 3.09 \times 10^{16}$ m, $k_{\rm B} = 1.38 \times 10^{-23}$ J K^{-1}, $m_{\rm h} = 1.67 \times 10^{-27}$ kg]

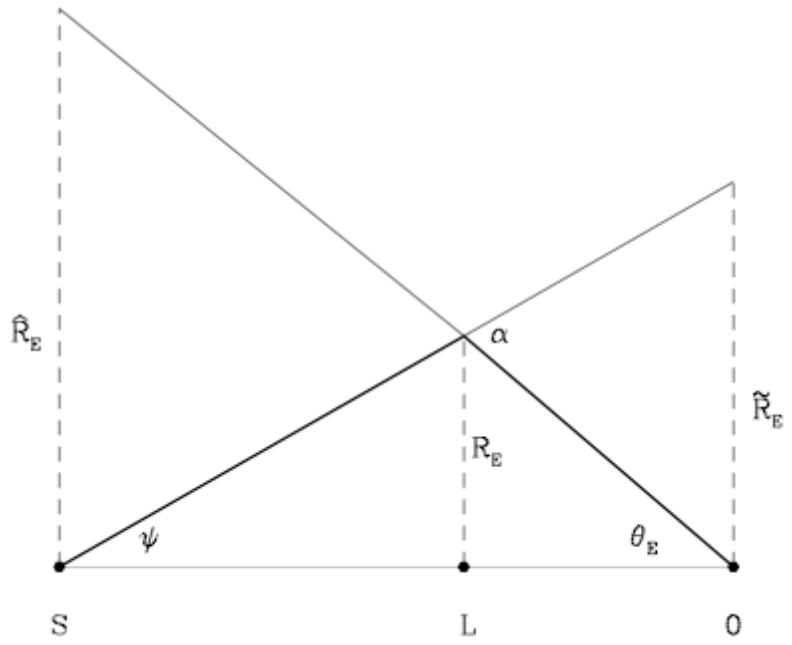

Figure 13.6: Situation where source S is gravitationally lensed by the lens L into an Einstein ring, seen by the observer O under an angle θ.

Contents